Affimers, protein-based residues as detection tools for the lectin-like low density lipoprotein 1 Scavenger receptor

Ahmed Salim Mohammed Al Aufi

Submitted in accordance with the requirements for the degree of

Master of Science Research

The University of Leeds

Faculty of Biological Sciences

School of Molecular and Cellular Biology

May 2023

The candidate confirms that the work submitted is his/her own, except where work which has formed part of jointly-authored publications has been included. The contribution of the candidate and the other authors to this work has been explicitly indicated below. The candidate confirms that appropriate credit has been given within the thesis where reference has been made to the work of others. Further details of the jointly-authored publications and the contributions of the candidate and the other authors to the work should be included below this statement.

Jointly authored publications

Chapter 2:

Roper, B.W.R., Al-Sayejh, B., **Al-Aufi, A.**, Cuthbert, G.A., Lacey, K., Homer-Vanniasinkam, S., Harrison, M.A., Tomlinson, D.C., Ajjan, R., and Ponnambalam, S. (2022). Purification and Analysis of Circulating Lipid Particles. Methods Mol Biol 2419, 193-212.

Acknowledgements

I graduated from medical school in Oman 13 years ago and during my time as a medical student, my exposure to the lab work has been very minimal. This experience was not just out of the norm for me but also was a great opportunity to explore my capabilities and to know that there is a broad spectrum to science that is yet to be uncovered. In the last 3 years ther has been may people who helped, offered support and were around to guide me. I would like to thank my principal supervisor Dr. Vas Ponnambalam for making this an enjoyable learning experience for me. I can't express enough gratitude to my co-supervisor Professor. Shervanthi Homer-Vanniasinkam for all her support and help. She has been and will continue to be a great role model. These thanks extend to the Leeds Hospitals Charity who funded this project and without whom none of this could have happened. In the lab I had more than just colleagues, I had friends who made my journey easier and more enjoyable. They offered help when I asked and even when I didn't. To Barney Roper, Will Critchley, Areej Alzahrani, Queen Saikia and Dhananjay Jade, thank you form the depth of my heart. I also thank my colleagues and supervisors in the Leeds vascular institute, who helped accommodate the needs of moving between research and clinical work. A special thank you to the person who all of this wouldn't have been possible without his guidance and support. To Dr. Edwin Stephen, my mentor in Oman, thank you ever so much for believing in me and seeing what I didn't see in myself. I have no words to express my thanks to my parents, who despite being 5000 miles away kept praying for me and offering emotional support that I needed during the toughest of times. I thank my children, Alkhalil, Yumna, Yousuf, Yaseen and Jana for making my life meaningful and being the motivation for me to work and keep working despite all the difficulties. Last , but no least , I thank the love of my life, my wife, Elham for being there always for me and being the loving, caring and understanding facilitators for me to carry on through this unpresented experience for me and for making me feel that every little I do is appreciated and matters.

Abstract

The role that lectin-like oxidised low-density lipoprotein receptor-1 (LOX-1) plays in atherosclerosis is an important research point. The current use of antibodies to inhibit LOX-1 activity is not promising and thus using antibody alternatives is a reasonable step to overcome the pitfalls of antibodies. Affimers, small protein scaffolds, are a potential LOX-1 inhibitors. They could be used in isolation of in combination with antibodies to identify and inhibit the uptake of oxidised low density lipoprotein (ox-LDL) into the endothelial cells. This work aims at establishing the ability of Affimers to bind and detect LOX-1 in vivo and in cell cultures in a preparatory step to test their use in animal and human –extracted tissues from disease and control subjects. The evolution of this technology will offer an advancement in the diagnostic and therapeutic modules of atherosclerosis.

Table of contents

List of figures

List of tables

Abbreviations

AcLDL Acetylated LDL

AGE Advanced glycation end-products

Akt Protein kinase B

AngII Angiotensin II

ApoA1-4 Apolipoprotein A1-4

ApoB-48 Apolipoprotein B-48

ApoB-100 Apolipoprotein B-100

ApoE Apolipoprotein E

BCA Bicinchoninic acid

BHT Butylated hydroxytolunene

BSA Bovine serum albumin

CAD Coronary artery disease

CD Cytoplasmic domain

CD36 Cluster of differentiation 36

CK-MB Creatine kinase MB

CRP C-reactive protein

CT Computerized tomography

CTLD C-type lectin-like domain

cTnT cardiac troponin T

CVD Cardiovascular disease

DAPI 4’. 6-diamidino-2-phenylindole

DARPins Designed Ankyrin repeat proteins

DiI 1,1’,di-octadecyl-3,3,3’3’-tetramethylindocarbocyanine

DMEM Dulbecco’s Modified Eagle Medium

DNA Deoxyribonucleic acid

ECD Extracellular domain

ECL Enhanced chemiluminescence

ECM Extra cellular matrix

EDTA Ethylene-diaminetetra acetic acid

EGF Epithelial growth factor eNOS Endothelial nitirc oxide synthase

ER Endoplasmic reticulum ERK1/2 Extracellular signal-regulated kinase 1/2 (p42/44)

FCS Foetal calf serum

GWAS Genome-wide association study

HBS HEPES buffered saline

HDL High-density lipoprotein

HEK-293 Human embryonic kidney -293 cells

HRP Horseradish peroxidase

HUVECs Human umbilical vein endothelial cells

ICAM-1 Intercellular adhesion molecule-1

IDL Intermediate density lipoprotein

IL Interleukin

lPTG lPTG Isopropyl β-D-1-thiogalactopyranoside

LB Luria-Bertani

LDL Low-density lipoprotein

LDLR Low-density lipoprotein receptor

LPS Lipopolysaccharide

LOX-1 Lectin-like oxidized low-density lipoprotein receptor-1

MAPK Mitogen-activated protein kinase

MCP-1 Monocyte chemoattractant protein-1

MCS Multiple cloning site

M-CSF macrophage-colony stimulating factor

MHC Major histocompatibility complex MI Myocardial infarction

MMP Matrix-metalloproteinases

mRNA Messenger ribonucleic acid MW Molecular weight NF-κβ Nuclear factor kappa B

Ni-NTA Nickel-nitriloacetic acid

NK Natural killer NO Nitric oxide

OLR1 Oxidized LDL receptor 1

OxLDL Oxidized LDL

PAGE Polyacrylamide gel electrophoresis

PBS Phosphate buffered saline

PCR Polymerase chain reaction

PEG Polyethylene glycol

PFA Paraformaldehyde

PI-3-K Phosphoinositide 3-kinase

PMSF Phenylmethylsulphonyl fluoride

PKC Protein kinase C

PPAR-γ Peroxisome proliferator-activated receptor-γ

PS Phosphatidyl serine

RAGE Receptor for advanced glycation end-products

ROS Reactive oxygen species

SCARB3 Scavenger receptor class B member 3

SDS Sodium dodecyl sulfate

scFv Single-chain variable fragment

sLOX-1 Soluble LOX-1

SNP Single-nucleotide polymorphism

SR Scavenger receptor

SRA1 Scavenger receptor class A type 1 (SCARA1)

SRB1 Scavenger receptor class B type 1 (SCARB1)

STEMI ST-elevation myocardial infarction

T2DM Type 2 diabetes mellitus

TBS Tris-buffered saline

TCEP Tris (2-carboxyethyl)phosphine

TEMED Tetramethylethylenediamine

TMB 3,3',5,5'-tetramethylbenzidine

VCAM Vascular cell adhesion molecule 1

VEGF Vascular endothelial growth factor -xv

VLDL Very-low-density lipoprotein

VSMC Vascular smooth muscle cell

Chapter 1
Introduction

1.1 Introduction to atherosclerosis

1.1.1 Historical background

The term atherosclerosis was first introduced in 1904 by Felix Marchand (Friedman, 1998; Mehta et al., 2002). Since then, the phenomenon of deposition of fat particles deposition in the arterial walls linking to hardening of the blood vessels became widely understood, leading to the use of atherosclerosis as a generic term that required no further definition or explanation globally. In the current era, doctors and healthcare workers almost always need no further descriptive terms when trying to explain an atherosclerotic process-related complication to a patient.

In the beginning of the 20th century, the beginnings of atherosclerosis as a biological phenomenon began to emerge; this was a mysterious science area and although descriptions of arterial disease existed before Marchand, the work done by these clinician-scientists and their colleagues have provided the foundations of our current understanding of the role of cholesterol imbalance in the initiation, development and progression of arterial disease (Ignatowski et al., 1909). Subsequently, immense research efforts have identified key features of this biological process. In 1910, Adolf Windaus demonstrated that atheromatous plaques have 6-fold increased levels of free cholesterol and 20-fold increased levels of esterified cholesterol compared to normal arterial walls (Konstantinov et al., 2006).

Generic definitions of this pathophysiological process argues that the deposition of lipid- and fat-enriched particles in the arterial wall is a central feature of atherosclerosis. However, viewed from a different angle, this is the endpoint of a long-standing biological process that eventually leads to arterial disease. All blood vessels are lined by a smooth surface of endothelial cells that, beside an important endocrine, exocrine and

paracrine function, also form a protective layer to the muscular layer below (Mannarino et al., 2008). Injury to this layer is a trigger point in the atherosclerosis pathway and the causes for such injury will be discussed at a later stage. The imbalance between circulating lipoproteins and chylomicrons leads to pathological deposition of lipids in the arterial wall which triggers an inflammatory reaction leading eventually to development of a fibrotic shell with a chronic inflammatory plaque that disrupts the function of all 3 layers of arterial wall (Mannarino et al., 2008; Milutinović et al., 2020). This eventually leads to narrowing of the blood vessel which results in ischaemia of the downstream tissues and organs. The disruption in blood flow and haemodynamics determines the differential atherosclerotic effects on large or small blood vessels (Kuller et al., 1994). Other systemic diseases like diabetes and rheumatoid inflammation also predispose to arterial disease via different mechanisms which will be described below.

While around 36-38% of atherosclerotic plaques are subclinical and lead to little or no pathological effects, they still possess the capability to progress over time and cause serious health consequences (Toth et al., 2008). In the Cardiovascular Health Study, >5000 adult subjects aged ≥65 years were screened for asymptomatic atherosclerosis; 36% of females and 38.7% of males had a significant atherosclerosis burden which increased with age (Toth et al., 2008; Kuller et al., 1994). Although some patients develop gradual symptoms which when progress add to the burden of atherosclerosis. Additionally some patients are at risk of significant morbidity and mortality without prior symptoms. This depends on time available for the affected body organ to form collateral circulation to sustain blood flow that match the demand of its tissues. However, the latter patients also have minimal capacity to deal with stress-induced ischaemia which renders them in need of interventions. Symptoms such as stable angina and intermittent lower limb claudication are examples of mismatch between tissue demand and supply during exercise and stress which are manifestation of atherosclerotic disease that is asymptomatic at rest. Patients with such symptoms may progress to acute life-threatening or limb-threatening symptoms with factors as simple as excess ischaemic stress or

a thrombotic or embolic event causing disruption of the collateral circulation or the remaining luminal flow.

1.1.2 Arterial histology and disease process

Blood and lymphatic vessels share 3 histologic layers named tunica intima, tunica media and tunica adventitia (Figure 1.1). The relative thickness of each layer is used to histologically differentiate arteries, veins, capillaries and lymphatic vessels. These histological differences pose significant implications in the development of disease as well as when treatment is considered. For example, tacking an 'unstable' intimal layer to the arterial wall after doing an endarterectomy of an artery becomes important to avoid dissection of the vessel on the antegrade flow direction. Aortic dissection, for instance, is a serious and usually acute disease that involves separation between the arterial wall layers. In-hospital mortality rates from aortic dissection are around 27%; besides close to 20% of the initially affected patients die before reaching a hospital setting (Kronzon et al., 2010**)**. This arterial disease also can lead to organ malperfusion and multi-organ failure resulting in considerable burden on health services as well as being resource-intensive to treat. A net cost of around US$30,000 is the median of treating a single patient with aortic dissection (McClure et al., 2020).

Figure 1.1: Cross section of arterial and venous blood vessels. Haematoxylin-eosin staining of tissue section containing blood vessels. Arterial walls have a thicker medial smooth muscle layer as opposed to venous blood vessel walls.

Another important aspect of understanding the histology is to develop and analyse biomarkers for different pathological processes. The intimal layer lines the luminal surface of the arterial wall and consists of longitudinally oriented specialised epithelial cells called endothelium. These cells act as a selective diffusion barrier separating the circulating blood from the rest of the arterial wall layers. Alongside their absorptive function, they also have essential autocrine, paracrine and endocrine functions by secreting bioactive substrates which ultimately control vessel tone, adhesion of platelets and white blood cells to the arterial wall. An elastic membrane separates the intima from the muscular layer below. With aging or when there is intimal injury, this membrane may get fragmented, duplicated or lost

focally (Jim et al., 2007). The disruption of this membrane can result in blood leaking into the sub-intimal space and triggering a sterile inflammatory response which is hypothesised to stimulate atherosclerosis (Ritman et al., 2007).

Theories of inflammation as a cause of atherosclerosis continue to be hypothesized including recently. In 2017 Alex Haverich, a German cardiologist, proposed that plaques result from inflammation of the vasa vasorum, which are small blood vessels found in the adventitial layer of large sized arteries and veins which act as nutrient blood vessels to the arterial wall (Jim et al., 2007; Ritman et al., 2007). Linking inflammation to atherosclerosis can also be evidenced by plaque histology showing accumulation of lymphocytes and macrophages surrounding a pro-inflammatory zone enriched for oxidised lipid particles (Stary et al., 1995). The description of a fibrous cap covering the atherosclerotic plaque also supports that inflammation is the main element of atherosclerosis as a process. This can be explained by fibrocytes taking over the function of acute inflammatory cells at the periphery of the plaque, similar to what occurs with any long-standing inflammation (Figure 1.2).

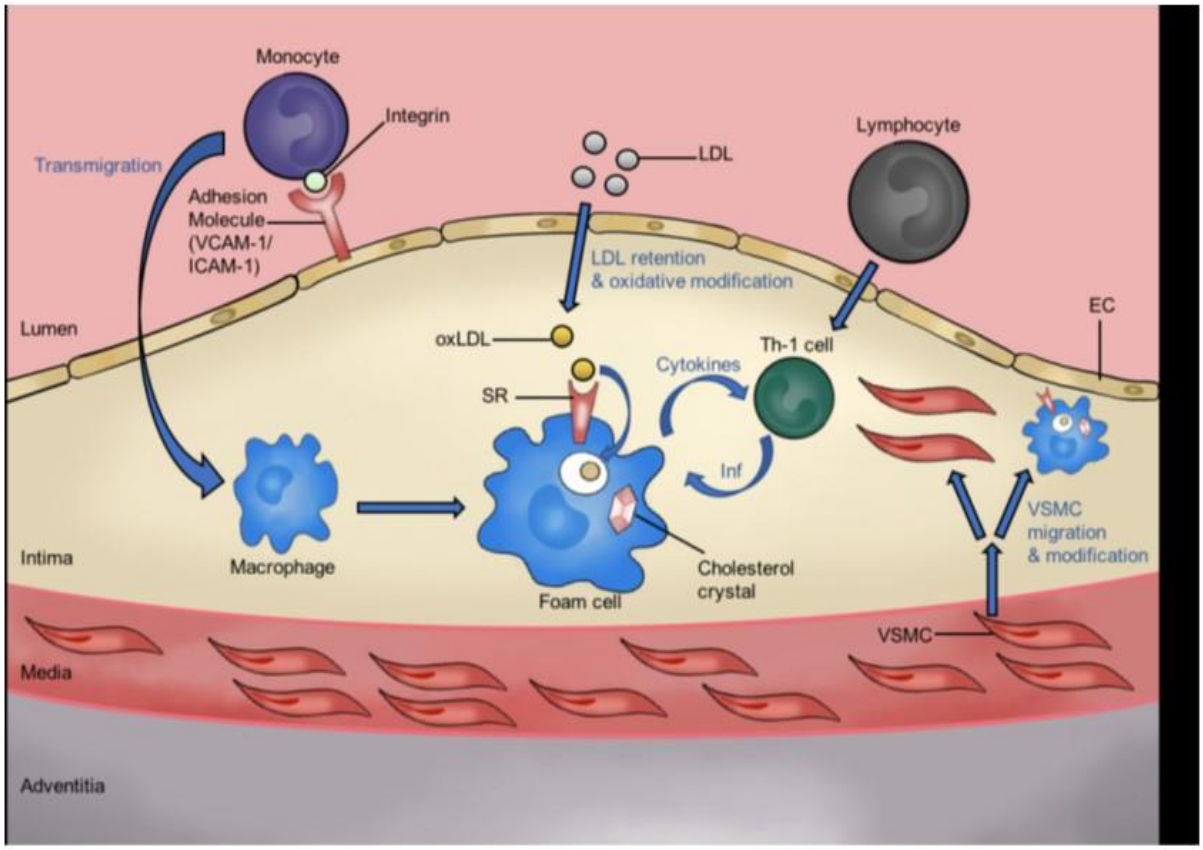

Figure 1.2: Formation of the atherosclerotic plaque. Within the blood vessel intima, LDL accumulation leads to a chronic inflammatory process leading to the transmigration of immune cells and the formation of foam cells. EC; endothelial cell. ICAM; intercellular adhesion molecule -1. Inf: interferon- gamma. LDL: low-density lipoprotein. oxLDL; oxidized low-density lipoprotein. SR: scavenger receptor. Th-1: T-helper 1 cell. VCAM: vascular cell adhesion molecule -1. VSMC: vascular smooth muscle cell. (Adapted from Gisterå et al., 2017).

1.1.3 Endothelial dysfunction and atherosclerosis

Ross and Glomset hypothesized the “response to injury hypothesis” which indicated that histological loss of the integrity of the endothelial layer is responsible for allowing the modified lipoprotein particles such as LDL to traverse the endothelial barrier and start the inflammatory process that eventually leads to the formation of atherosclerotic plaque (Gimbrone et al., 2016). As this may sound logical, overt physical loss of the intimal lining integrity, as found subsequently in animal modules, is not a mandatory precursor for atherosclerosis to commence and progress. Oxidative stress from nitric oxide imbalance which is a result of multiple disease processes (Table 1.1) or changes of intraluminal flow haemodynamics are thought to be the offending agent resulting in loss of intimal continuity (Gimbrone et al., 2016). The change of haemodynamics can be used as evidence to explain the common observation of atherosclerotic plaques taking place at arterial branching (Morbiducci et al., 2016). The response to injury theory was beyond attractive pure scientific study topic. This is evidenced by proof that growth factors and injury-repair mechanisms result in inflammation and subsequently atherosclerosis.

The endothelial dysfunction phenomenon replaced this theory to a great extent and suggested a widely accepted and physiologically acceptable explanation for an oxidative stress response even in the absence of physical dysfunction of the endothelium (Boisvert et al., 2016; Swirski et al., 2007). The evolution of this concept revolutionized the current understanding of the atherosclerosis process. This theory suggests that the endothelial permeability and regeneration process may be as much responsible for the inflammatory changes as is loss of continuity of the endothelial layer.

Hypercholesterolaemia (e.g., oxidatively modified lipoproteins)
Diabetes, metabolic syndrome (e.g., advanced glycation end products, reactive oxygen species, adipocytes)
Hypertension
Sex hormonal imbalance (e.g., oestrogen deficiency, menopause)
Ageing (e.g., advanced glycation end products, cell senescence)
Pro-inflammatory cytokines (e.g., interleukin-1, tumour necrosis factor)
Infectious agents (e.g., bacterial endotoxins, viruses)
Haemodynamic forces (e.g., disturbed blood flow, turbulent flow)
Environmental toxins (e.g., cigarette smoke, air pollutants)

Table 1.1: Disease processes that promote atherosclerosis.

The chemotactic process initiated by platelet adhesion and secretion of platelet-derived growth factors stimulates blood cells to migrate to the endothelial site of dysfunction, leading to local inflammatory changes and eventually leading to the formation of a fibromuscular plaque (Ross et al., 1999). Statins are a group of medications used widely to reduce circulating cholesterol levels, usually associated with low-density lipoprotein (LDL) particles. Statins are also thought to have anti-inflammatory properties and anti-plaque development and progression (Antonopoulos et al., 2012). The pathways by which statins exhibit this anti-plaque function involves hepatocytes and endothelial cells. They reduce circulating levels of C-reactive protein (CRP), tumour necrosis factor (TNFα), interferon gamma (IFNγ) and interleukin 6 (IL-6) which are vital pro-inflammatory factors in

plaque formation and progression. Recent evidence suggests that high dose statins have better cardio-protective capability mainly due to their anti-inflammatory action. Kim et al. (2012) concluded that increasing statin dosage reduced pro-inflammatory factors in atherosclerosis and arterial disease. Loss of physiological capabilities of promoting vasodilatation, fibrinolysis and anti-adhesion are the markers of endothelial dysfunction rather than physical loss of the endothelial layer barrier.

1.2 Vascular disease

1.2.1 Spectrum of vascular disease

Many references and researchers use the term vascular disease interchangeably with cardiovascular disease which is not scientific and not accurate. The commonly described vascular disease refers to the chronic vaso-occlusive disease that is almost always caused by atherogenic occlusive plaques. Cardiovascular disease certainly gained more attention because of statistical abundance of the disease and the mortality related, being the highest disease- related cause of mortality worldwide. Cerebrovascular disease leading to disabling strokes and peripheral arterial disease causing significant morbidity and being the leading cause of lower limb amputation are manifestation of vascular occlusive disease. Peripheral arterial disease may be thought of as a visible marker of cardiovascular and cerebrovascular disease mainly because it usually presents with symptoms that patients and clinicians can easily appreciate whereas the latter two can be asymptomatic till a major incident take place.

The clinical manifestations of arterial occlusive disease occur when there is a mismatch between tissue demand and supply. The symptoms will depend on the organ affected and the degree and extent of ischaemia. For instance, extensive cardiac ischaemia will result in ST-segment elevation myocardial infarction (STEMI) which is a cardiological emergency with significant mortality that often necessitates urgent re-vascularization. Similarly, the acuteness of limb ischaemia and presence of collateral circulation

determine the options of revascularization for critical limb ischaemia and the time frame at which an intervention should be done. A surgical image representing stenotic arterial plaque is displayed in Figure 1.3.

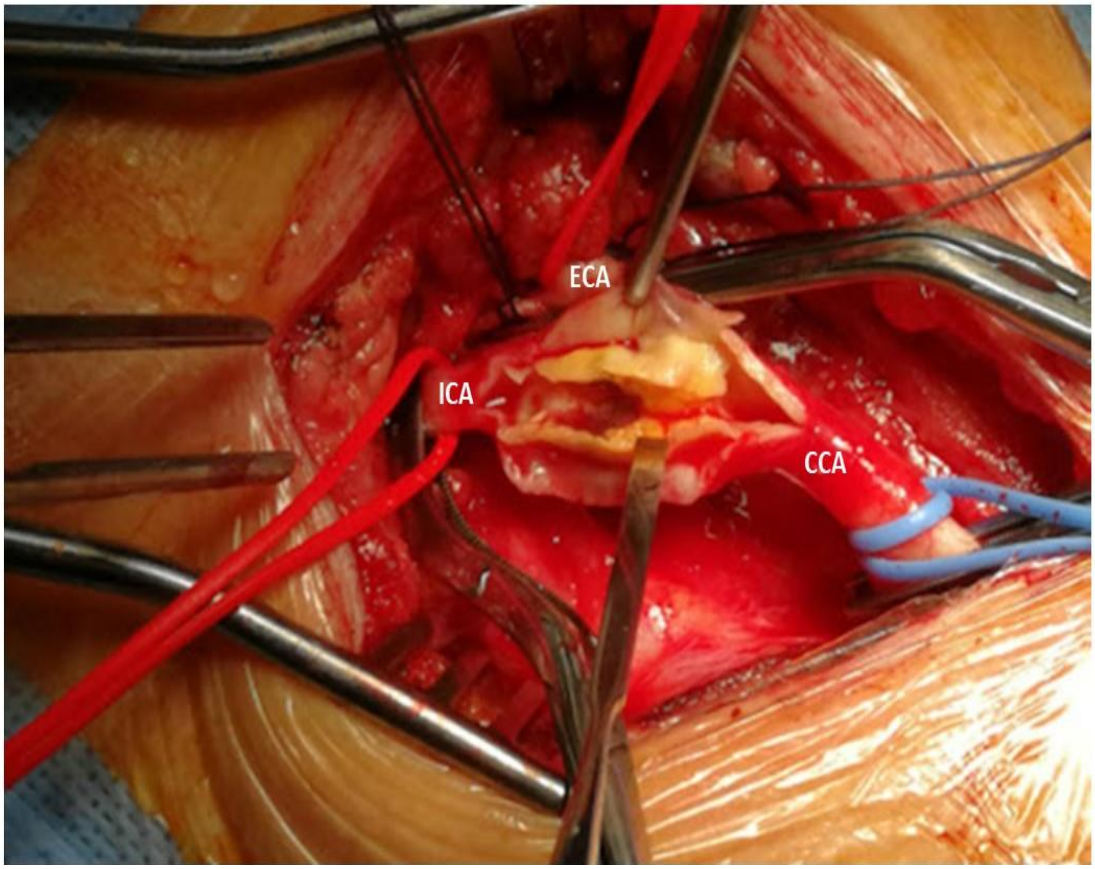

Figure 1.3: Carotid plaque removal by surgery. Surgical image during a carotid endarterectomy showing the atheromatous plaque (yellow, arrow) being dissected off the common and internal carotid arteries. Blue sling around common carotid artery (CCA) red slings around internal (ICA) and external(ECA) carotid arteries. [Patient's consent was recorded for the data collection A. Al-Aufi, operating surgeon, Leeds General Infirmary, Leeds, UK].

1.2.2 History of vascular disease

Although cardiovascular disease is widely thought of as a disease of the modern era, studies on ancient Egyptian mummies have shown definitive and probable atherosclerosis in 34% out of 137 mummies (Allam, et al., 2018). Whole body computed tomography (CT) examination of these mummies that have been preserved for over 4000 years from 4 different civilizations across the globe demonstrated that atherosclerosis is as ancient as these mummies. The probable reason why we are observing a rise in cardiovascular disease currently is likely due to more easy access to health facilities and diagnostic tests, beside of course the actual increase in incidence, which is attributable to lifestyle changes in the modern era.

The technology of CT scanning performed on those mummies enabled scientists to establish evidence of atherosclerotic disease without the need for surgical dissection. This, however, was not the case during earlier times. Greek anatomists, Herophilus and Erasistratus, performed the first dissections in Alexandria, Egypt. Later, Roman law prohibited dissection and autopsy of the human body and as autopsies were banned untill the 14th century, no further dissection was performed and hence no physical evidence of atherosclerosis was documented. Despite the return of autopsies thereafter the clinical correlation with findings of atherosclerosis during dissections was not made and hence no major scientific advances were achieved. The clinical description of angina pectoris that dates to around 3000 BC derived from links to anatomy and remains just descriptive symptoms of what is referred to as “threat of death”.

Similar reference to cardiac disease was made in Arabic literature referring to a famous poet, “Majnun Laila”, who is thought to have died of a myocardial infarct following a failed love story (Hajar et al., 2017). The description of his sad love experience was similar to the symptoms of an acute cardiac event. Scientists quote the poem below when referring to the death of “Majnun Laila” caused by what seems to be a heart attack.

“My heart is firmly seized

By a bird's claws.

My heart is tightly squeezed,

When Lila's name flows.

My body is tightly bound,

When the wide world I found

Is like a finger ring around”

1.2.3 Burden of vascular occlusive disease

There are two main types of pathophysiological blockages for vascular ischaemic events, embolic and occlusive. Embolic blockage is usually linked to cardiac arrhythmias or aneurysmal disease and when an embolus breaks off, it can travel and lodge into a distal blood vessel. The burden of the embolus and the affected organ will determine a patient’s presentation and ability to recover. An occlusive blockage usually refers to a chronic gradual process of arterial narrowing caused by an atheromatous plaque which can reach a stage of total occlusion. Symptoms are usually less acute than embolic events, particularly because there is time for collateral vasculature to develop. This, however, is not always the case and depending on the organ affected and whether collateralization has taken place or not, the affected organ may be at risk of irreversible ischaemia.

The focus of many statistical analyses with regards to the incidence, morbidity, mortality and cost of treatment of vascular disease refers mainly to cardiovascular disease which constitute the major bulk of vascular occlusive disease (Figure 1.4). The other two major constituents of vascular disease also contribute to the overall disease burden and account for considerable health consequences and expenditures. For instance, limb amputations are possible end results of peripheral arterial disease and they cause significant disability and consume human and financial resources. Combination of more than one system affected is also a common

manifestation of vascular disease and it is not infrequent to encounter patients suffering from concomitant heart and limb vascular disease, for example. This displays the spectrum of vascular disease and by linking the associated morbidity and disabilities with those conditions, one can assess the heft of these diseases on the health systems. Although their prevalence of these diseases may vary between countries or in different socioeconomic zones, it remains the most concerning health related issue globally (Roussouw et al., 1990).

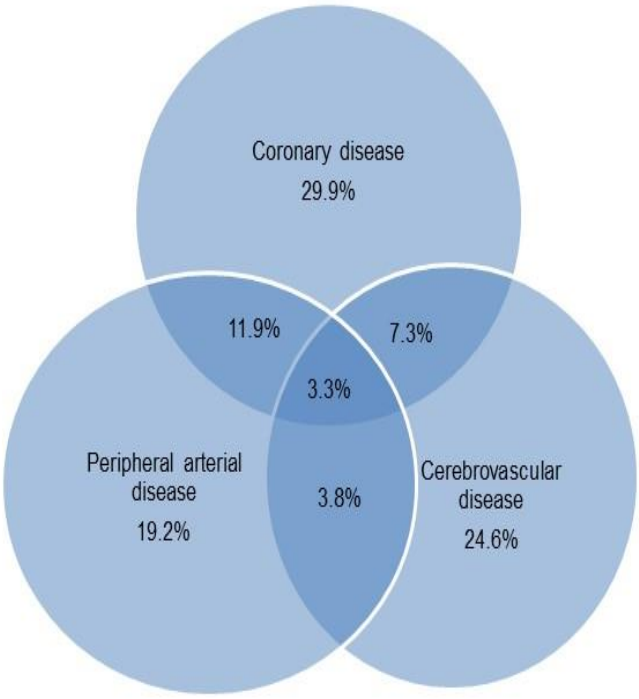

Figure 1.4: Vascular disease incidence and mortality. A Venn diagram representation of the risks of different vascular disease states and mortality.

1.3 Lipid lowering therapy

Evidence compiled over the last three decades strongly shows the association between increased total cholesterol, LDL and triglycerides and the mortality from cardiovascular events. In addition to this, lower levels of high-density lipoprotein (HDL) cholesterol are also linked to increased CVD events and death related to them (Roussouw et al., 1990). It is then sensible to hypothesize that lowering the levels of LDL, triglycerides and total cholesterol would reduce mortality in people who are at risk or who have existing CVD. This was proved extensively by many clinical trials. For instance (Gitsels et al., 2016) showed that the all-cause mortality is reduced in people taking statins at age >65 years compared to the placebo group. Given that 75% of the deaths in people with existing coronary disease occur as a result of cardiovascular events, it was essential to establish a secondary preventive strategy for CVD. Lipid lowering agents are an important pillar of this secondary prevention module which act in conjunction with antiplatelet therapy to reduce the risk of major adverse cardiovascular events (MACE) and major adverse limb threatening events (MALE) in people with cardiovascular disease. The target LDL levels postulated for this category of people varies based on their risk factor profiling. To exemplify, people with established atherosclerotic disease (EAD) who are either diabetic or have chronic kidney disease have an LDL target of <70 mg/dL as opposed to those with multiple risk factors (MRFs) without established atherosclerotic disease, who have a set LDL target level of<100 mg/dL (Krittayaphong et al., 2019).

Statins are the most commonly used lipid lowering agents worldwide; over 129 million people took some form of statins in 2018 and this number is thought to have grown significantly over the last few years (Blais et al., 2021). High dose statin is proposed to be as effective as a lipid lowering

therapy in people with dyslipidaemia; in addition to their low side effects gives more patient compliance (Sharma et al., 2009). The hepatic metabolism of most statins also allow their use with no need for renal adjustments in people with chronic kidney disease (Sharma et al., 2009). These characteristics as well as their easy production and low production cost contribute to their wide usage (Chong et al., 2001). Statins act predominantly on hepatocytes and exhibit their LDL-c lowering effect by competitively blocking the enzyme HMG-CoA reductase in the mevalonate pathway which is the rate limiting step in this pathway that is a precursor for cholesterol synthesis (Buhaescu et al., 2007).

Statins not only reduce total serum cholesterol, but also have a pleotropic effects on the vascular beds including improvement of the function of the endothelial cells, reducing the vascular inflammation and stabilizing atheromatous plaques (Liao et al., 2001).There is strong evidence of the reduction of mortality and incidence of cardiovascular events in high and moderate risk patients using statins compared to placebo. Studies with high degree of reliable evidence generated from double blinded randomized clinical trials including the 4S (Scandinavian Simvastatin Survival Study Group 1994), JUPITER (Ridker et al., 2008), PROVE IT-TIMI 22 (Cannon et al., 2004), WOSCOPS (Freeman et al., 2001), TNT (LaRosa et al., 2005) and IDEAL (Waters et al., 2011) trials. These studies demonstrated statin-based reduction in mortality and morbidity in high-risk patients and also compared different regimes of statin therapy as mono- or combination therapies.

Beside direct inhibition of the cholesterol production pathway, statins also exhibit an anti-inflammatory response which is an important feature especially during the initial period following a major cardiovascular or cerebrovascular accident. It is during this period that the plaque ruptures leaving a raw surface vulnerable to a blood clot or thrombus. This is the reason that most clinicians insist that a patient with a recent cardiovascular event should be promptly started on statins.

1.4 Lipid particles in disease

As early as 1913, the connection between cholesterol and the formation of atherogenic arterial plaques were postulated in studies on rabbits on a fat-rich diet (Anitschkow, 1913). Compilation of evidence at a later stage proved that raised serum LDL levels are linked to increased incidence of cardiovascular disease (Stamler et al., 1986; Castelli et al., 1986). Lipids and fats are essential parts of the mammalian diet, but these hydrophobic entities they are enclosed within lipid micelles and transported in circulatory fluids e.g. blood. Lipoprotein-, lipid- and fat-containing particles are formed in the liver and circulated to the rest of the tissues and where the excess constituents are transported back to the liver to be excreted by a process known as “reverse cholesterol transport” (Marques et al., 2018).

Lipid particles are complex substances consisting of a central hydrophobic core of non-polar lipids, primarily cholesterol esters and triglycerides, which is surrounded by a hydrophilic membrane consisting of phospholipids, free cholesterol, and apolipoproteins (Figure 1.5). Lipid particles can be subdivided into 7 classes based on their molecular weight, lipid composition and apolipoproteins (Figure 1.6). Of the seven classes of lipid particles, LDL is widely considered to be the most pro-atherogenic owing to the following properties. LDL particles can display a reduced affinity to the LDL receptor (LDLR) and are therefore retained in the circulation for longer. LDL particles enter the arterial wall more easily compared with larger lipid particles. LDL particles contain the 500 kDa apolipoprotein-B100 (Apo-B100), which binds avidly to intra-arterial proteoglycans leading to trapping within the arterial wall. LDL particles are more susceptible to oxidative modification, with oxLDL being rapidly taken up by macrophages. Apo-B100 is the major structural component of very low-density lipoprotein (VLDL), intermediate-density lipoprotein (IDL) and LDL particles. There is a single molecule of apo-B100 per VLDL, IDL or LDL particle. Ionic bonds between positively charged intra-arterial proteoglycans and negatively charged Apo-B100 lead to the retention of LDL within the arterial wall.

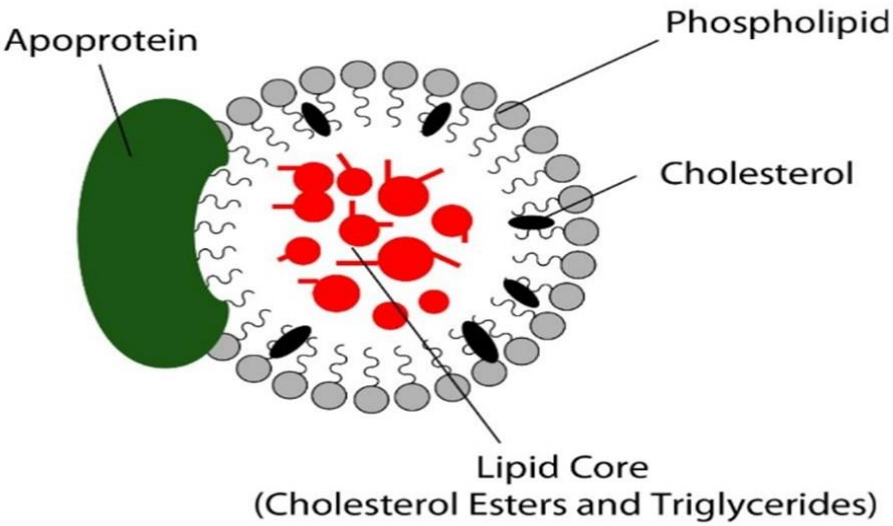

Figure 1.5: Schematic diagram showing the molecular composition of a lipoprotein particle. The difference between the various subtypes of lipoproteins is the percentage of the different concentrations of these components. Created using Biorender.com.

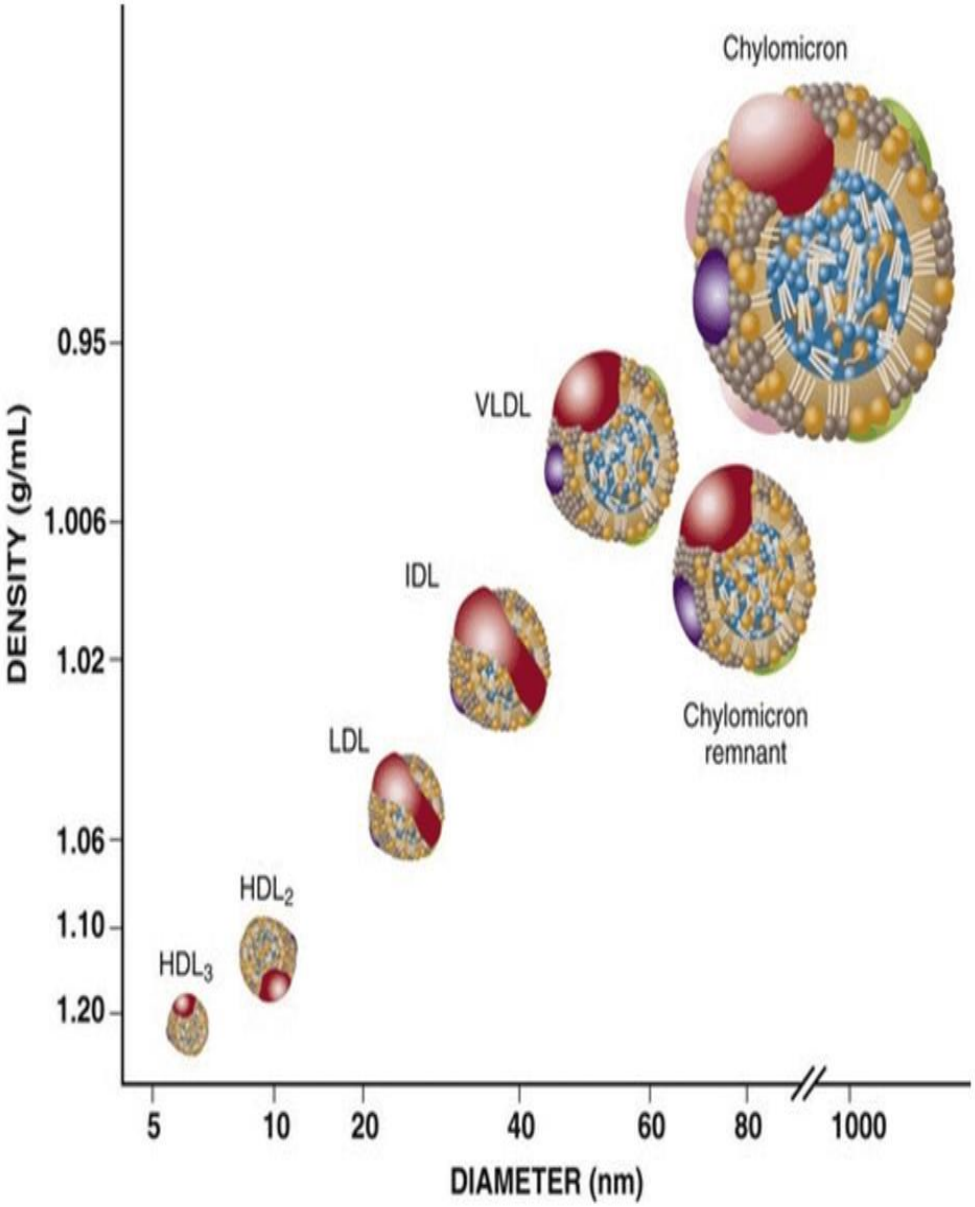

Figure 1.6: Lipoprotein particle heterogeneity and properties. The specific density (g/mL) vs. average diameter of each class of known lipid particles. Created using Biorender.com.

1.5 Scavenger receptors

1.5.1 Scavenger receptor family

The family of scavenger receptors (SRs) include ten classes of transmembrane protein receptors that are involved in a wide range of functions including binding, transmembrane transportation and elimination of multiple ligands such as microbes, apoptotic cells and denatured proteins (Canton et al., 2013) (Figure 1.7). More recently, a member of the SR family, the HDL scavenger receptor B type 1, was shown to facilitate the entry of severe acute respiratory syndrome coronavirus 2 (SARS-CoV-2) that was responsible for the Coronavirus-19 pandemic, into host cells via an angiotensin-converting enzyme 2 receptor (ACE2) –dependent mechanism (Wei et al., 2020). The crossover of ligand and antigen recognition of these subclasses of SR is linked to redundancy in the immune system allowing multiple receptor binding to the same antigen. For instance, modified LDL can bind to six of these subclasses, although this binding is at different levels of strength and possibly to different binding sites on the protein receptors (Moore et al., 2006).

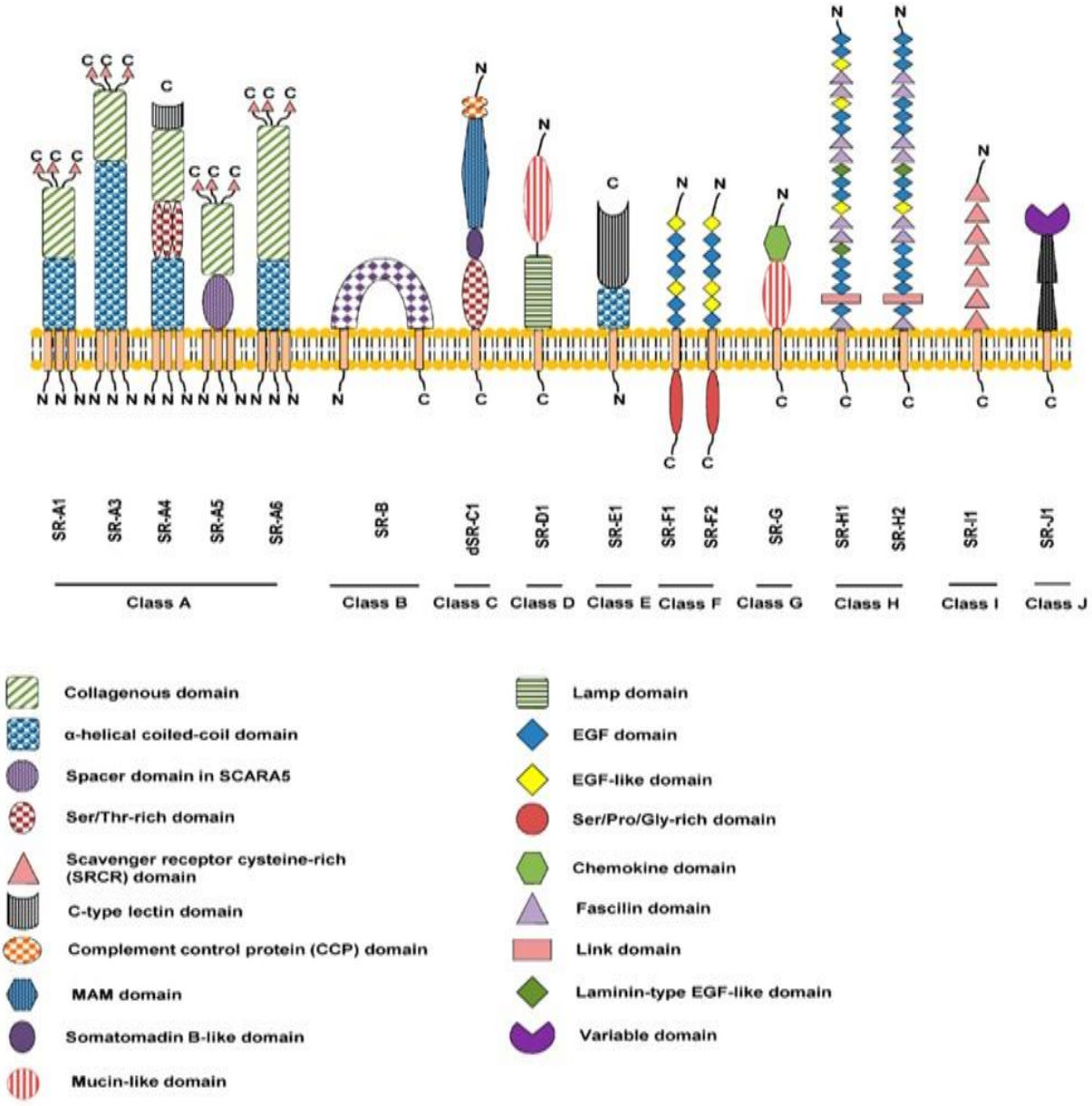

Figure 1.7: Schematic representation of the scavenger receptor supergroup. Structural similarities and differences of the ten classes of SRs. Class A and E proteins have specific affinity for oxLDL. Adapted from Abdul Zani et al 2015.

Scavenger receptors class A consist of three groups that have exclusive affinity to ox-LDL. These receptors consist of an extracellular C-terminus, a cytoplasmic N-terminus and a single pass transmembrane segment (Kodama et al., 1990). They are subdivided into 5 groups and these are expressed in different cell types. Amongst these groups is scavenger receptor with C-type Lectin (SRCL) which is expressed on endothelial cells and has high affinity to ox-LDL (Levitan et al., 2010). The lectin-like ox-LDL receptor 1 (LOX-1, OLR1) is the single member of class E-SR and is predominantly found on endothelial cells and is one of the most studied SR as it is linked to development of atherosclerosis. This is discussed in depth in the following section.

1.5.2 Lectin-like low Density lipoprotein receptor-1 (LOX-1)

1.5.2.1 LOX-1 receptor structure

Human LOX-1 (OLR1) is a membrane receptor and a type II membrane glycoprotein that is made of 273 amino acids, with an apparent molecular weight of ~45-50 kDa due to N-glycosylation. The C-type lectin-like domain (CTLD) makes up most of the bulk of the glycoprotein (130 residues) and contains an important hydrophobic channel, a neck domain, a transmembrane domain and a 34-residue cytoplasmic domain (Figure 1.8). The hydrophobic tunnel is enclosed in a quasi-conical mixed hydrophilic and hydrophobic structure. Mutations in this structure have beeng linked to impairment of binding capability of LOX-1 receptor to specific ligands (Biocca et al., 2009). LOX-1 is found on macrophages, platelets, endothelial and vascular smooth muscle cells (Chen et al., 2001; Yoshida et al., 1998).

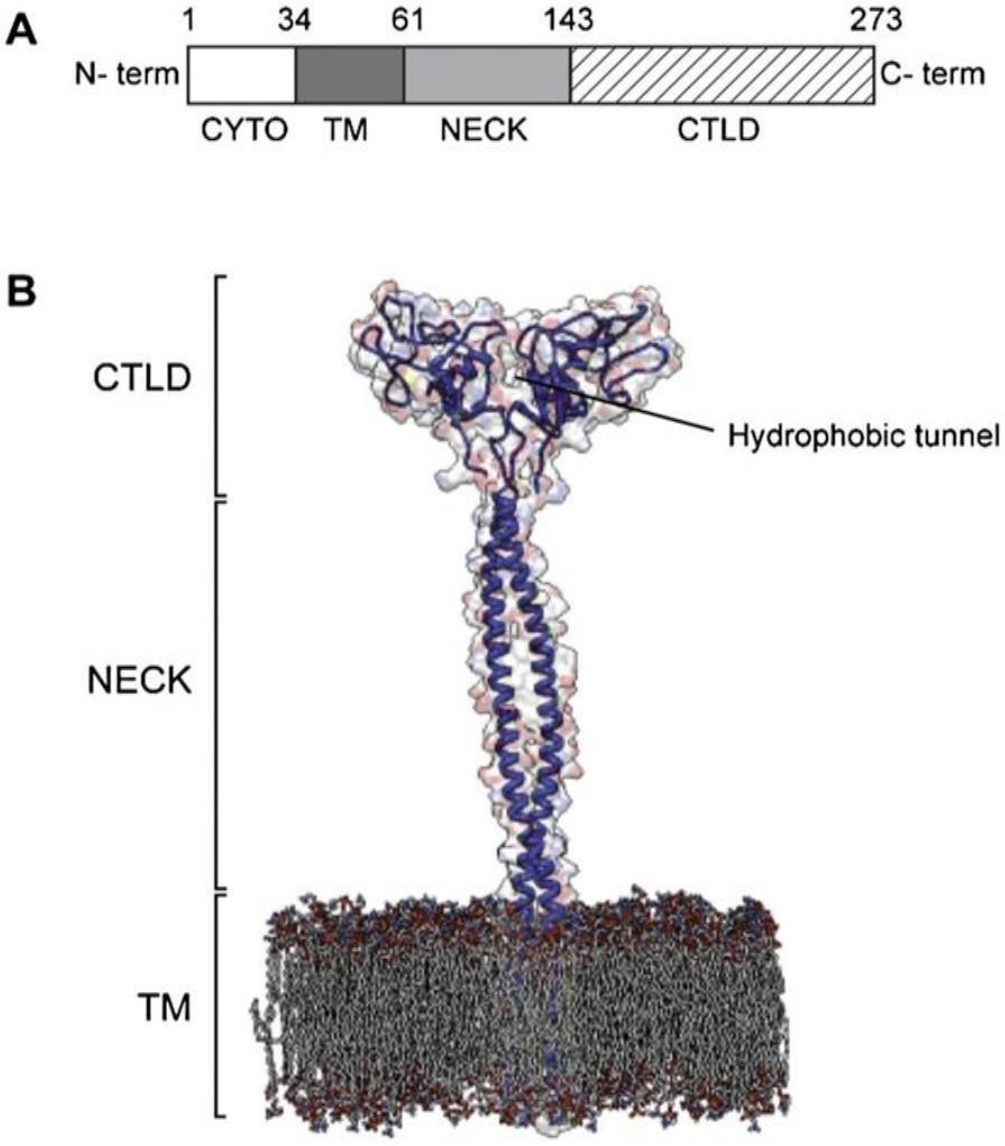

Figure 1.8: LOX-1 domain structure. (A) Schematic representation of the LOX-1 membrane protein. (B) Model of the different aspects of the LOX-1 membrane protein excluding the cytoplasmic domain. Abbreviations: CTLD, C-type lectinlike domain; Neck, helical stalk or neck domain; TM, transmembrane domain. Adapted from Kore et al.,2022.

The LOX-1 (OLR1) gene is located on the short arm of human chromosome 12 called and is within the loci encoding innate immunity receptors. In contrast to other scavenger receptors, LOX-1 has a structure and sequence similar to a class of immune receptors found on natural killer (NK) cells (Yamanaka et al., 1998; Aoyama et al., 1999). The OLR1 gene is made of 7000 base pairs in the form of 6 exons and 5 introns. Single nucleotide polymorphic mutations in these segmental coding bases were shown to have a wide array of consequences with variable importance (Sentinelli et al., 2006; Palmieri et al., 2013; Biocca et al., 2009). Whilst some of these polymorphic forms are of uncertain significance, a deletion of exon 5 resulting in loss of a segment of the CTLD domain is proven to have an anti-atherogenic effect (Mango et al., 2011).

In normal homeostatic state, LOX-1 receptors are expressed in low concentrations and contribute to the innate immunity versatility. They dispose of circulating apoptotic cells and cellular debris. Certain pathological conditions including atherosclerosis, carcinogenesis, obesity, cellular transformation and inflammatory response trigger induction of LOX-1 receptors expression (Binder et al., 2016). Activated LOX-1 receptors triggers an oxidative stress response leading to destabilization of atheromatous plaques and consequently plaque rupture leading to atheroembolization that results in the clinical cardiovascular, cerebrovascular and peripheral arterial disease presentations associated with atherosclerosis (Boullier et al., 2000). Animal experimental work on ORL1 knockout mice showed that the resultant atherosclerotic lesions were considerably limited and less dense compared to the ORL1 expressing mice. These mice also were protected from periaortitis (inflammation of the aorta and the periaortic tissues) and developed a reduced response to ischaemia and reperfusion injury (Mehta et al., 2002). Additionally, induction of LOX-1 expression and the higher concentrations of ox-LDL were linked to cell dysfunction, inflammation and injury in the same animal module.

1.5.2.2 LOX-1- signalling pathway

The activation of LOX-1 receptors by bondage of oxLDL and other ligands activates a sequence of interconnecting cellular signalling pathways that result in foam cell formation, proliferation of vascular smooth muscle cells, platelet activation, generation of reactive oxygen species (ROS), and collagen degradation which are the key steps in atherogenesis (Xu et al., 2013); (Pothineni et al., 2017). The specific signal activation and transduction is shown in Figure 1.9 below. The imbalanced state of oxidative stress caused mainly by reduction of nitric oxide (NO) and increased production of ROS leads to endothelial cell dysfunction which is the rate limiting step in atherogenesis (Ogura et al., 2009); (Kataoka et al., 2001).

1.5.2.3 LOX-1 receptors and disease process

LOX-1 receptors have been studied in a spectrum of pathological processes. Examples of these pathologies are given below. Figure 1.9 gives a summary of disease processes that are linked to LOX-1 receptors.

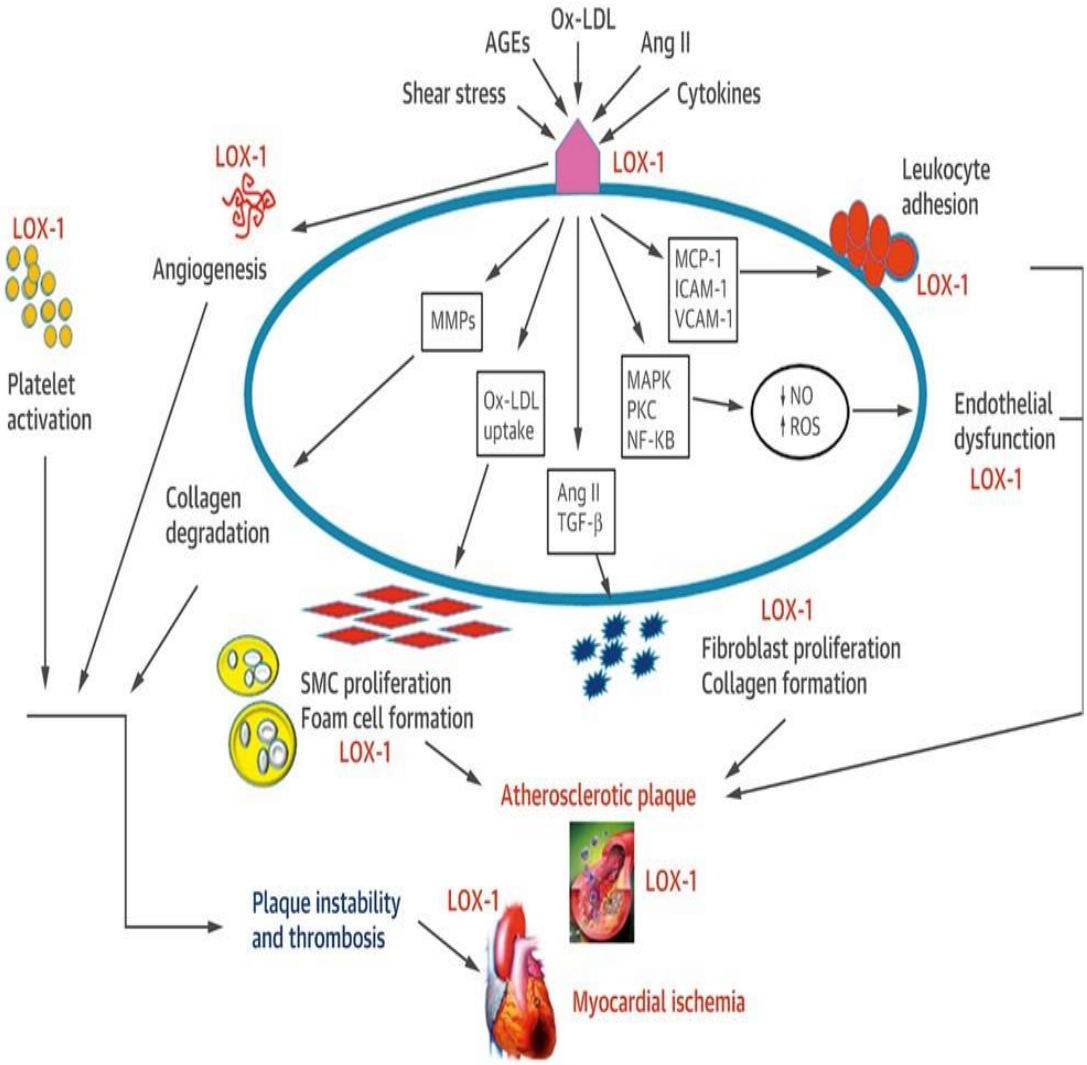

Figure 1.9: LOX-1-mediated signalling in physiology and pathology. Schematic representation of role of LOX-1 in different signalling processes impacting on cell and tissue responses. Abbreviations**:** ↑, increased; ↓, decreased; AGE, advanced glycation end product; Ang II, angiotensin II; ICAM-1, intercellular adhesion molecule-1; MAPK, mitogen-activated protein kinase; MCP, monocyte chemoattractant protein; MMP, matrix metalloproteinase; NF-κB, nuclear factor–kappa B; NO, nitric oxide; PKC, protein kinase C; TGF, transforming growth factor; VCAM-1, vascular cell adhesion molecule-1. Adapted from Pothineni et al. (2017).

1.5.2.3.1 Endothelial dysfunction

Endothelial dysfunction is characterized by reduction of endothelium-dependent relaxation, endothelial cell apoptosis and increased monocyte adhesion to endothelial cells, (Xu et al., 2013). As shown in Figure 1.9, activation of LOX-1 receptors leads to reduction of NO production which is an important stimulus for smooth muscle relaxation. Reduced levels of NO expectedly lead to lack of arteriolar dilatation of vascular beds resulting in myocardial infarction and cerebrovascular events (Shi et al., 2011). Evidence from experiments on atherosclerosis-prone apolipoprotein E (APO-E) deficient mice which had existing atherosclerotic lesions and were treated with Anti-LOX-1 antibodies demonstrated that the balance of NO-mediated coronary dilation was restored. The same antibody treatment showed no effect in wild-type mice (Xu et al., 2007).

As formerly mentioned, recruitment of inflammatory cells is crucial in atherogenesis. Recruitment of inflammatory cells to the endothelium is crucial in the, the development of atherosclerosis. Incubated human endothelial cells extracted from coronary arteries in an ox-LDL-rich media showed increased monocyte chemoattractant protein-1 (MCP-1) production as well as monocyte adhesion to HCAEC (Li and Mehta, 2000). Human LOX-1 antisense RNA seems to inhibit this response which supports the key role of LOX-1-mediated monocyte adhesion in atherogenesis.

1.5.2.3.2 Vascular smooth muscle cells migration and proliferation

Vascular smooth muscle cells (VSMC) migration and proliferation is one of the defining characteristics of atherosclerosis. Overexpression of LOX-1 receptors due to ox-LDL bindings activates NF-κB- and JNK-signalling which consequently leads to VSMC growth and proliferation. This pathway was inhibited by using LOX-1 antisense mRNA in vitro (Xu et al., 2013). This was also supported by the work of Hinagata and co-workers who gave anti-LOX-1 antibody to rats after inducing an intimal injury with an angioplasty balloon. The treated rats demonstrated suppression of oxidative stress, VSMC proliferation and leucocyte infiltrates (Hinagata et al., 2006).

1.5.2.3.3 Macrophage foam cell formation

At early stages of atherosclerosis it is known that the internalization and processing of ox-LDL by macrophages forming foam cells contributes to the atherogenic process. In his work, Popovic and co-workers examined the effect of incubating human macrophage cells with inflammatory mediators, Interleukin-4 (IL-4) and interferon Gamma (IFNγ), and compared them to untreated macrophages. The induced macrophages formed more foam cells and also showed increased expression of LOX-1 receptors which support that foam cell formation is a LOX-1 mediated pathway (Popovic et al., 2017).

1.5.2.3.4 Platelet activation and thrombosis

Platelets express LOX-1 receptors and hence have the capability to internalize ox-LDL. This leads to suppression of nitric oxide synthase and platelets aggregation (Chen, Mehta and Mehta, 1996). Platelets retrieved from atherosclerotic plaques in post mortem examination of patients suffering from angina showed increased expression of LOX-1 receptors (Chen et al., 2001). Animal studies where anti-LOX-1 antibodies were used to block LOX-1 receptors showed reduction in the formation of an arterial thrombus and reduced platelets count in the atherosclerotic plaques (Kakutani et al., 2000). Additionally, platelet activation varied significantly when polymorphic LOX-1 platelets were exposed to ox-LDL (Puccetti et al., 2007).

1.5.2.3.5 Hypertension

The renin-angiotensin system (RAS) is an important determinate of blood pressure homeostasis so imbalance in this system leads to hypertension. Data suggest that RAS is activated by increasing levels of circulating oxLDL (Chen and Mehta, 2006). Increased levels of ox-LDL also induce LOX-1 receptor expression, not only by direct signalling, but also by means of stimulating RAS which triggers LOX-1 receptors as shown in Figure 1.7 (Pothineni et al., 2017). Angiotensin receptor (ATR) blockers were used by

Nagase and colleagues on an APO-E null mice fed on a cholesterol-rich diet and these mice showed reduced extent and burden of atherosclerosis (Nagase et al., 1997). Furthermore, the same group investigated the expression of LOX-1 receptors on aortic samples from hypertensive mice and those receptors were found to be overexpressed compared to healthy mice, which proves the linkage of hypertension to LOX-1 expression (Nagase et al., 1997).

1.6 Antibodies and alternative synthetic protein technology

1.6.1 Introduction

Antibodies are proteins that occur naturally to bind antigens (non-self) molecules or pathogens as a means of immune recognition and defense. Antigen targeting using antibodies with predefined specificity is a technology that was first introduced in 1970s (Köhler and Milstein, 1975). Since then this technology gained much attention and is used in biomedical research for diagnostics, disease treatment and different applications. The approach to produce clonal antibodies has been exploited to produce large quantities of a specific antibody directed to a specific ligand. In the past 40-50 years, antibody production techniques have improved tremendously. For instance, bacteriophage display systems can be used to screen and identify clonal antibodies to target pathological antigens (Clementi et al., 2012). The concept of polyclonal and monoclonal antibodies was also an area of development in the past few decades. Polyclonal antibodies are derived from multiple cells and tissues and have wide binding properties, whereas monoclonal antibodies are clonal, derived from a single cell line and bind to a single epitope or defined antigen.

1.6.2 Applications and limitations of antibodies

Monoclonal antibodies are a fundamental tool in immunoblotting (Magi and Liberatori, 2005), immunoprecipitation (Kaboord and Perr, 2008) and immunohistochemistry (Stack et al., 2014) amongst other uses. These

abilities of antibodies give them the advantage of being used to analyse animal and human blood and other fluids by tests like enzyme-linked immunoassay (ELISA) (Lequin, 2005) and immunosensors (Luppa et al., 2001). The specificity and sensitivity of antibodies binding to cell surface proteins is a feature with important applied medical usage. For instance rheumatoid arthritis (RA) is treated with monoclonal antibodies that target ligands on certain inflammatory cells and disrupt their function, which controls the patient's symptoms and the disease progression (Bossaller and Rothe, 2013). Similar uses exist for inflammatory bowel disease (Shah and Mayer, 2010), neoplasms (Scott et al., 2012) and hypercholesterolaemia (Sabatine et al., 2017). Antibodies have also been used to enhance drug delivery systems in certain diseases to improve the tissue concentration and bioavailability of the medication in that specific tissue which reduces the systemic side effects of the medication (Firer and Gellerman, 2012). Different ways of utilizing antibodies in target detection are shown in Figure 1.10.

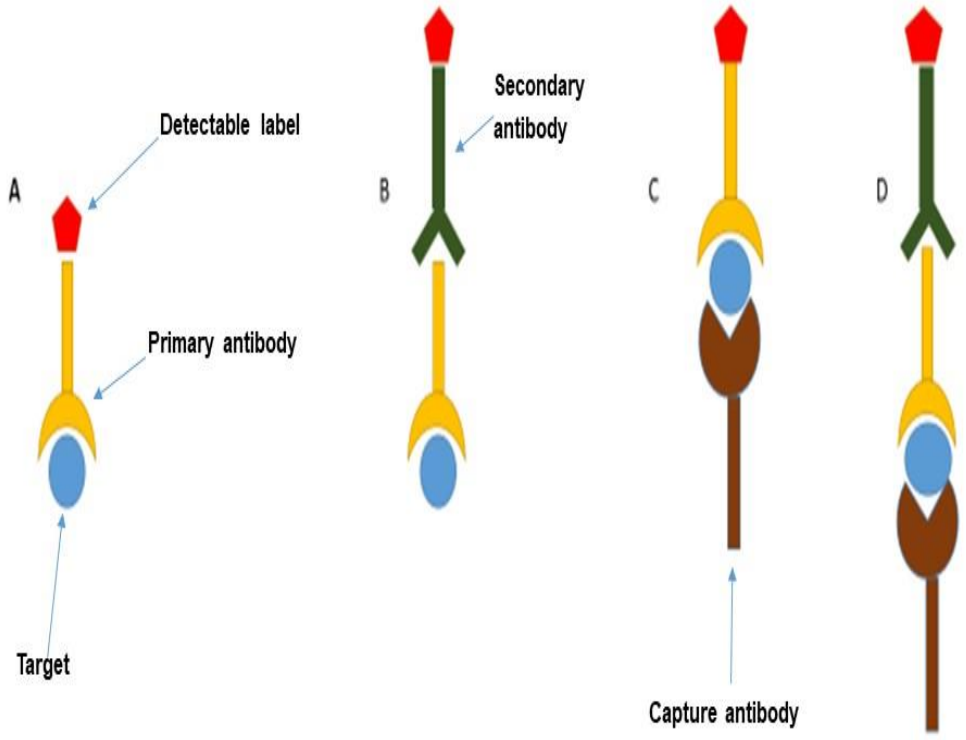

Figure 1.10: Different methods of immunoassay. (A) Direct immunoassay, (B) indirect immunoassay, (C) sandwich immunoassay, and (D) indirect sandwich immunoassay. Created using Biorender.com.

Despite their versatile abilities and usefulness, antibodies have some technical limitations. Polyclonal antibodies, for instance, have a wide batch variability which renders them less useful and as there is a long process of trial and error to get the desired antibody at the desired concentration, this requires time and money and hence limits their commercial use (Bradbury and Pluckthun, 2015). Isolation of monoclonal antibodies resolves the issue

of batch variability; however, it still doesn't address the matter of cost. Furthermore it, still requires animal hosts for production and it is technically demanding and this consequently prolongs the production time. Monoclonal antibodies are generally favoured in therapeutic application because as they are raised from a single clone and should interact with a single target epitope, their effects should be consistent and predictable. The cost is the most limiting factor for the wide spread use of monoclonal antibodies in clinical circumstances. Alemtuzumab, for example, is a monoclonal antibody used in the treatment of leukaemia which costs £37,000 per year per patient (Shaughnessy, 2012). Another issue with antibodies is their relatively large size (150 kDa) which limits their permeability to certain tissue in the body.

Alternative technologies are under development to overcome the shortcomings of antibodies. Fragment antigen bindings (Fab) and single-chain variable fragments (scFv) are examples of these particles. As they lack the constant fragment (Fc) region, their size is considerably smaller and hence offers more versatility compared to the original antibody they are derived from (Bird et al., 1988; Xenaki et al., 2017) (Figure 1.11). Moreover they also can be expressed in bacterial cells for mass production and this helps reduce the cost. Despite these characteristics these particles also have limitations. For instance, they are grown in bacteria which lack the capability to form disulphide bonds and the exposed hydrophobic residues, thus rendering these fragments unstable (Helma et al., 2015). This challenge could to some extent be resolved by using strains of engineered Escherichia coli (E.coli) bacteria (Bertelsen et al., 2021). These fragments are also prone to protein aggregation which can cover their binding surface and disable their function especially when expressed as intrabodies (intracellular expression) (Ewert et al., 2004). The need for alternatives to antibodies and antibody fragments, to express the benefits and limit the pitfalls (Helma et al., 2015)), has given rise to antibody mimetics, non-antibody scaffolds or nanobodies (Helma et al., 2015).

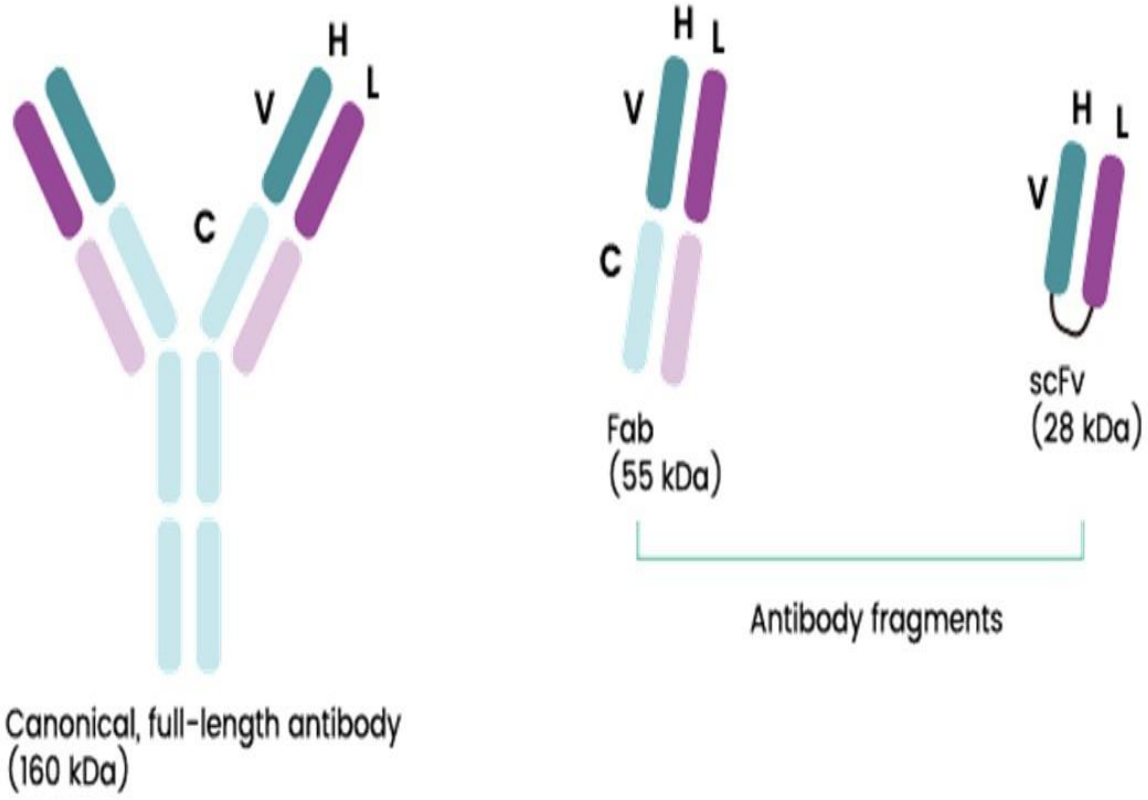

Figure 1.11: Antibody structure and variations. Basic structure and sizes of antibodies, antibody fragments and single chain variable fragments. Adapted from www.SinoBiological.com.

1.6.3 Antibody alternatives

Antibody alternatives are synthetic scaffolds that carry the ability to bind specific ligands, as do classical antibodies, and simultaneously overcome some of the shortcomings of antibodies. They are smaller in size with simpler structure and relatively easier and cheaper to produce (Sternke et al., 2019). The use of these scaffolds have being described and experimented for medical uses including toxin neutralisation (Jenkins et al., 2019). Figure 1.12 shows examples of these scaffolds and some of them are discussed in more depth in the next section.

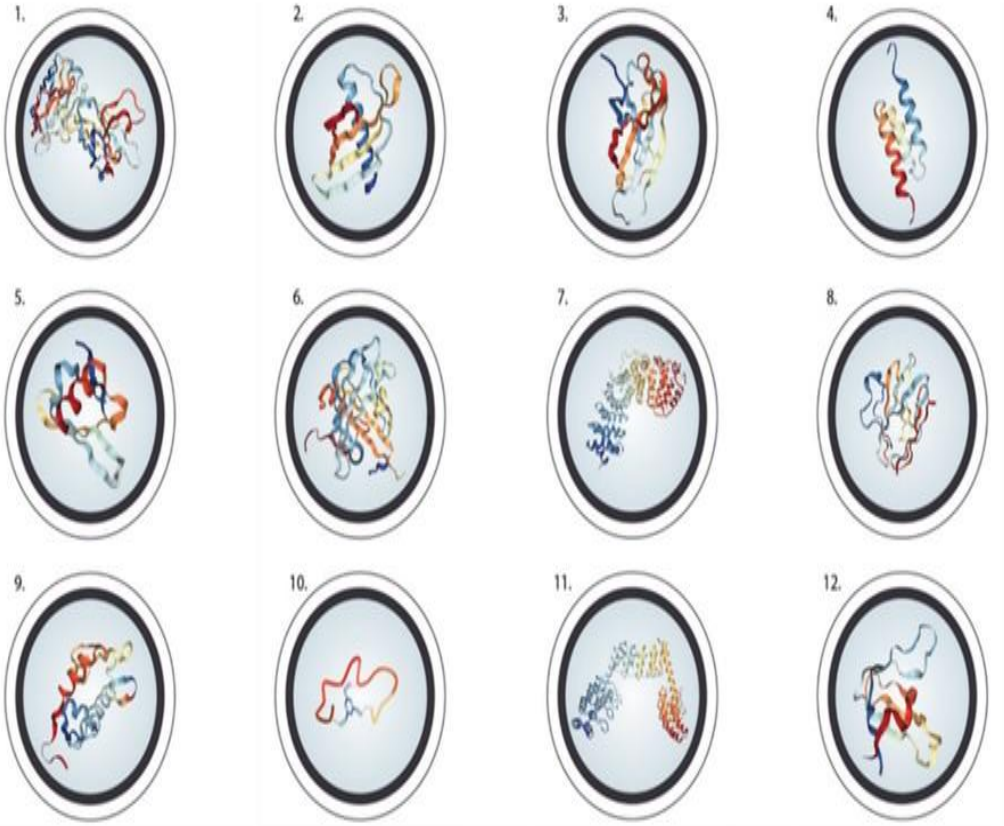

Scaffold	Parental Protein	Structure	Randomization	MW (kDa)	T_m	Ct Phase	YoD
1. Nanobodies	Camelid Antibody	β-sheets, seperated by loop regions	Loop randomization	12-15 kDa	Up to 86 °C	Phase II (completed)	1989
2. Affimers	Phytocystatin	β-sheet core & α-helical center	Loop randomization	~11 kDa	Up to 101 °C	NA	2014
3. Adnectins	Fibronectin (type III)	β-sheet	Loop randomization Beta-strand randomization	~10 kDa	Up to 84 °C	Phase II (completed)	1998
4. Affibodies	Z-domain (protein A)	α-helical	Helix-randomization	~6 kDa	Up to 75 °C	Phase I (completed)	1997
5. Affitins	Sac7d	β-sheet	Surface and loop randomization	~7 kDa	Up to 87 °C	Phase I (completed)	2007
6. Anticalins	Lipocalin	β-sheet & α-helical terminus	Loop randomization Beta-strand randomization	~20 kDa	Up to 79 °C	Phase I (completed)	1999
7. Armadillo repeat proteins	Armadillo repeat domains	Right-handed super helix	Helix randomization	~4.6 kDa	Up to 70 °C	NA	1980
8. Avimers	A-domain	Ca^{2+} binding & Disulfide constrained	Loop randomization	~4 kDa	Up to 80 °C	Phase I	2005
9. Beta-hairpin mimetics	HDM2	β-hairpin motif	Loop randomization	~1.7 kDa	NA	Phase III (in progress)	2004
10. Bicyclic peptides	Peptide	Chemically constrained	Loop randomization	1.5-2 kDa	NA	Phase I (recruiting)	1978
11. DARPins	Ankyrin repeats	α-helical β-turn	Helix-randomization Beta-turn randomization	14-18 kDa	Up to 90 °C	Phase III (completed)	2003
12. Fynomers	SH3 domain (fyn kinase)	β-sheet	Loop randomization	~7 kDa	Up to 70°C	Phase II (terminated)	1989

Figure 1.12: Antibody alternatives and their characteristics. Adapted from Jenkins et al. (2019). Abbreviations: MW, Molecular weight,; Tm, Denaturation temperature; Ct, Current Phase; YoD, Year of Development.

1.6.3.1 Nanobodies (Nbs)

These nanobodies (Nbs) are IgG-based particles are composed of 110-136 amino acids and consist of a single heavy-chain region and a variable domain (VH) which includes the antigen binding site (Conrath et al., 2005). They are much more thermostable then classical antibodies and have a small molecular weight that varies between twelve and fifteen kDa which gives them the ability of higher deep tissue penetration (Dolk et al., 2005). The complementarity determining region 3 (CDR3) loop is the binding site on the variable domain and this loops is extended on Nbs which combined with their small size allows them to bind and neutralize hidden epitopes that regular antibody cannot bind to (Manglik et al., 2017).
Nbs have a short half-life (1-6 h) secondary to their different pharmacokinetic behaviour and this characteristic is considered a “double-edged sword” ,where in situations where rapid clearance is needed it is an advantage, whilst if longer tissue availability is key in treatment then multiple dosing will be required (Van Audenhove et a.l, 2016). Trials to improve the Nbs half-life by glycation using polyethylene glycol (PEG) has some success; however, it resulted in reduction of Nbs-PEG tissue penetration due to increased size (Holt et al., 2003).

1.6.3.2 Adnectins

Adnectins or monobodies are structurally based on the type III domain of the adhesive glycoprotein, fibronectin (Lipovšek et al., 2011). Fibronectin is abundant in human blood and extracellular matrix and is easily extractable thus adnectins are relatively easy to synthesize and they bear resemblance to the variable domains of antibodies (Ramamurthy et al., 2012). These factors, in addition to their compact size of ≤12 kDa, led to the interest in these particles as antibody alternatives (Ramamurthy et al., 2012). They are made up of seven β-strands joined by six loops arranged in a double antiparallel β-sheet fold (Lipovšek et al., 2011). Disulphide bones and free cysteine residues contribute to their thermostability, as these bonds require a temperature of 84°C to breakdown in addition to a reducing condition and this makes them suitable to be produced in bacterial cells (Plaxco et al., 1997). They can reach high volumes of distribution and rapid penetration of tissues due to their small size and soluble nature, although this eventually

leads to rapid clearance by the kidneys (Mitchell et al., 2014). Oncological studies at phase II of trials are taking place to investigate the potentials of adnectins, but some studies suggest that their use in other fields is controversial (Vazquez-Lombardi et al., 2015; Koutsoumpeli et al., 2017).

1.6.3.3 Designed ankyrin repeat proteins (DARPins)

As the name suggests, these synthetic protein scaffolds are based on ankyrin repeats (AR) which are protein-protein interaction domains found in many species (Bork, 1993). DARPins consist of two or three internal AR domains joined by a six-residue β-turn which is the binding site for potential protein targets (Binz et al., 2003). The β-turn can be modified to adapt to a wide range of targets by altering the sequence of the amino acids (Plückthun et al., 2015).

DARPins are easily expressed in *E.coli* and have a molecular mass of 15-18 kDa (Binz et al., 2017). Owing to their high thermostability and adaptive pharmacokinetics, they can be used intravenously, topically, nasally, orally or by inhalation (Stumpp et al., 2008). Clinical Phase II trials have assessed the use of DARPins in oncological treatment as a tissue-specific delivery system. This is thought to reduce hepatotoxicity from some chemotherapeutic agents (Münch et al., 2013). They also exhibit the capability to bind to and neutralize protein targets useful in toxicology work (Rodon et al., 2015).

1.6.3.4 β-Hairpin mimetics

These consist of two antiparallel β-strands connected by a loop with an exceptionally small size (approximately 1.7 kDa) which allows good tissue penetration and distribution (Fasan et al., 2004). Their ability to activate the p53 tumour suppressor protein led to investigations for their use in early cancer management and therapy (Fasan et al., 2006).

1.6.3.5 Anticalins

Anticalins are derivatives of lipocalins that consist of 150-180 synthetic residues and have an extremely high affinity to certain protein targets that are involved in tumour growth and inflammation (Rothe et al., 2018). Fifteen naturally occurring anticalin isotopes have been isolated from human plasma which are thought to play an important role in the inflammatory response and carcinogenesis (Rothe et al., 2018).

1.6.3.6 Affimers

First described by Tomlinson, McPherson and colleagues, these plant phytocystatin synthetic scaffolds gained global interest due to their desirable characteristics (Tiede et al., 2014). For instance, they are extremely thermostable and degradation occurs beyond water boiling point (Tiede et al., 2017). The core structure is an α-helix reinforced by four antiparallel ß-strands forming a β-sheet with two variable regions that act as potential binding sites for targets (Figure 1.11). A bacteriophage-based Affimer library can be screened against a specific target with up to $1.3x10^{10}$ independent Affimer clones within the library (Tiede et al., 2014). The targets can include proteins, DNA, lipids or small molecules. Affimers have been isolated to different antigens such as tubulin, vascular endothelial growth factor receptor 2 (VEGFR2), ion channel TRPV2 and cancer antigen tenascin C (Tiede et al., 2017). Discussions on Affimers will follow in the later chapters.

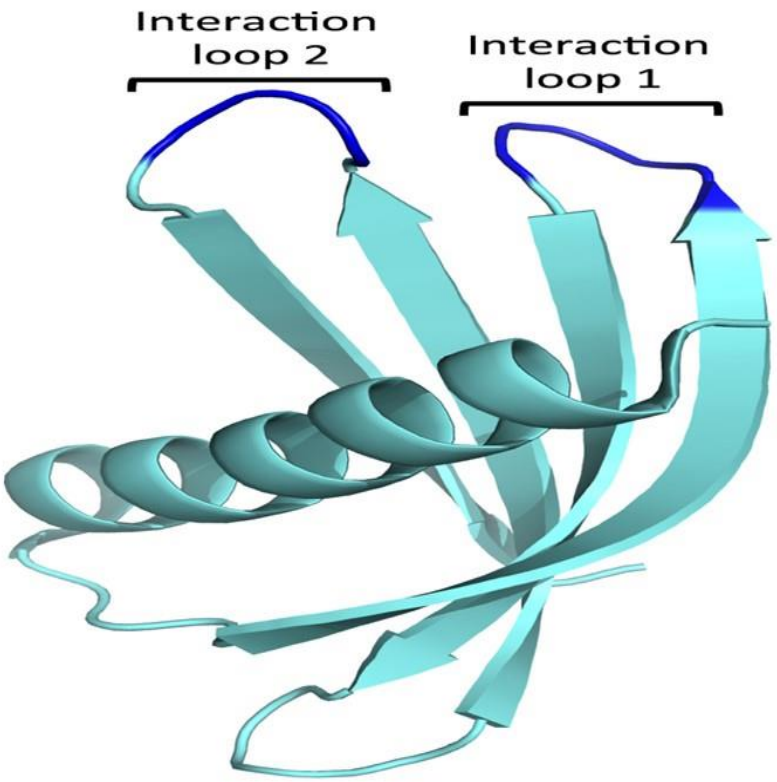

Figure 1.11: Affimer structure. The core Affimer scaffold (80 residues) is composed of a single α-helix supported by a β-sheet made of four anti-parallel β-strands. Two flexible variable loops (interaction loops 1 and 2) contain 9 residues each and their sequence is randomized in a bacteriophage library. Affimers with variable loops confer specific target antigen which could be identified and isolated using phage display. Created using Biorender.com

1.7 Summary and hypothesis

In this work we detail the experiments that seek better understanding of the LOX-1 protein in the uptake of oxLDL by endothelial and vascular cells using a novel class of synthetic protein scaffold called Affimers. Five different anti-LOX-1 Affimers were isolated human LOX-1 as a target antigen. To better evaluate the properties of Affimers on LOX-1 recognition, we developed assays to assess Affimer-based recognition of LOX-1-mediated oxLDL recognition and uptake. We hypothesise that Affimers are as a better antibodies-alternative in detecting LOX-1 receptors and blocking the uptake of ox-LDL by endothelial cells. Our findings provide the basis for development of synthetic scaffold proteins (Affimers) to LOX-1 as a new route for diagnostics and therapeutics.

Chapter 2
Materials and methodology

2.1. Materials

2.1.1 Chemicals and reagents

All chemicals and reagents are sourced from Sigma-Aldrich (Poole, UK), Thermo Fisher Scientific (Loughborough, UK) or BDH (Poole, UK) unless otherwise stated. Restriction enzymes were obtained from New England Biolabs (Hitchin, UK), Promega (Southampton, UK) or Fermentas Life Sciences (York, UK).

2.1.2. DNA plasmids

DNA plasmids encoding recombinant Affimer cDNAs were used for expression and purification of the five LOX-1-specific Affimers; these were obtained from B. Roper (University of Leeds, UK). Plasmids were made in E.coli XL-10 bacterial strain and purified using plasmid DNA preparation kits as specified by manufacturer (Thermo Fisher Scientific). Purified plasmid was stored at -20°C and transformed into E.coli BL21*(DE3) bacterial strain for production and purification the respective LOX-1-specific Affimers.

2.1.3 LOX-1 Plasmids

Plasmid pET15b expression vector encoding either human LOX-1 extracellular domain (ECD-LOX-1; residues 68-273) or the C-type lectin domain (CTLD-LOX-1; residues 143-273) were previously cloned by R. Vohra (University of Leeds, UK) was kindly provided by S. Ponnambalam, (University of Leeds, UK).

2.1.4 Bacterial Strains

The XL-10 Gold E.coli strain TetrΔ(mcrA)183 Δ(mcrCB-hsdSMR-mrr)173 endA1 supE44 thi-1 recA1 gyrA96 relA1 lac Hte [F′ proAB lacIqZΔM15

Tn10 (Tetr) Amy Camr] was from Stratagene (CA, USA) and was used for plasmid propagation and cloning. The BL21*(DE3) E.coli strain (F– ompT hsdSB (rB – mB –) gal dcm rne131 (DE3)) was from Novagen (Nottingham, UK). BL21*(DE3) is a modified bacterial strain specifically engineered to use the T7-based plasmid expression system resulting in enhanced protein expression. It also harbour an RNaseE (rne131) gene mutation which is the major source of mRNA degradative enzymatic action. BL21*(DE3) was used for recombinant soluble LOX-1 production.

2.1.5 Human cell lines

Tetracycline-inducible LOX-1 expressing HEK293 T-Rex cells were provided by Mr. B. Roper and I. Abdul-Zani (University of Leeds, UK).

2.1.6 Antibodies

Antibodies used for the experimental work were purified in-house or brought as readymade antibodies as follows:

Mouse anti-FLAG M2 (Sigma-Aldrich, Poole, UK), horseradish peroxidase (HRP)-conjugated secondary antibody (ThermoFisher, AlexaFluor-488 and -594 conjugated secondary antibodies (Invitrogen, Paisley, UK). The following antibodies were produced in the Ponnambalam laboratory (University of Leeds, UK): sheep anti-LOX-1 (Diagnostics Scotland, Edinburgh, UK), rabbit anti-LOX-1 (Eurogentec, Seraing, Belgium). Antibodies used in this project are listed in Table 2.1 with concentrations and sourcing details.

Antibody	Source	Host	Original concentration (mg/ml)	Dilution (Western blot / Immunofluorescence)
Monoclonal anti-FLAG	Sigma Aldrich (Poole, UK)	Mouse	1	WB 1:1000 IF 1:300
Polyclonal anti-LOX-1 (crude serum)	Ponnambalam lab, purified from crude serum	Rabbit	10 mg/ml (total IgG)	WB 1:1000
Polyclonal anti-LOX-1	Ponnambalam lab, purified from crude serum	Sheep	1	WB 1:1000 IF 1:500
HRP-conjugated anti □-tubulin	Proteintech (Rosemont IL, USA)	Mouse	2	WB 1:5000

AlexaFluor™ 488 conjugated anti-mouse secondary	Thermo Fisher (Waltham, MA, USA)	Donkey	2	IF 1:500
HRP conjugated anti-rabbit secondary	Jackson Immuno Research (Ely, UK)	Donkey	0.8	IF 1:1000
HRP conjugated anti-sheep secondary	Jackson Immuno Research (Ely, UK)	Goat	0.8	IF 1:1000
HRP conjugated anti-mouse secondary	Jackson Immuno Research (Ely, UK)	Goat	0.8	IF 1:1000

Table 2.1: Antibodies used in these studies.

2.2 Experimental methods

2.2.1 Preparation of competent bacterial cells

BL21*(DE3) or XL-10 cells were streaked onto Luria-Bertani (LB) agar plates (1% (w/v) bacto-tryptone, 1% (w/v) NaCl 0.5% (w/v), bacto-yeast extract, 1.5% (w/v) agar, pH 7.0) and grown at 37°C overnight, using a single colony and inoculating it in a flask containing 50 ml of LB media (1% (w/v) bacto-tryptone, 0.5% (w/v) bacto-yeast extract and 1% NaCl, pH 7.0). This was incubated at 37°C for 24 hours with continuous shaking. Using a dilution of 1:20, the stationary phase bacteria were grown until the OD600nm reached a density of ~0.5. The culture was then put on ice to cool for 15 min. Following this the cultures were spun in a pre-cooled benchtop centrifuged at 4000 rpm for 5 min at 4°C. Supernatant was poured out and the cell pellet resuspended in the residual liquid by vortexing. 20 ml of ice cold TfbI (100 mM $RbCl_2$, 50 mM $MnCl_2$, 30 mM potassium acetate, 10 mM $CaCl_2$ and 15% (v/v) glycerol, pH 5.8) was then added per 50 ml of original culture and cells gently resuspended before incubating on ice for 45 min. Following this the cells were then centrifuged in a pre-cooled 4°C benchtop centrifuge at 4000 rpm for 10 min. Supernatant was decanted by pouring and cells gently resuspended in 4 ml of ice cold TfbII (10 mM MOPS, 75 mM $CaCl_2$, 10 mM $RbCl_2$ and 15% (v/v) glycerol, pH 6.5) per 50 ml of original culture. Cells then incubated on ice for 30 min before aliquotting into 50-100 µl aliquots and snap frozen on dry ice for storage at -70°C.

2.2.2 DNA transformation into competent bacterial cells

Plasmid DNA (1.5 µl) was added to 100 µl of thawed competent cells (prepared from previous section). E.coli XL10 gold (for bacterial plasmid replication) or BL21*(DE3) (for protein expression) were the cells of choice. These cells with the added plasmid were then incubated on ice for 5 min. Cells were heat-shocked by placing in a water bath at 42°C for 1 min and returned to ice for 5 min. Sterile LB media at 1 ml of was added to cells and incubated while shaking at 37°C for 1 h. Cells were then plated onto LB

plates containing ampicillin 100 µg/ml and incubated at 37 °C overnight before selection of a bacterial colony now incorporating the recombinant plasmids. Alternatively the culture plates could be stored at 4 °C for two weeks.

2.2.3 DNA purification

A single colony of E coli XL-10 gold transformed with the plasmid of interest was selected from LB-agar plates and inoculated into 3 ml of LB containing ampicillin 100 µg/ml and incubated at 37°C for 18 hours in a shaking incubator (150 rpm). Following this, 1.5 ml of the culture was centrifuged at 16000 g for 5 minutes to pellet the bacterial cells. Plasmid DNA was extracted using a miniprep kit (Qiagen, Crawley, UK) according to the manufacturer's instructions.

2.2.4 Plasmid DNA sequencing

600 ng of the plasmid samples were purified using commercial kits as previously described then made up to 25-30 ng/µl in a 20 µl volume using deionized water. These were sent to the DNA Sequencing Service (Dundee University, UK) for analysis. DNA sequences were emailed back after analysis.

2.2.5 E.coli expression of recombinant human soluble LOX-1

Human LOX-1 plasmid was transformed into E.coli BL21*(DE3) cells and selected on Luria-Bertani (LB) agar plates with ampicillin (100 µg/ml) and incubated overnight at 37°C . A single colony was inoculated in a sterile 50 ml LB medium (1% (w/v) bacto-tryptone, 0.5% (w/v) bacto-yeast extract and 1% (w/v) NaCl, pH 7.0) with added 100 µg/ml ampicillin, which was then incubated with shaking overnight at 37°C. A 20 ml overnight culture was then added to a 1 L culture of LB medium with 100 µg/ml of ampicillin and incubated with shaking at 37°C until the OD600nm ~0.6. At this stage isopropyl β- d-1-thiogalactopyranoside (IPTG) at 0.1 mM was added (1:10 000 dilution from 1 M IPTG stock) to induce the cultures to induce

recombinant protein expression which then were returned to the incubator for 16 hours at 25°C for continued protein expression. Next day, bacterial cultures were centrifuged at 4000 rpm for 30 min at 4°C and supernatant was discarded.

2.2.6 Purification of recombinant human LOX-1

The bacterial pellet was resuspended in 20 ml of lysis buffer (10 mM Tris pH 7.8, 1 mg/ml lysozyme, 1 mM PMSF, 1 U/ml benzonase) and incubated on ice for 30 min. The cell suspension was sonicated for 6 x 30 sec each at 15 µM amplitude. The lysed cells were then centrifuged at 10 000 rpm for 15 min. The supernatant was removed and the inclusion body pellet were resuspended in 40 ml solubilization buffer (10 mM Tris pH 8.0, 6 M GnHCl, 100 mM NaH_2PO_4) before vortexing and sonicating them for 6 x 30 sec bursts. This was centrifuged again as before; the solubilised protein was incubated with ~0.5-1 ml of washed nickel-agarose resin (in a 20 ml column) on a rotator at 4°C for 30-60 min. The column was allowed to drain and flow-through kept for later analysis. Columns were washed 2 x column volumes (~40 ml) with solubilisation buffer plus 1% TX-100 (w/v). The columns are then washed in 10-20 ml solubilization buffer (+ 1% TX-100 + 20 mM imidazole) to get rid of non-specific bound proteins. The column was washed backed into 10-20 ml solubilisation buffer (no detergent or imidazole). The peak fractions were then eluted in 5-10 x 1 ml fractions of solubilisation containing 250-500 mM imidazole. Elution fractions with measured absorbance OD280>0.1, now containing the soluble LOX-1 protein, were pooled together for refolding and dialysis. Purity of soluble LOX-1 was checked by running it against BSA in 12% agarose gel.

2.2.7 Recombinant human sLOX-1 refolding process

To the pooled LOX-1 fractions from previous section, 100 mM dithiothreitol (DTT) was added, gently mixed and incubated at 4°C for 1 hour. To remove the DTT, the LOX-1 fractions were then placed in a dialysis membrane and dialysed overnight at 4°C using the initial dialysis buffer (4 M GuHCl, 50 mM Tris pH 8.0). Then to allow correct format of refolding, the purified sLOX-1

protein was sequentially dialysed using 6 variable-constitution dialysis buffers and each is used for at least 12 hours. Buffer 1 (50 mM Tris-HCl pH 8.5, 4 M GuHCl, 0.4 M L-Arginine, 0.4 sodium chloride, glycerol (v/v)10%, 0.5 mM oxidized glutathione, 5 mM reduced glutathione). Buffer 2 (50 mM Tris-HCl pH 8.0, 3M GuHCl, 0.4 M L-arginine, 0.4 sodium chloride, glycerol (v/v)10%, 0.5 mM oxidized glutathione, 5 mM reduced glutathione). Buffer 3 ((50 mM Tris-HCl pH 8.5, 3 M GuHCl, 0.4 M L-arginine, 0.4 sodium chloride, glycerol (v/v)10%, 0.5 mM oxidized glutathione, 5 mM reduced glutathione). Buffer 4 (50 mM Tris-HCl pH 8.5, 1 M GuHCl, 0.4 M L-arginine, 0.4 sodium chloride, glycerol (v/v)10%, 0.5 mM oxidized glutathione, 5 mM reduced glutathione). Buffer 5 (50 mM Tris-HCl pH 8.5, 0.4 M L-arginine, 0.4 sodium chloride, glycerol (v/v)10%, 0.5 mM oxidized glutathione, 5 mM reduced glutathione). Buffer 6 (50 mM Tris-HCl pH 7.5, 50 mM sodium c
hloride). If precipitations form (Figure 2.1), the dialysate is centrifuged at 100 000 g for 30 min at 4°C and returned to the dialysis membrane. After the final dialysis and centrifugation, sLOX-1 fraction was mixed with an equal volume of 50% (v/v) glycerol (25% (v/v) glycerol final concentration), snap frozen, and stored at -80°C.

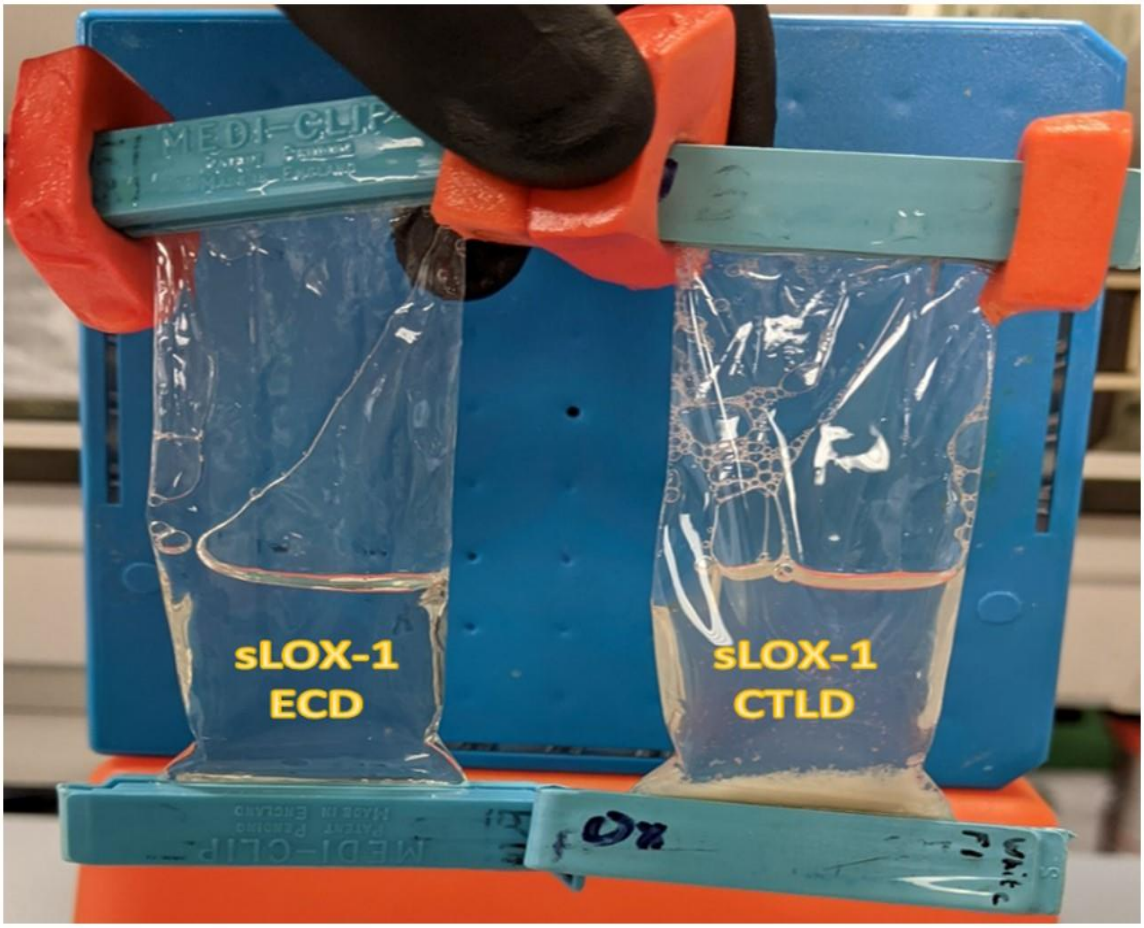

Figure 2.1 Dialysis of sLOX-1 proteins against buffer 4. The soluble LOX-1 proteins were dialysed extensively against buffer 4 (see Materials and Methods). sLOX-1-ECD (left) remained clear whilst sLOX-1-CTLD (right) contained solid white precipitated protein. These precipitations could be removed by centrifuging at 100 000 g for 30 min at 4°C before further dialysis.

2.2.8 Affimers production and purification

10-50 µl aliquots of BL21*DE3 cells were thawed on ice allocated before adding 1 µl of the 5 LOX-1-specific plasmids encoding Affimers which were incubated on ice for 30 min. Following a heat shock at 42°C for 2 min, the cells were returned to ice for 5 minutes. The resultant Affimer plasmid-transformed bacterial cells are then spread separately on LB agar + ampicillin (50 µg/ml) culture plates and kept in an incubator at 37°C overnight.

Single colonies of the respective cultured bacteria harbouring the Affimer plasmids, were selected and added to 3 ml of 2xYT (16 g/L bactotryptone, 10 g/L yeast extract, 5 g/L NaCl) and then incubated overnight at 37°C with shaking. Pre-warmed 50 ml 2xYT culture was inoculated with 1 ml of the incubated cultures and then put back in the incubator until absorbance OD600 reached ~0.6. Following this, the cultures were induced with 0.1 mM IPTG and incubated overnight at 25°C with shaking. The following day, the cultures were centrifuged at 4,000 rpm 4°C for 15 min. The supernatant was decanted and 1 ml lysis buffer (50 mM NaH_2PO_4, 300 mM NaCl, 20 mM imidazole, 10% (v/v) glycerol, 0.1 mg/ml lysozyme, 1% (v/v) Triton X-100, 10 U/ml benzonase pH 7.4) was used to resuspend the cell pellets before applying them to sonication at 50% power for 30 sec bursts x4 to avoid denaturing the proteins with the generated heat from sonication. These were then placed on a rotator wheel at 4°C for 20 min. Meanwhile preparation of the nickel-based agarose resin was prepared by washing 300 µl/Affimer subtype of Ni-NTA agarose resin (Invitrogen) in 1ml of lysis buffer, gently mixed, centrifuged at 1,000 g for 1 min and the buffer decanted. This washing process was repeated 3 times. In a prewarmed water bath at 50°C, the lysates are incubated for 30 min and then on ice for 3-5 min before centrifuging at 4,000 g for 20 min at 4°C. At this stage the lysates are added to the resin and kept on a wheel rotator for 2 h at 4°C. The resin binds to the Affimers leaving other proteins free to be collected by centrifuging at 1,000 g for 1 min following the 2 h incubation period. These

unbound proteins were stored at -20 °C for analysis. The resin bound Affimers were then repeatedly washed by adding 1 ml wash buffer (50 mM NaH_2PO_4, 500 mM NaCl, 20 mM imidazole, pH 7.4) and centrifuging at 1000 rpm for 1 min. Wash fractions with OD_{280} ≥0.05 were pooled and eluted to free the Affimers from the resin using the elution buffer (50 mM NaH_2PO_4, 500 mM NaCl, 300 mM imidazole, 10% (v/v) glycerol, pH 7.4) in 150 µl fractions. Elutions repeated until A_{280} readings on a NanoDrop Spectrophotometer were consistently <0.01. Elution fractions with A_{280} readings >0.05 were pooled and dialysed with PBS containing 10% (v/v) glycerol.

2.2.9 Maleimide-based biotinylation of Affimers

Following elution from Ni-NTA, Affimers were biotinylated at the C-terminal cysteine residue. 150 ml of lysate containing Affimer was bound to Tris (2-carboxyethyl) phosphine (TCEP) immobilized resin (ThermoFisher Scientific) and washed with 300 ul PBS containing 1 mM EDTA, mixing thoroughly and centrifuged at 1000 rpm for 1 min. The supernatant is then aspirated and 4 ul PBS containing 50 mM EDTA was added. To this, 150 ul of a 0.5 mg/ml concentration of each Affimer is added and left on a wheel rotator (20 rpm) for 1 h at bench temperature. The solution was spun at 1000 rpm for 1 min and, carefully aspirating 130 ml of the supernatant, was transferred into a tube containing 6 ml of 2 mM biotin-maleimide (Sigma-Aldrich) and incubated at room temperature for 2 h. Zeba spin desalting columns (Thermo Fisher Scientific) were prepared according to the manufacturer's protocol and the Affimers were added to the columns and centrifuged at 1000 rpm for 5 min to remove excess biotin.

2.2.10 N-Hydroxysuccinimide biotinylation of Affimers

Where biotin-maleimide binds to the cysteine residues of Affimers, biotin-N-hydroxysuccinimide modifies exposed terminal amines. NHS-biotin (Sigma-Aldrich) was prepared by dissolving the powder form and using serial dilution in dimethyl sulfoxide (DMSO) to reach a concentration of 0.25

ng/ml. Affimers at concentration of 0.5 mg/ml were added to the NHS-biotin in a volume ratio of 4:1 to the desired volume and incubated on ice for 1 hour and then desalted using Zeba spin desalting columns (Thermo Fisher Scientific).

2.2.11 Alexafluor-488 maleimide as a fluorescent tag for Affimers

Using the Affimers that were “freshly” eluted from Ni-NTA resin, 150 µl fractions at 0.5 mg/ml concentration were incubated with 150 µl of washed Tris (2-carboxyethyl) phosphine (TCEP) immobilized resin (ThermoFisher Scientific) and incubated for 1 h at room temperature with agitation. The resultant solution was then centrifuged at 1,500 g for 1 min and 120 µl of the supernatant was extracted. To this, 6 µl/Affimer of 2 mM AlexaFluor 488 C5 maleimide (Thermo Fisher Scientific) was added, gently mixed and incubated for 2 h at room temperature and protected from light by wrapping in foil. Zeba 7 kDa MWCO desalting columns (ThermoFisher Scientific) were used to remove unbound AlexFluor 488 according to the manufacturer’s instructions.

2.2.12 Preparation of cell lysates

Media was aspirated from flasks and cells were washed thrice in ice-cold PBS. Cell lysis was achieved by adding in 2% (w/v) SDS in PBS containing 1 mM PMSF and protease inhibitor cocktail (Roche) and scraped into microcentrifuge tubes. Following this the lysates were incubated at 95°C for 5 min and then burst sonicated for 5 sec.

2.2.13 Bicinchoninic acid (BCA) assay for determining protein concentration

Protein concentration was measured using bicinchoninic acid (BCA) assay. To generate a standard curve, 10 µl of bovine serum albumin (BSA) controls at concentrations of 0, 0.2, 0.4, 0.6, 0.8 and 1.0 mg/ml were pipetted into the wells of a 96-well polystyrene ELISA plate (Nunc, Roskilde, Denmark) in duplicate to generate test samples of 0, 2, 4, 6, 8 and 10 µg of BSA. The protein of interest was then pipetted at 1, 5 and 10 µl. Pierce BCA protein assay reagents A and B (Thermo Fisher Scientific) were mixed

together in a 50:1 ratio. 200 µl/ well of the mixture was added before incubating the plate at 37°C for 30 min. The readings were analysed using a Tecan plate reader running Magellan version 6.0 software (Tecan, Reading, UK). The standard curve generated from BSA was used by the programme to determine the protein concentration of the test protein.

2.2.14 Sodium dodecyl sulphate polyacrylamide gel electrophoresis (SDS-PAGE)

Polyacrylamide-based gel 12% or 15% at 1.5 mm thickness was used for protein analysis. The composition of the different gel concentrations making 20 ml of gel is shown in table 2.2. These were topped with stacking gel that and a well comb was used to create the well spaces. Stacking gel composition for 200 ml was as follows:

- 30% Acryl 33.3 ml
- 1 M Tris 25 ml
- 10% SDS 2 ml
- ddH2O 139.7 ml
- 10% APS 2 ml
- TEMED 0.2 ml

TEMED should be the last component to be added.

Solution (volume in ml)	Gel percentage %					
	6	7	8	10	12	15
30% Acryl	4	4.7	5.3	6.7	8	10
3M Tris	2.5	2.5	2.5	2.5	2.5	2.5
ddH2O	12.9	12.2	11.6	10.2	8.9	6.9
10% SDS	0.2	0.2	0.2	0.2	0.2	0.2
10% APS	0.4	0.4	0.4	0.4	0.4	0.4
TEMED	0.016	0.016	0.016	0.016	0.016	0.016

Table 2.2: Percentage composition of polyacrylamide gels.

A mass of 10-25 µg of whole lysates and 1-10 µg of purified protein would be run on the gels alongside a visible protein marker for referencing. Gels

were stained using Instant Blue Protein Stain (Stratech Scientific, Newmarket, UK) and imaged using a Syngene G Box:Chemi (Cambridge, UK). SDS-PAGE running buffer was prepared from 10X stock (30.3 g Tris, 144.2 g glycine) making 1 l solution. 100 ml of this was then used in addition to 10 ml of 10% SDS and made up to 1 l by adding ddH2O to make up 1x SDS-PAGE running buffer.

2.2.15 Western blotting

Buffers were prepared as follows

- 1X Transfer buffer: 200 ml 10x transfer buffer, 400 ml 20% methanol, 1400 ml ddH2O, PH 8.1
- 10X Transfer buffer: 30.3 g Tris, 144 g glycine were dissolved in 900 ml of ddH2O and made up to 1 l volume, PH 8.1
- TBS-T: 10 mM Tris, pH 7.5 , 150 mM NaCl , 0.1% Tween-20

6 pieces of 3MM Whatman blotting paper and one strip of nitrocellulose membrane (BioRad) per gel were cut at the size of the gel and the top left corner of the nitrocellulose membrane was marked for easy orientation at later stages. The nitrocellulose membrane and the blotting papers are soaked in transfer buffer before stacking them. The gel was inverted on the nitrocellulose membrane and 3 blotting papers were used to sandwich them on either side ensuring air bubbles are removed from all the layers of the stack. This was then placed in the transfer cassette and placed in a transfer tank that was prefilled with transfer buffer. At constant current of 300mA at 4° C the transfer tank was kept overnight to complete the protein transfer into the nitrocellulose membrane.

To ensure protein transfer is complete, the nitrocellulose membrane was placed in Ponceau S solution to cover the membrane; the presence of visible bands confirm successful transfer. Remaining red stain from the Ponceau S was rinsed off with ddH2O followed by 3-5 washes with TBS-T. The membrane was then incubated in TBS-T with 1-5% (w/v) non-fat skimmed milk to a volume enough to cover the membrane 1 h and then washed with TBS-T 3 times for 10 min each. 1° antibody was prepared by

mixing 1% (w/v) non-fat skimmed milk in 20 ml TBS-T and adding 1° antibody to 1:1000-10,000 of serum final concentration. The nitrocellulose membrane was incubated in the TBS-T containing 1° antibody overnight at 4° C. After the 1° antibody solution was drained and stored for one more useable time, the membrane was washed 3 times with TBS-T for 10 min each. In 20 ml of TBS-T, 2° antibody was diluted to 1:2500 in with1% skimmed milk and then added to the washed membrane and incubated at room temperature for 1 h on a rocker. The 2° antibody was drained and the membrane is washed 3 times for 10 min each time with TBS-T. Enhanced chemiluminescence (ECL) solution was made up by mixing reagents A and B in a 1:1 ratio to a volume ~500 µl total volume per membrane strip. The ECL solution was pipetted onto a sheet of plastic acetate to cover an area equal to the size of the membrane and the membrane blot was inverted a few times onto the ECL solution and ensuring that air bubbles between the sheet and the membrane are removed and the ECL activated membrane is allowed to set for 1 min then covered with a second acetate sheet. At this stage the membrane is ready to be imaged using a chemiluminescence workstation.

2.2.16 Affimer-based ECD and CTLD detection

LOX-1 ECD and CTLD domains were transferred on a nitrocellulose membrane along with tetracycline-induced and un-induced cell proteins. These membranes were then added to a dish containing a mixture of 20 ml TBS-T, 1% (w/v) skimmed milk and un-labelled Affimers at 1:1000 and incubated at room temperature overnight. These were done for all 5 LOX-1 specific Affimers. The following day, TBS-T was decanted and the membranes washed with TBS-T and then incubated for 2 h at room temperature against TBS-T containing 2° antibody and 1% skimmed milk. Membranes were then washed with TBS-T 3 times for 10 min each and then treated with ECL as described in the previous section before imaging them in a chemiluminescence workstation. These were compared to standard 1° antibody tagged membranes.

2.2.16 Lipoprotein particle purification from blood

18 ml blood sample were taken from consenting volunteers in accordance with the University of Leeds Faculty of Biological Sciences protocol and using local ethical approval and licence (University of Leeds reference BIOSCI 15-007). The blood was added to a falcon tube containing 2 ml of 3.8% (w/v) trisodium citrate as an anticoagulant before centrifuging the sample at 3,000 rpm for 10 min at 4°C. The plasma layer (yellow) was carefully aspirated to isolate it from the precipitant blood cells (red) and then transferred into a falcon tube containing Opti-prep density gradient medium (Sigma) at a 4:1 ratio. The plasma was then pipetted out using a sharp glass pipettes and layered beneath 1 ml of HBS (0.85% (w/v) NaCl, 10 mM Hepes, pH 7.4) that was initially pipetted to a 4.7 ml Optiseal centrifuge tube (Beckman Coulter, High Wycombe, UK). The centrifuge tubes were sealed by placing black bungs and tube collars on all tubes. Tubes were balanced and placed in a TL-110 rotor inside a Beckman Optima-MAX centrifuge and ran at 100 000 g for 3 h at 16 °C. At this stage the different lipoproteins formed distinct layers that could be aspirated and analysed as shown in Figure 2.2. Tubes were wrapped in Sellotape to reduce accidental mixing of the layers when piercing the tube with the needle. The tubes were then placed in clamps and using a 25-gauge needle and 1 ml syringe, the LDL band was aspirated (Figure 2.3). The LDL was then dialysed against PBS overnight at 4°C. BCA was used to measure the concentration of LDL following dialysis and concentration was adjusted to 1 mg/ml with PBS.

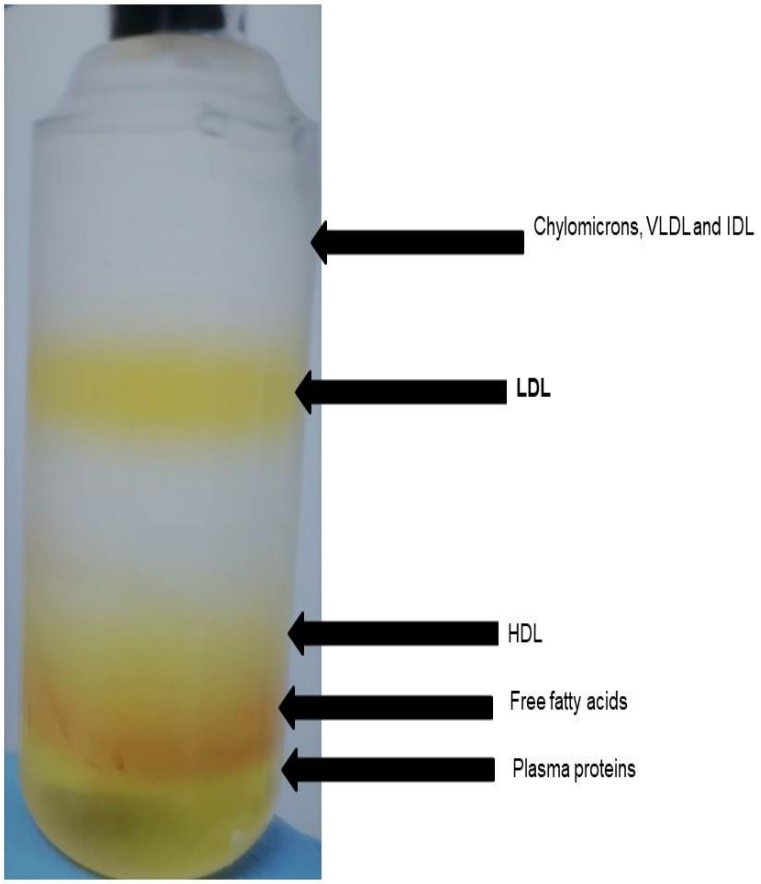

Figure 2.2: Preparation of LDL from plasma. Plasma was extracted from whole blood and centrifuged at 100,000 g for 3 h (see Materials and Methods). This procedure separates LDL from HDL, LDL and VLDL. Abbreviations: VLDL, very low-density lipoprotein; IDL, intermediate-density lipoprotein; LDL, low-density lipoprotein; HDL, high-density lipoprotein particles.

Figure 2.3: Aspiration of lipoproteins. A 19 gauge needle attached to a 1 ml syringe is used to aspirate the different lipoproteins after separation using ultracentrifugation. A 1-2 ml band of LDL was aspirated from each tube and these were pooled and dialyzed in BPS overnight.

2.2.17 Oxidation of LDL particles

The LDL sample generated from previous section was divided into 2 fractions. The first was was treated with 100 µM EDTA and 20 µM BHT (final concentrations) were added from stock solutions. This was wrapped in foil and stored at 4°C for up to 4 weeks and used as native- LDL (non-oxidised) for comparative analysis alongside ox-LDL. The other fraction was processed for oxidation LDL sample for oxidation by incubating with 5 µM CuSO4 for 24 h at 37°C with protection from light by wrapping in tinfoil. After this period lapsed, 100 µM EDTA and 20 µM BHT were added to the

ox-LDL to halt the oxidation process and the tube placed on ice. Successful oxidation could be visibly observed by a colour change from yellow of the LDL to clear of ox-LDL. The final step was to dialyse the ox-LDL sample in PBS at 4°C with protection from light before measuring and recording the final concentration of ox-LDL and the native-LDL was determined by BCA assay.

2.2.18 Agarose gel electrophoresis-based analysis of lipid particles

4 µg of oxLDL and native LDL were loaded in 5x sample buffer (50 mM Tris pH 8, 50% glycerol, 0.025% bromophenol blue) onto a 0.5% (w/v) agarose gel running at 100 V for 45 min. The agarose gel was then fixed with a solution of 75% (v/v) ethanol and 5% (v/v) acetic acid at room temperature for 15 min. This solution was then decanted before using Sudan black in 60% (v/v) ethanol and 0.05% (w/v) NaOH to stain the agarose gel. The gel was destained by washing briefly in ddH2O then incubating overnight in 50% (v/v) ethanol at 4°C. By this stage the gel with visible LDL bands was ready for digital imaging.

2.2.19 DiI-labelling of oxLDL

The red fluorescent dye DiI DiIC18(5)-DS (1,1'-Dioctadecyl-3,3,3',3'-Tetramethylindodicarbocyanine-5,5'-Disulfonic Acid; Thermo Fisher Scientific) was used to label native and oxidised LDL particles. DiI was prepared by dissolving the powder form of the dye in DMSO to yield a concentration of 10 mg/ml. 30 µl of fluorescent dye in DMSO was mixed per milligram of lipoprotein particles and incubated at 37°C overnight with protection from light. The following day the solution was centrifuged at 10,000 rpm for 10 min to pellet any residual unbound DiI and protein aggregates. The supernatant now containing the ladled LDL was then dialysed in PBS for 24 h in a sealed, dark box, stored at 4°C. Final concentration was assessed by BCA.

2.2.20 Epithelial human embryonic kidney 293 (HEK293) culture

HEK293-LOX-1-FLAG cells were cultured in Dulbecco's modified eagle medium (DMEM) that was prepared by adding the following:

- MEM non-essential amino acids, 2 mM L-glutamine)
- 10% (v/v) Foetal Bovine Serum Gold (PAA laboratories, Pasching, Austria)
- 50 U/ml penicillin
- 50 ug/ml streptomycin

Cell culturing was achieved under humid, aseptic conditions at 37°C, 5% CO2.

Cell passaging was done by incubating every 2-3 days with PBS + 5 mM EDTA for ~3 min, this is done until complex detachment of the cells is achieved. 9 ml of the previously prepared DMEM was used to quench the reaction and cells were plated at ~20% confluency. Cells were split at 3:1 ratio before 1 mg/ml poly-L-lysine (Sigma-Aldrich) was used to coat fresh culture plates and coverslips which were then incubated for 30 min at room temperature then washed with PBS. Plates were allowed to 2 hs before seeding cells. The resultant lysates were stored at -20 °C.

2.2.21 Cell lysis

Cold PBS was used to wash the cells and get rid of any residual medium. Lysis buffer (PBS, 2% (w/v) SDS and protease inhibitor cocktail (1:1250, Merck)) was then added to the cells which were then detached from the tubes using a cell scraper. To complete the lysis process, cells were then transferred on ice for 5 min and then sonicated for 5 times for 5 sec each at 50% sonication power before applying a heat-shock at 95°C for 5 min to. Heating is used to stop the protease activity as well as to denature proteins. The final concentration of the protein was determined using BCA assay.

2.2.22 Using Affimers as probes for LOX-1 on HEK293-LOX-1-FLAG cells

Tetracycline-induced HEK293-LOX-1-FLAG cells were prepared by seeding coverslips in DMEM + 10% FBS on 24-well plates at 25% confluence and when confluence reached 50% confluence tetracycline was added and cells incubated for 16 h. Following this the media was aspirated and Opti-MEM media with added 0.2% BSA and 25 µg/ml of AlexaFluor488-labelled Affimers and incubated on ice for 10-30 min. Cells were then transferred into a new 24-well plates containing 0.5 ml PBS. Cells were washed 3 times with PBS which is carefully aspirated after each wash then the cells were fixed using 3% (w/v) paraformaldehyde for 20 min at room temperature, and then washed further with PBS 3 times. Coverslips were then incubated with 500 ul PBS plus DAPI (1 µg/ ml) at room temperature for 2 h before washing the cells again PBS 3 times. Finally the coverslips containing the fixed cells were mounted onto microscope slides using Fluoromount-G™ Mounting Medium (Cat. No. 00-4958-02, ThermoFisher).

HEK293-LOX-1-FLAG cells stained with antibodies were prepared differently. After tetracycline-induction, cells were immediately fixed with 3% (w/v) paraformaldehyde for 20 min at room temperature. Coverslips were washed 3 times with PBS before incubating with PBS, 0.5% (w/v) BSA for 30 min. Coverslips were then washed with PBS 3 times. The coverslips were then removed from the 24-well plates inverted onto 25 µl droplets of anti-FLAG antibody suspended in PBS, 0.1% (w/v) BSA then incubated overnight at room temperature with light-protected in a moist chamber. The following day, coverslips were subsequently washed 3x with PBS then inverted in a 25 µl droplet of secondary AlexaFluor 488 antibody conjugate (4 µg/ ml) (Cat. No. ab150105; Abcam, Cambridge, UK) suspended in PBS containing 0.1% (w/v) BSA and DAPI (1 µg/ml). The coverslips were then incubated at room temperature for 2 h before washing them with PBS 3 times and then the coverslips were mounted in Fluoromount G (ThermoFisher) onto glass slides for imaging. Images were taken with the Zeiss LSM 700 confocal microscope using the Plan-Apochromat 40x/1.30 Oil objective lens. Laser at 405 nm wavelength was used to agitate DAPI

and the resultant emission were collected at 435 nm (filter range 493 – 1000) whilst AlexaFluor 488-labelled Affimers and antibodies were excited at wavelength of 488 nm with emission collected at 518 nm (filter range 493 – 1000).

2.2.23 Using Affimers to block LOX-1-dependent oxLDL uptake

Using the same technique of cell seeding described above, the HEK293-LOX-1 cells were seeded at 50% confluence onto poly-L-lysine coated glass coverslips in 24 well plates until achieving confluence of 70% at which stage they are induced in Opti-MEM medium with 0.2% BSA and 1 µg/ml tetracycline for 16 h at room temperature. Following this the medium was changed and the cells were then incubated on ice for 30 min. The media at this stage had the LOX-1 specific Affimers (A1, A3, B1, G1 and H1) added to each media flask. 3 concentrations of Affimers were tried 10, 100, and 1000 ng/ml. Anti-LOX-1 antibody (JTX92) was used at 1 µg/ml as a positive control. DiI-labelled oxLDL was added to the excited media at 10 µg/ml and incubated for 30 min on ice before washing the cells with 500 µl PBS 3 times and fixed using 3% PFA for 15 min. Subsequently cells were washed with 500 µl of PBS 3 times and then incubated at room temperature in PBS with1 µg/ml DAPI for 30 min. Finally 3 washes with 500 µl of PBS were done and then the cover slips were mounted on microscope slides using Fluoromount G anti-fade medium (Thermo Fisher Scientific) for imaging. Images were taken with the Zeiss LSM 700 confocal microscope at 40x magnification. DAPI was excited with a 405nm laser and emission collected at 435nm (filter range 0-585 nm) whilst DiI was excited with a 555 nm laser and emission collected at 585 nm (filter range 560-1000 nm).

2.2.24 Statistics

Mean ± standard error of the mean (SEM) were used to express data. Error bars in graphs denote ± SEM. The statistical analysis was performed using the unpaired 2-sided t-test for two sets of data or one-way analysis of variance (ANOVA) followed by appropriate post-hoc test for multiple

comparisons as mentioned in the image legends. The statistics were done on the online tool Statistics Kingdom. Significant differences between control and test groups were evaluated with p values less than 0.05, 0.01, 0.001 and 0.0001 were indicated on the graphs.

Chapter 3
Results

3.1 Introduction

Atherosclerosis is a primer for many disease processes that result in clinical manifestations. Cardiovascular disease, cerebrovascular disease and peripheral arterial disease are commonly seen examples of these manifestations. The main focus on anti-atherosclerosis management that is used currently is the use of statins (Kwak et al, 2003; Almeida et al, 2019). Statins work by reduction of the total circulating cholesterol by reducing its synthesis which ultimately reduce the available cholesterol particles that can deposit in the arterial walls (Schiffrin et al, 2002). The side effects and intolerance issues with statin therapy call for the need for other options of treatment aiming at reducing the cardiovascular risk of patients.

The oxLDL lipid particle is believed to be the main precursor for atherosclerosis development and progression and is recognised by scavenger receptors (SRs) (Zani et al., 2015). Multiple classes are included in the SR family and SR classes A, B and E play important roles of variable extent in atherosclerosis especially the LOX-1 receptor which is a member of class E SRs and is a multiligand receptor (Xu et al., 2003). The versatility of LOX-1 receptor functions and its direct involvement in the uptake of ox-LDL makes it a logical target for treatment options to halt or control the progression of atherosclerosis. LOX-1 receptors are versatile and are found macrophages, endothelial and smooth muscle cells of arterial beds, so the dysfunctional effects of LOX-1 over-expression on these cells is largely linked to endothelial dysfunction leading to atherosclerosis (Sun and Chen, 2011; White et al., 2011; Wang et al., 2019). In addition to this, activation of LOX-1 results in loss of smooth muscle relaxation due to inhibition of endothelial nitric oxide synthase (eNOS) activity thus resulting in rigidity of the arterial wall (Cavieres et al., 2014).

The use of antibodies for various medical intentions has been around for at least a few decades now and their uses extend to a wide range of medical applications including cancer treatment, autoimmune diseases and musculoskeletal disorders (Gligorov et al., 2022; Lu et al., 2020; Hafeez et al., 2018). Due to various issues with antibodies including cost of production, thermal and pressure stability conditions, cross reactivity and target specificity and structure complexity. These matters limited the use of antibodies and urged to exploit other particles to be used that exhibit the pros of the antibodies and has limited drawbacks.

Affimers are small protein-based scaffolds that offer a solution for the pitfalls of antibodies and offer a good advantage of target-customisation. These targets can be screened via the phage library (Tiede et al., 2017; Tiede et al., 2014). Affimers have features including, small molecular weight, easy predictability in bacterial cells, thermal and pressure stability and low cost of production (Tiede et al., 2017; Tiede et al., 2014). These features favours the use of Affimers as potential LOX-1 antagonists which offers possibilities in the treatment of atherosclerosis as monotherapy or combination therapy. Five LOX-1-specific Affimers have been identified and they will be analysed experimentally in this study.

3.2 Isolation and purification of lipid particles from human blood

Blood was extracted from volunteers and run in a low-speed centrifuge to separate blood cells from the supernatant plasma which is then centrifuged at high-speed to separate the lipoprotein particles according to density (see Materials and Methods). These were then separated and used for biochemical analysis. These lipid particles were run on 0.5% (w/v) agarose gels to assess their migratory properties and then stained with Sudan black dye (figure 3.1).

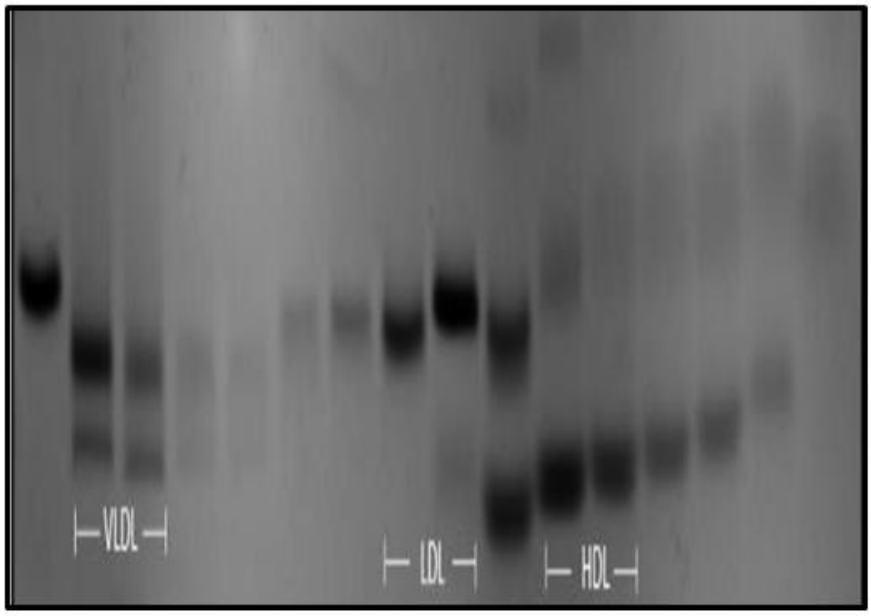

Figure 3.1 : Lipoprotein particle analysis on agarose gel. Fractions (3 µl) of centrifuged samples after ultracentrifugation were loaded from top (left) to bottom (right) of the centrifuge tube. Fractions were loaded onto 0.5% (w/v) agarose gel and stained with Sudan black dye (see Materials and Methods).

The migration of these lipoprotein particles is dependent on their relative density and the proportion of protein content which carries the negative charge of the lipoprotein and hence effects the response to electrophoresis in the gel. For instance, chylomicrons are noted to remain in the upper gel due to their large size and this could be explained by their high density and low protein portion. VLDL on the other hand migrates more in the gel compared to the more dense LDL and this is related to its higher content of negatively charged ApoB-100 and apolipoproteins A5,C1,C2,C3 and E. To further analyse the protein content of these lipoproteins, 25 µl of each lipoprotein were ran on 6-20% denaturing SDS-PAGE gel and stained with Coomassie blue dye (Figure 3.2).

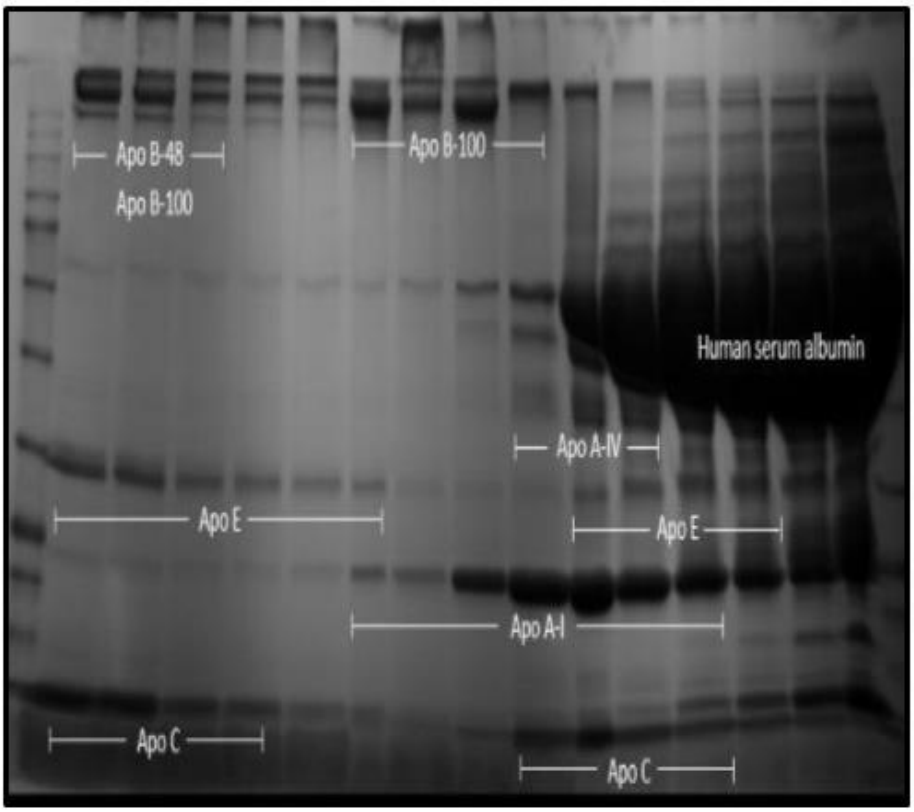

Figure 3.2: Lipoprotein particle analysis on SDS-PAGE. Fractions of centrifuged samples after ultracentrifugation were loaded from top (left) to bottom (right) of the centrifuge tube. Fractions were loaded onto 6-20% SDS-PAGE and stained with Coomassie blue dye (see Materials and Methods).

3.3 Lipid particle oxidation and fluorescent labelling

As mentioned earlier, ox-LDL is the metabolically active form of LDL and it is linked to atherosclerosis. In most healthy people, the levels of circulating ox-LDL are very low and this is linked to anti-oxidative processes and reducing conditions in the plasma (Malekmohammad et al., 2019). For these reasons, obtaining ox-LDL from plasma is not feasible and it is easier to produce in vitro. Using 10 μM copper sulphate is the main method of oxidation adapted for the purpose of this work. LDL and other lipoproteins could be labelled by a fluorescent label called DiI (1,1′-dioctadecyl-3,3,3′,3′-tetramethylindocarbocyanine perchlorate) which adds two long C18 chains to the lipid bilayer of the lipoproteins giving a red-orange fluorescence to the lipid particles (Figure 3.3). This allows the study of their cellular uptake.

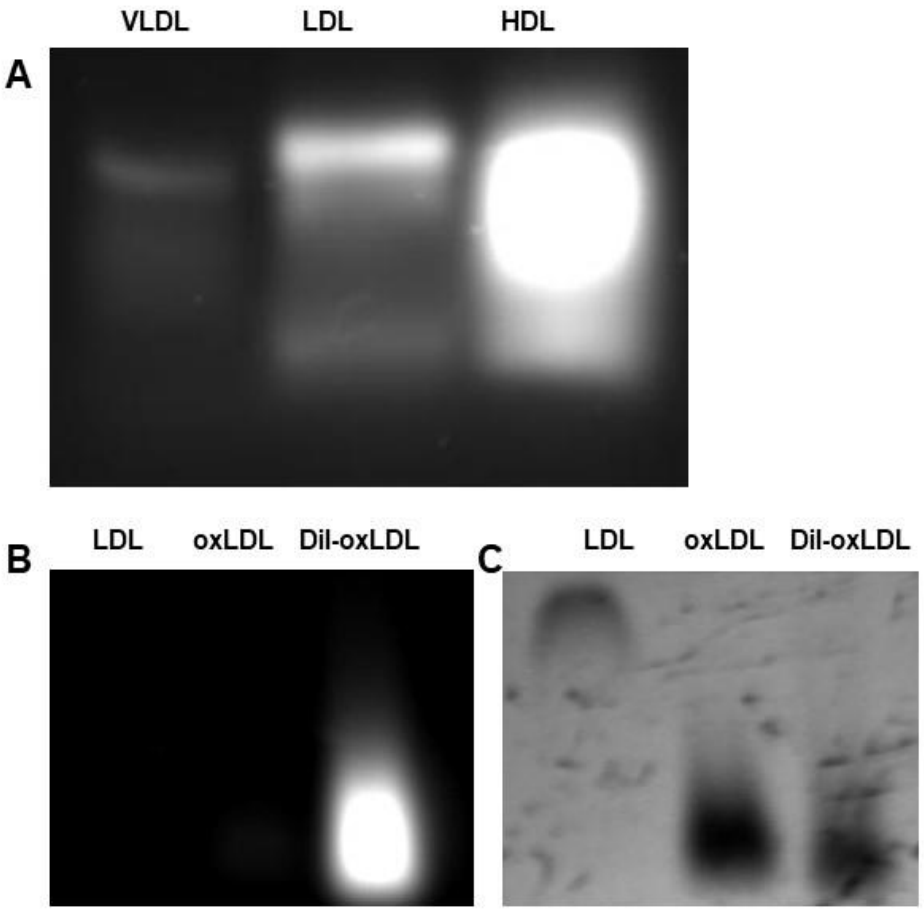

Figure 3.3: Fluorescence labelling of oxLDL. (A) Fluorescent DiI-labelling of VLDL, LDL and HDL particles. The visibly red-orange DiI dye was incubated with 4 µg worth of protein content of each lipoprotein particle, ran on a 0.5% agarose gel and imaged at 550 nm excitation and emission at 570 nm. (B) DiI labelling of native LDL and oxLDL. Purified LDL was oxidised by incubation with 10 µM copper sulphate overnight. Oxidised LDL was then labelled with fluorescent DiI dye and analysed as described in panel A. (C) Agarose gel electrophoresis of native LDL and oxLDL upon staining with Sudan black dye. As seen, following chemical modification, the oxidised LDL gains higher net negative charge which result in increased electrophoretic mobility.

3.4 Expression and purification of LOX-1 protein

The production purification and refolding process of sLOX-1 is discussed in this section. This step is mandatory before screening the Affimer library for possible targets for LOX-1. Production process was achieved by incorporating the LOX-1 plasmid into E. coli BL21* (DE3) bacterial strain. sLOX-1 plasmid was cloned in pER-15b bacteria vectors using PCR. The configuration of the resultant LOX-1 protein intentionally lacked the cytoplasmic and transmembrane segments to allow solubility ECD domain which included the neck domain in addition to the CTLD domain (residues 61-273) (Figure 3.4) in the cellular cytoplasm during the expression process. Two constructs of sLOX-1 were created, CTLD which was formed by residues 136-273 and the LOX-1 plasmid which was engineered to contain a hexahistidine (His6) tag that binds to Ni-NTA resin, a tobacco etch virus cleavage site (TEV) and thrombin cleavage site that could be used to exclude the His6 tag.

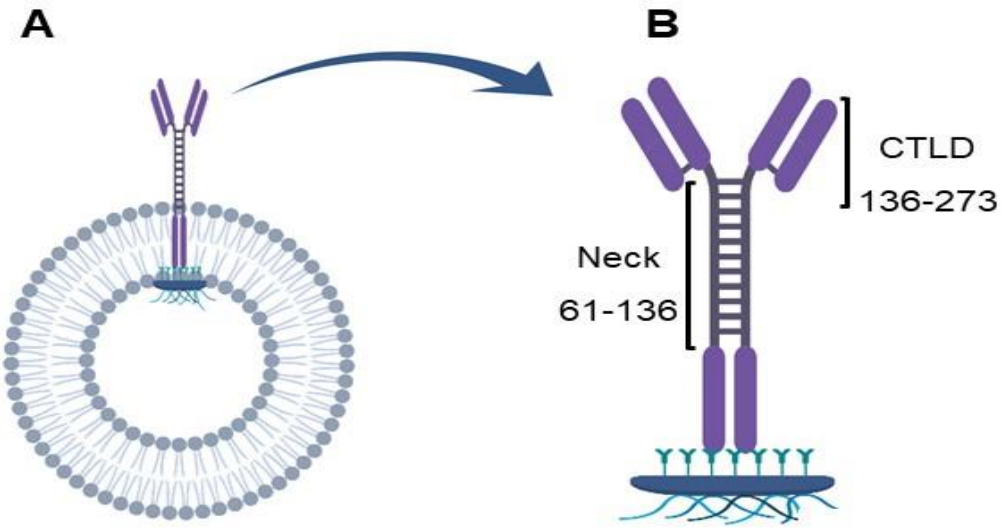

Figure 3.4: **LOX-1 binding to oxLDL.** Schematic representation of LOX-1 binding to oxidised or 'cryptic' epitopes on oxLDL particles. Key: CTLD, C-type lectin domain; TM, transmembrane domain; CD, cytoplasmic domain. Created using BioRender.com

Following the protocol (Chapter 2), pET-15b sLOX-1 plasmids were transformed into the E. coli BL21* (DE3) plasmid and large volume cultures were produced. When OD600 was around 0.4, LOX-1 production was induced with IPTG overnight. LOX-1 protein present in the human body is naturally in a dimeric form as a disulphide bond links two monomers together, however, this does not occur when LOX-1 is produced in bacterial cells. To resolve this, the protein underwent a series of reduction and then refolding (Figures 3.5 and 3.6).

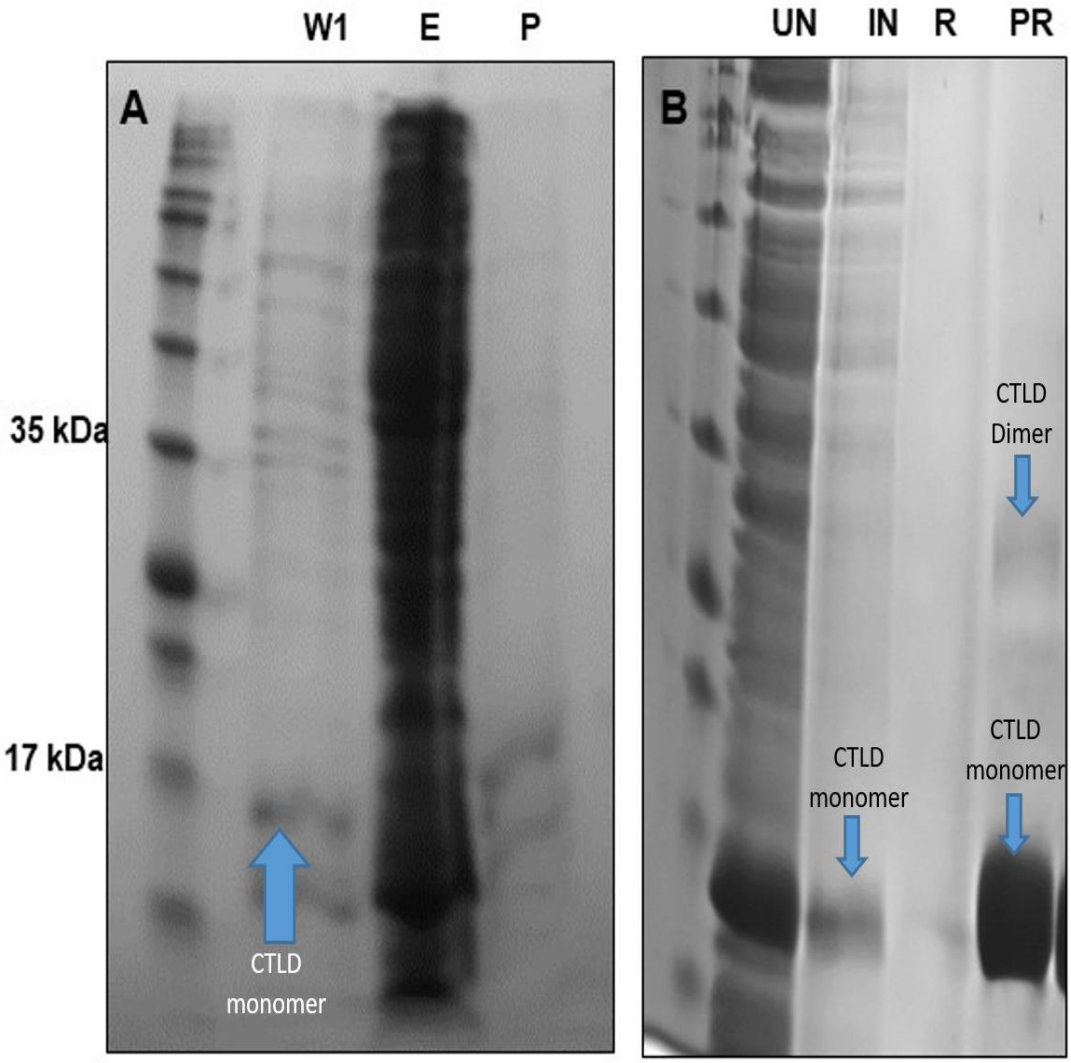

Figure 3.5: **SDS-PAGE gel analysis of the sLOX-1-CTLD domain.** (A) Purified recombinant sLOX-1-CTLD domain is produced in a monomeric form lacking the disulphide bonds that are required to form dimers. The sLOX-1-CTLD domain after first wash before refolding (W1), after eluting from the Ni-NTA resin (E) and the purified monomeric form before refolding process (P). The pattern of heavy smearing seen in elution samples is expected due to the high salt concentration in the elution buffer. (B) Purified dimers and monomers of sLOX-1-CTLD domain (35, 17 kDa respectively) when the protein is partially reduced using DTT and denaturation at 72°C for 1 min (PR). In fully reducing conditions with DTT and incubation at 72 °C for 5 min (R), the monomeric form of sLOX-1-CTLD is only seen. These were compared to induced (IN) and uninduced (UN) bacterial cell lysates.

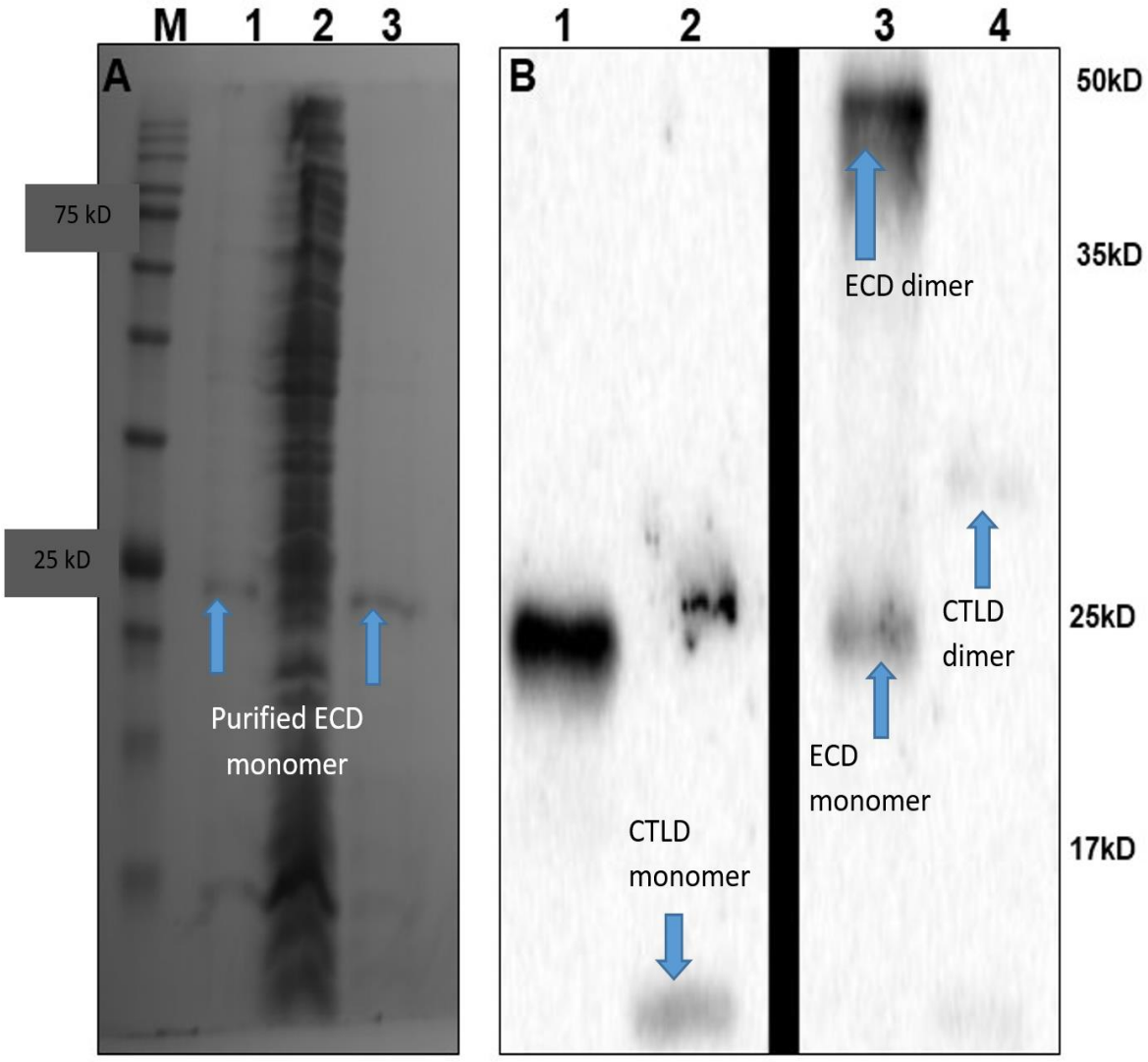

Figure3.6: SDS-PAGE analysis of reduced and non-reduced sLOX-1 proteins. (A) Purified denatured sLOX-1-ECD is produced lacking the disulphide bonds that are required to form sLOX-1 dimers. To reform these dimers the protein undergoes a process of refolding (chapter 2). Lane 1, the sLOX-1-ECD domain after first wash before refolding (W1), after eluting from the Ni-NTA resin (E) and the purified monomeric form before refolding process. The pattern of heavy smearing seen in elution samples is expected due to the high salt concentration in the elution buffer (lane 2). (B) Purified non-reduced sLOX-1-ECD (lane 3), sLOX-1-CTLD (lane 2), reduced dimers and monomers and of sLOX-1-ECD (lane 3) and sLOX-1-CTLD (lane 4). Molecular mass markers indicated on right hand side of panel.

3.5 Selection of LOX-1 specific Affimers

The Affimer phage display is a system used to match Affimers to target ligands. This system was first described by Tiede and co-workers at the University of Leeds (Tiede et al., 2014). Screening the sLOX-1 ECD domain previously identified five Affimers as LOX-1-specific. The process starts by capturing the biotinylated ECD domain on streptavidin-coated plates before adding an Affimer phage library which consist of 30 billion random-structure Affimers. After a period of incubation, the un-bound Affimers were washed and the ones with affinity to ECD were eluted. These then were incorporated in E.coli ER2738 strain to amplify their numbers and then used to target ECD in another round of panning. After repeating the phage-display for 3 times the strongest binding Affimers remain and these were the LOX-1-specific Affimers. Using bacteriophage genome, these Affimers were then cloned into pET-11a expression vectors and the resultant plasmid can later be used for protein production in E.coli BL21*(DE3) strain. The Affimers are labelled as A1, A3, B1, G1 and H1. Figure 3.7 shows a schematic diagram of the process of panning.

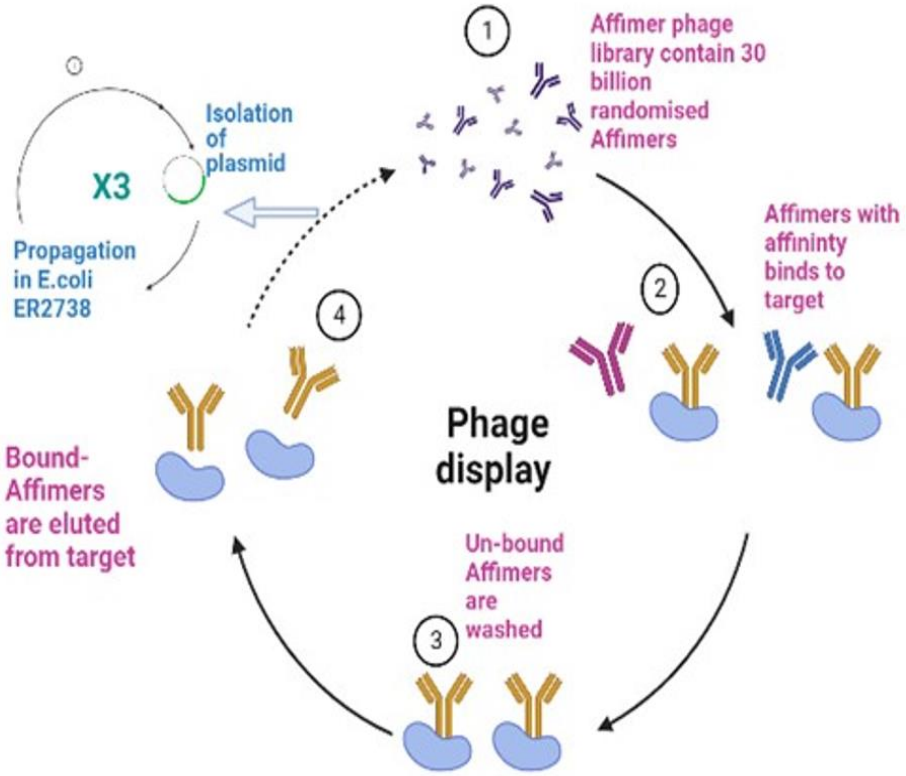

Figure 3.7: Screening and purification of LOX-1-specific Affimers. Schematic showing rounds of panning of an Affimer-based phage display library over immobilized sLOX-1-ECD protein. Created using BioRender.com.

3.6 Expression and purification of LOX-1-specific Affimers

Unlike the process of LOX-1 purification where refolding is required to reform the disulphide bonds between the monomers, Affimers lack disulphide bonds and rapidly form a folded stable structure; hence Affimer purification from E.coli is a single step process. The plasmids of the five LOX-1-specific Affimers which were previously isolated by the BioScreening Technology Group (BSTG) were subcloned into pET-11a bacterial expression vectors (Tang et al., 2017; Tiede et al., 2014). Induction using IPTG is the rate limiting step in the production pathway after which step the cells were lysed and the lysates were incubated with Ni-NTA resin that binds to the Affimers but not the other proteins. These were then washed until protein fractions were at negligible concentrations. High imidazole (250 mM) buffer was then used to elute bound Affimers from the Ni-NTA resin. Fractions during the Affimer purification process were analysed using SDS-PAGE (Figure 3.8).

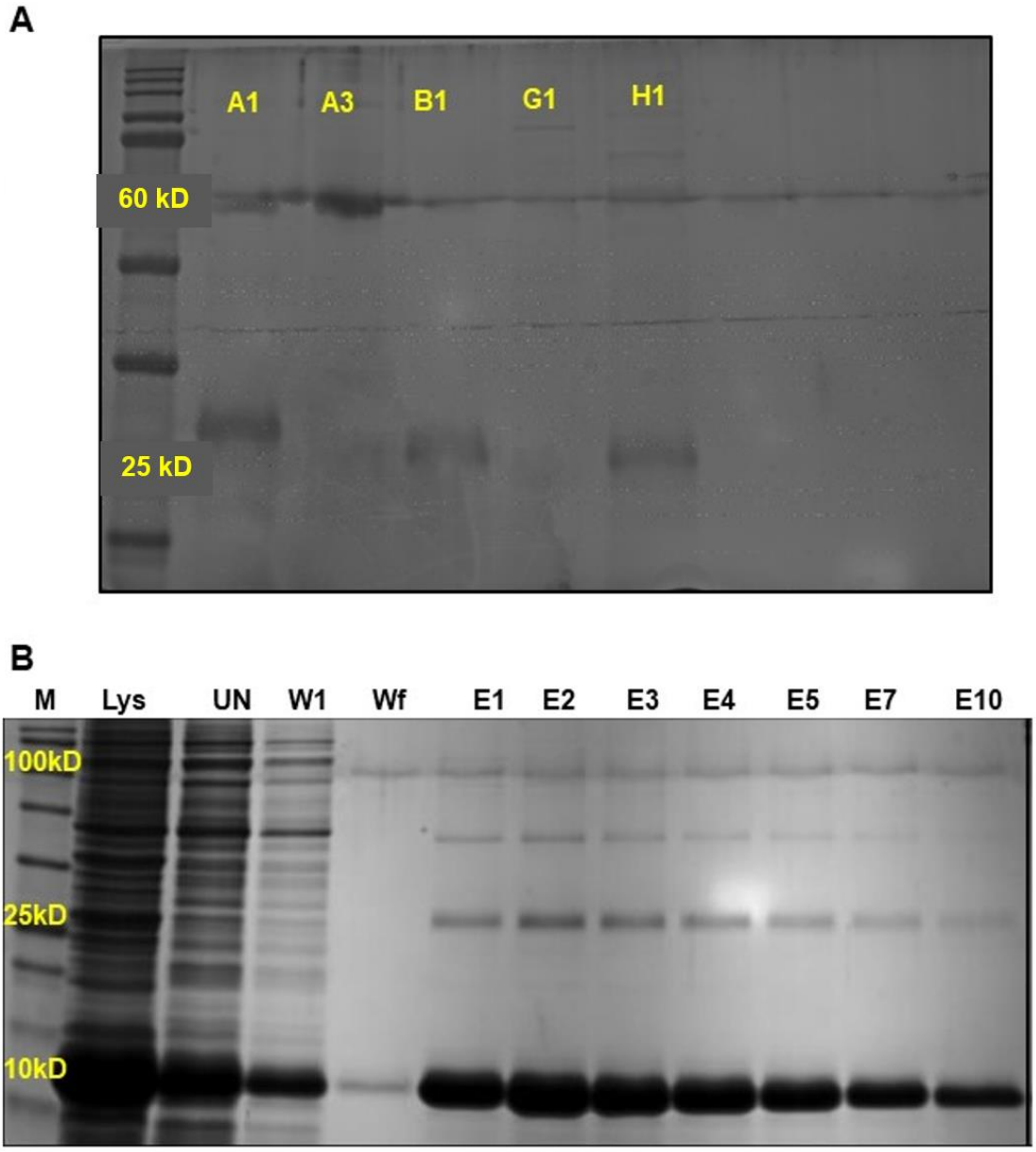

Figure 3.8: SDS-PAGE analysis of purified Affimers. (A) Purified Affimers were purified as described in Materials and Methods. 5 µg of each Affimer was analysed using 12% SDS-PAGE. Affimers showed bands at 60 kDa (tetramer) and 30 kDa (dimer). Very faint bands are seen at around 15 kDa representing the monomeric Affimer form. Affimer G1 routinely gave the lowest yield and is only present at very low amounts. (B) Different stages of purification of Affimer H1 from bacteria. Key: M, protein marker; Lys, lysate proteins following cell lysis; UN, unbound proteins; W1, proteins following the 1st was after lysis; Wf, proteins after final wash; E, elution with respective number of batch elution step.

3.7 Affimers as LOX-1 probes using blotting technique

Testing Affimers as LOX-1-specific probes was needed to assess their use in different assays. One test is to use the purified Affimers and assess binding to sLOX-1-ECD or sLOX-1-CTLD; a comparison to anti-LOX-1 antibodies (positive control) and BSA (negative control) was used under blotting conditions. Multiple samples of sLOX-1-ECD, sLOX-1-CTLD, BSA and HEK293-LOX-1-FLAG cell lysates were probed using blotting techniques. The antibodies were used in sequence as follows:

Affimers were used directly on the membrane strips. All were labelled and incubated for 24 h at room temperature before preparing for digital imaging. Affimers showed comparable ability to detect LOX-1 protein domains on Western blots compared to the standard anti-LOX-1 antibodies (Figure 3.6). This required further validation to ensure that the binding is linked to the variable loop of the Affimers and hence the next step was to directly label the Affimers and use these as probes for recombinant sLOX-1 proteins.

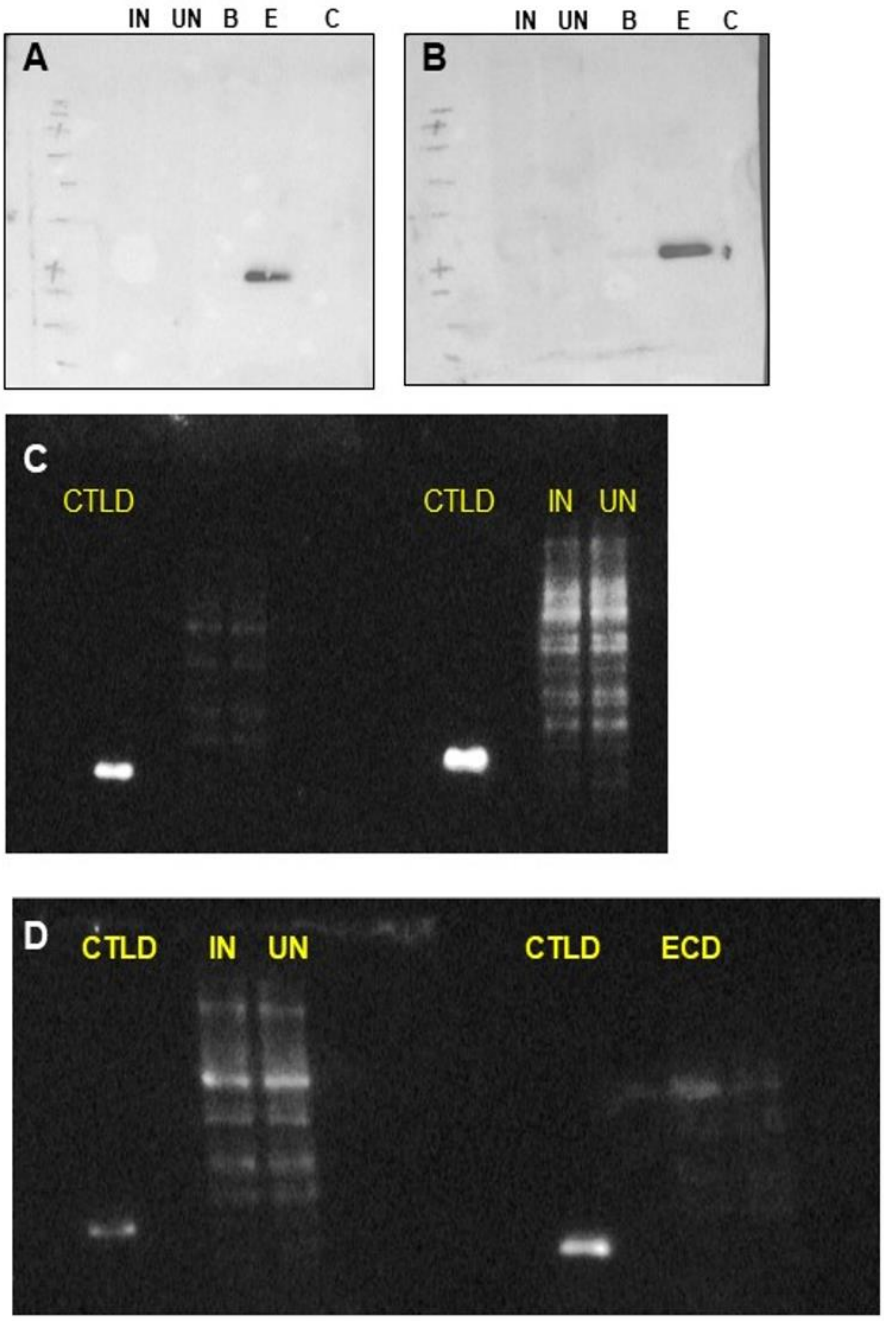

Figure 3.9: Comparison of antibody and Affimer-based detection of LOX-1 proteins using blotting techniques. (A, B) Sheep-anti-LOX-1 antibodies used at (A) 0.1 µg/ml or (B)1 µg/ml used to detect sLOX-1-ECD (E). For comparison, BSA (B) and CTLD (C) were used; these were not recognised bysheep anti-LOX-1. (C) Affimer A1 (left) was compared to anti-FLAG M2 antibody (right) to detect purified CTLD domain in blots (D). Sheep anti-LOX-1 antibodies (left) to vs. Affimer H1 (right) detecting sLOX-1 CTLD and ECD proteins. Key: IN, induced lysates; UN, un-induced lysates; B, Bovine serum albumin; E, sLOX-1-ECD; C, sLOX-1-CTLD.

3.8 Affimer labelling and applications

3.8.1 Maleimide-based biotinylation of Affimers

Labelling of antibodies and proteins including Affimers is a useful approach to assess ligand recognition, abundance and distribution in cells and tissues. Besides these features it also adds to the specificity of the interaction with the target. All the LOX-1-specific Affimers contain an added cysteine residue at the end of the C-terminus. This allows using the maleimide chemistry to label the Affimers. The process is done immediately after the Affimers are purified and eluted from the Ni-NTA resin. The Affimers were incubated with washed TCEP (Tris(2-carboxyethyl)phosphine hydrochloride) resin to break any preformed di-cysteine bonds between Affimers and freeing the cysteine residues to bind to biotin. Following this the Affimers were added to maleimide-conjugated biotin and the unbound biotin is removed using desalting columns. The conjugated Affimers were then run alongside the unconjugated counterparts in a 12% SDS-PAGE gel and transferred into a nitrocellulose membrane which was then probed with streptavidin-HRP (Figure 3.10). Multiple attempts using maleimide-biotin to label Affimers were not successful. The use of alternate reducing agents such as DTT, heating the samples before SDS-PAGE and finally using ELISA to check for biotinylation was again not successful.

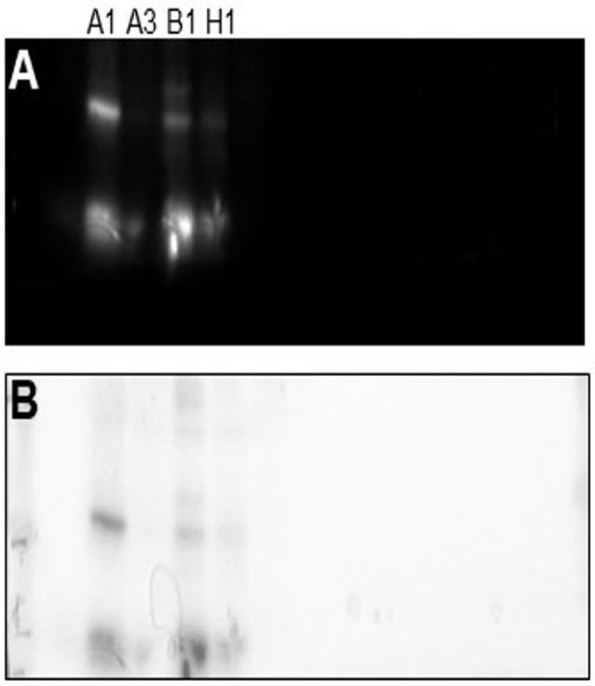

Figure 3.10: Biotinylation of Affimers. (A, B) LOX-1-Specific Affimers A1, A3, B1 and H1 (5 µg/sample well) on a 12% SDS-PAGE gel and in the following well spaces the maleimide-biotinylated counterparts were loaded. These were then transferred into a nitrocellulose membrane and probed with streptavidin-HRP and ECL. As shown the unlabelled Affimers are displaying a monomeric and dimeric forms, however the biotinylated Affimers are not showing any bands.

3.8.2 N-Hydroxysuccinimide-biotin labelling of Affimers

An alternative approach using NHS-biotin to label terminal amines on lysine residues was tried. The biotinylation process is simple and uses a fixed concentration of NHS in a high pH (pH>8.0) non-amine buffer. Affimers were incubated with 0.25 mg/ml of NHS-biotin for 30-60 min and then desalting columns were used to remove the excess biotin. Affimers and the NHS-biotinylated Affimers were analysed by SDS-PAGE and then blotted before probing with streptavidin-HRP (Figure 3.11).

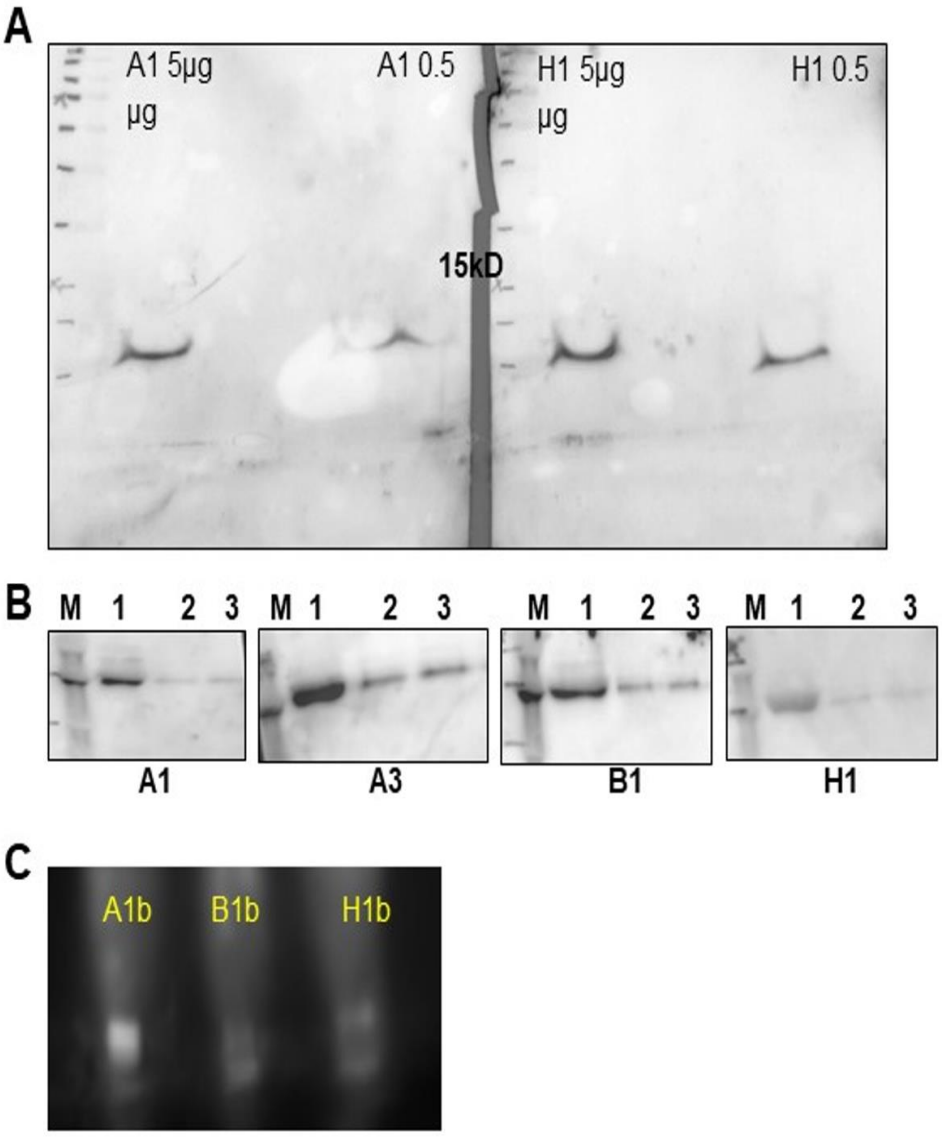

Figure 3.11: Western blot detection of sLOX-1 using NHS-biotinylated Affimers. (A) Biotinylated Affimers A1 and H1 loaded at 5 µg and 0.5 µg in SDS-PAGE probed with streptavidin-HRP and ECL detection.(B) Loading of different Affimers at 5 µg, 2 µg and 1 µg of each Affimer and detection using streptavidin-HRP and ECL. (C) Comparison of NHS-biotinylated Affimers to maleimide-biotinylated and unlabelled Affimers. Only NHS-biotinylated Affimers show bands when probed with streptavidin-HRP and ECL.

3.5.2 Fluorescent labelling of Affimers

Affimers were labelled on the free cysteine residue with maleimide AlexaFluor-488. Fluorescent Affimer-488 was detected using excitation with 488 nm light and detection by emission at 520 nm. These showed that AF488-labelled Affimer could indeed be detected for all 5 purified Affimers (Figure 3.11). SDS-PAGE and Coomassie Blue staining was used to check the presence of Affimer protein bands (Figure 3.12). Thus fluorescent Affimer probes could be made using this approach.

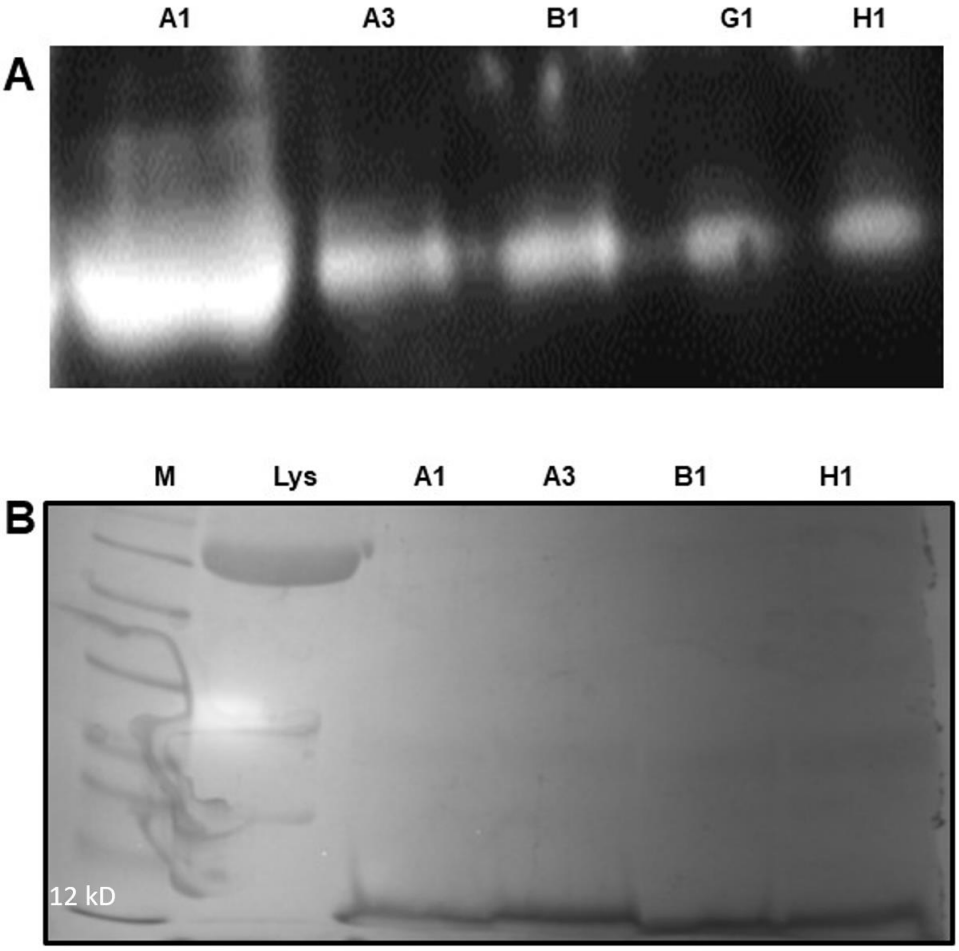

Figure3.12: Fluorescent Affimers. AlexaFluor-488 labelling of LOX-1-specific Affimers. (A) Analysis of AF488-labelled Affimers after SDS-PAGE imaged at 488 nm excitation and 520 nm emission. (B) Coomassie Blue stained SDS-PAGE gel to confirm the presence of Affimer protein bands. Key: Lys, Lysates; M, Protein marker.

3.9 Labelled Affimers as probes on Western blots

Biotinylated Affimers were used to assess recognition of purified recombinant sLOX-1-ECD and sLOX-1-CTLD domains. A 96-well ELISA plate was used to immobilize the ECD and CTLD domains of human sLOX-1 and simultaneously mouse LOX-1 and bovine serum albumin (BSA) and water were used as negative controls or to test cross-reactivity. Biotinylated Affimers were then added to the plate wells compared to anti-human VEGFR1-specific Affimer 37c (negative control) which shares the same basic structure as LOX-1-specific Affimers but differs in the structure of the variable regions which binds to antigens such as LOX-1. This is to ascertain the specificity of Affimer recognition in the assay. After this the unbound Affimers were removed and streptavidin-HRP was added to probe for biotinylated bound Affimers. By using a specific HRP substrate i.e. ONPD, this was used to detect (Figure 3.13).

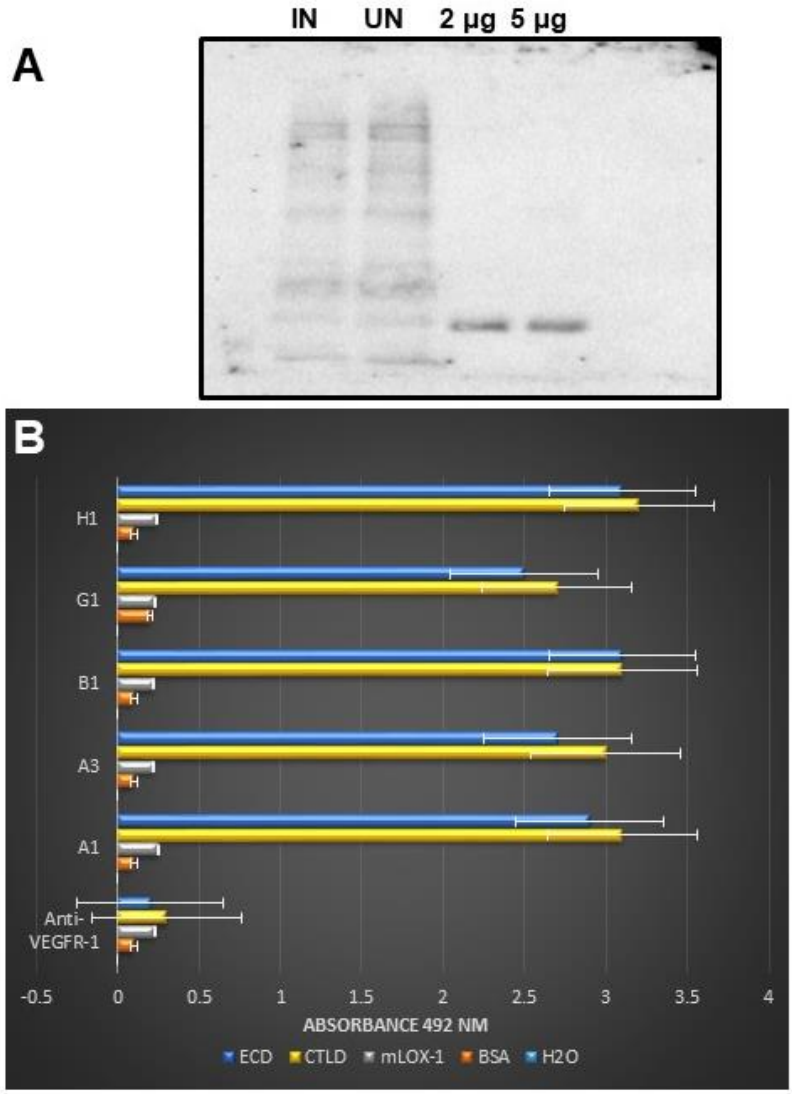

Figure 3.13: Biotinylated Affimer application for LOX-1 detection. (A) NHS-biotinylated H1 Affimer used to detect sLOX-1-ECD at 2 µg and 5 µg loaded onto SDS-PAGE. These were tested alongside HEK-293-LOX-1 cell lysates (LOX-1-FLAG, ~ 40 kD). Blots were probed with streptavidin-HRP and ECL. (B) 96-well plates were incubated with recombinant human sLOX-1-ECD (extracellular domain) or sLOX-1-CTLD (C-type lectin domain) variants or recombinant mouse sLOX-1 (msLOX-1). BSA and blank wells were negative controls. Recombinant sLOX-1 proteins detected using biotinylated Affimers followed by streptavidin-HRP. The anti-VEGFR1 Affimer 37C was a negative control. After addition of TMB substrate, the OD450 was read after 5, 15 and 30 min. The 15 min dataset is displayed. Error bars show mean ±1 SD. Significance tested by 2- way ANOVA 37c negative control Affimer.

3.10 Using Affimers as probes for LOX-1 on HEK293-LOX-1-FLAG cells

The need for showing the expression of LOX-1 on Human Endothelial Kidney (HEK293-LOX-1-FLAG) cells was required before testing the ability to detect the protein using Affimers. As LOX-1 is linked to apoptosis, studying its functions on cells is challenging (Li and Mehta, 2009). Using tetracycline induction is a system that was created to overcome the apoptosis and allow study of LOX-1 functions (Abdul-Zani, 2017). These cells were induced with tetracycline along a negative control HEK293 cells that were transfected with an empty plasmid (empty vector) and after incubating the induced cells for 16 hours, sheep anti-LOX-1 antibodies were used to demonstrate the presence of LOX-1. As shown in Figure 3.14, the HEK293-LOX-1-FLAG expressed LOX-1 as opposed to the empty vector cells.

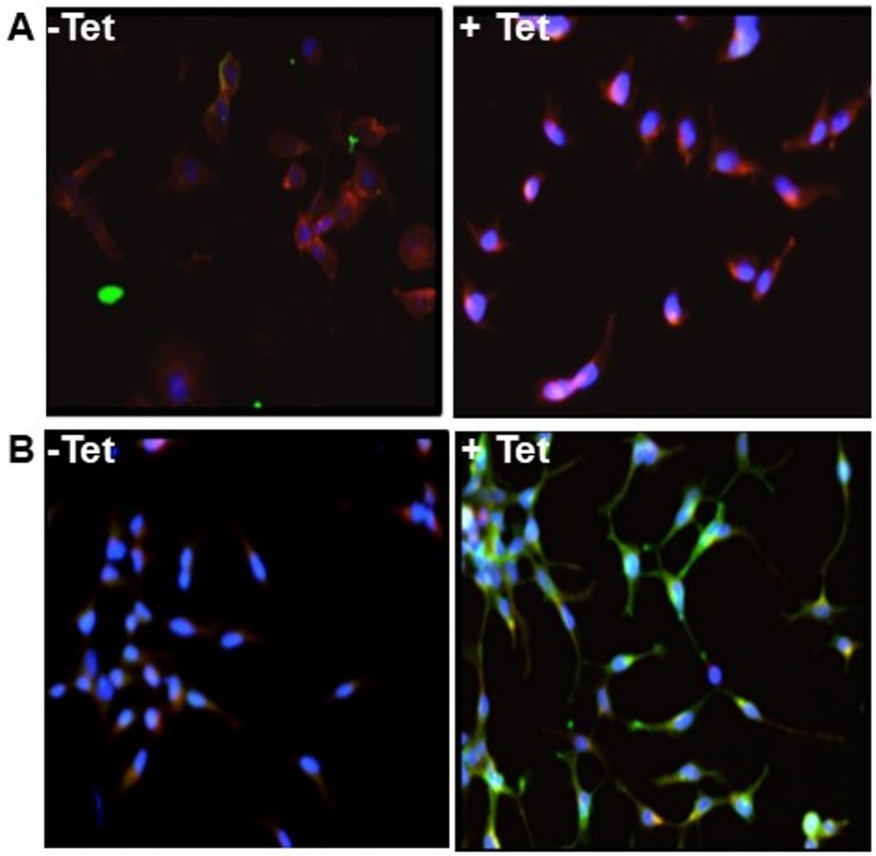

Figure 3.14: Tetracycline-regulated expression of human LOX-1. (A) Empty vector HEK293 cells induced with tetracycline and probed with sheep anti-LOX-1 Antibodies. (B) HEK293-LOX-1 cell line induced with tetracycline probed with sheep anti-LOX-1. Sheep anti-LOX-1 (green) and nuclear stain DAPI (blue).

The same experiment was repeated and the cells were probed with AlexaFluor-488 labelled Affimer A1 and the uptake was assessed using fluorescent microscopy (Figure 3.15). LOX-1-expressing HEK293 cells labelled for AF488-Affimer A1 (Figure 3.15A), but not for control cells lacking LOX-1 expression (Figure 3.15B).

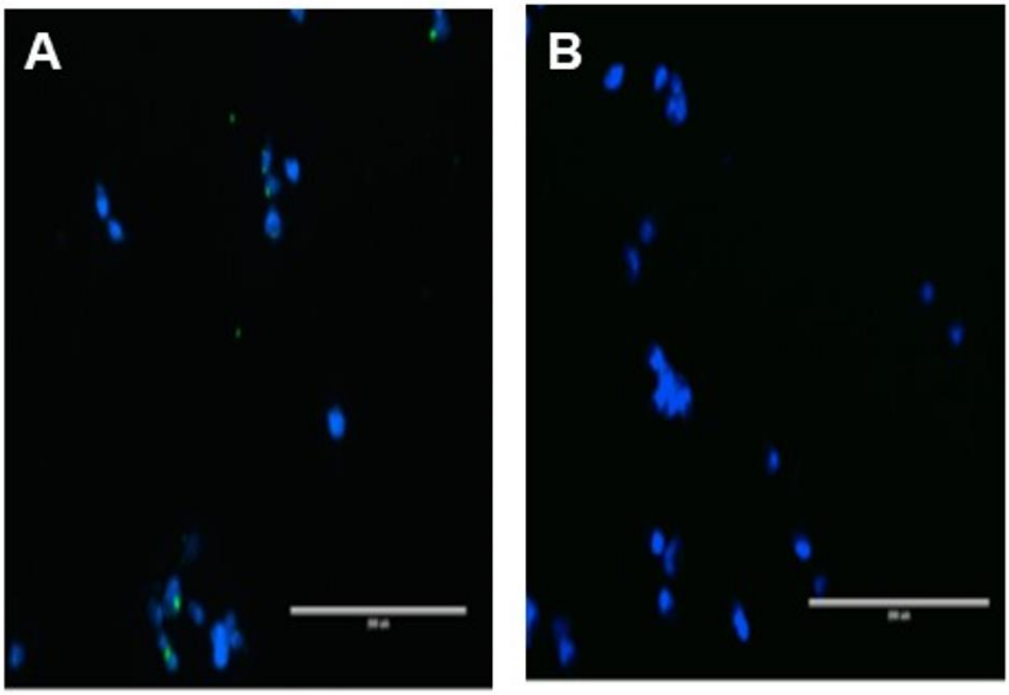

Figure3.15: Labelled Affimer uptake by LOX-1-expressing cells. (A) Tetracycline-induced HEK293-LOX-1-FLAG cells when incubated with AlexaFluor-488-labelled Affimer A1 for 2 h. The uptake of labelled Affimer appears as dots (green, arrows). (B) Tetracycline induced-Empty Vector HEK293 cells incubated with labelled Affimer A1. As expected there is no fluorescence visible.

3.11 Using Affimers to block LOX-1-dependent ox-LDL uptake

As shown previously, LOX-1-specific Affimers can bind to membrane LOX-1 protein. This offers a potential to examine the ability of these Affimers to inhibit the uptake of oxLDL into cells. HEK293-LOX-1-FLAG cells along with Empty Vector (EV) HEK293 cells as controls were used and incubated with variable concentrations of Affimers for 2 hours. Then these were incubated with Dil-Labelled oxLDL (see Materials and Methods for details) for 15 min before fixing the cells and imaging them using fluorescent microscopy. The Affimers displayed the ability to inhibit the uptake of oxLDL in LOX-1-FLAG cells and the inhibition was Affimer concentration dependent (Figure 3.16). The inhibition of oxLDL uptake seems is maximal at 1 µg/ml Affimer concentration; additional increase in Affimer levels shows minimal additional inhibitory effects (Figure 3.16).

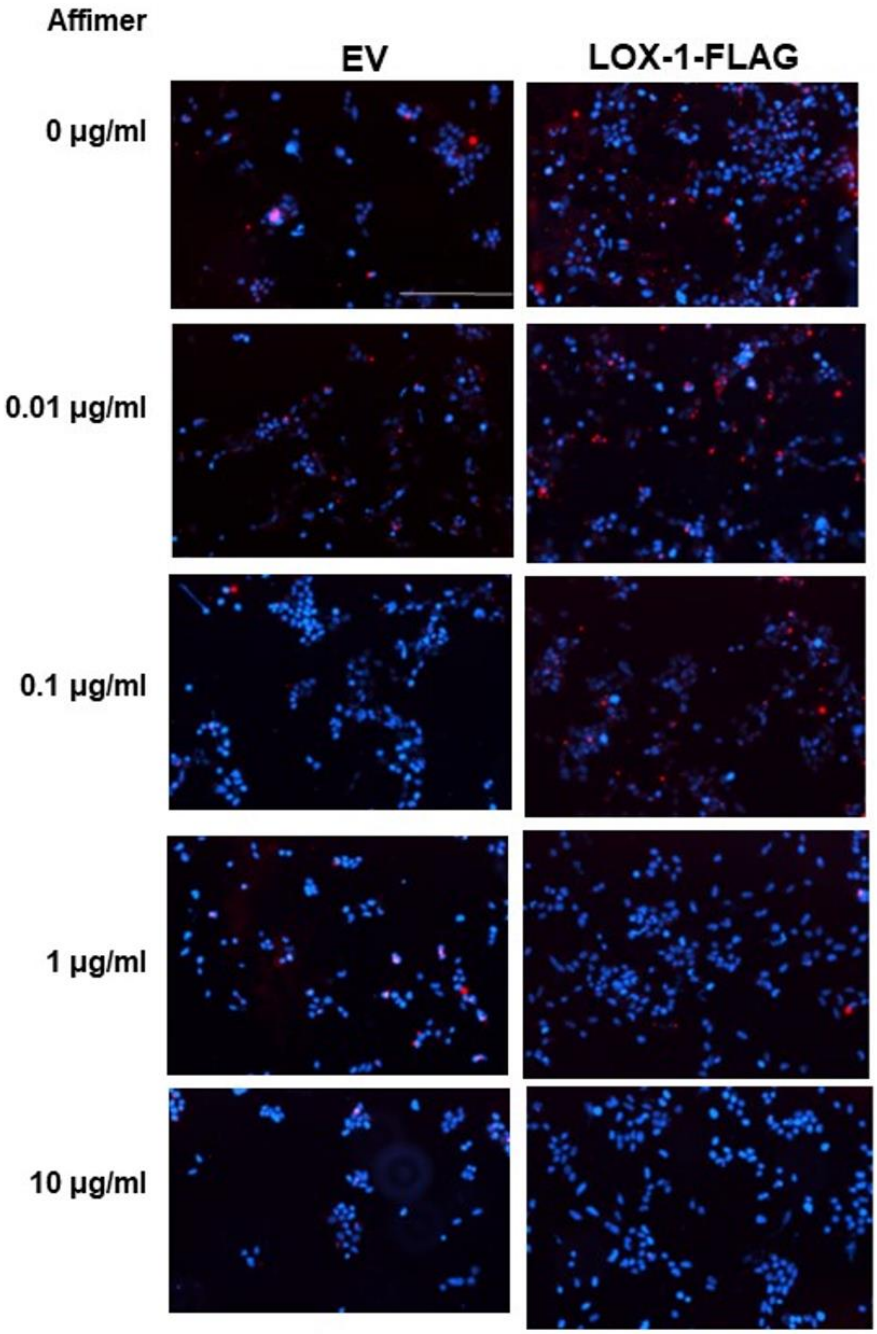

Figure 3.16: Affimer effects on labelled oxLDL uptake in HEK293 cells. Fluorescence microscopy imaging of HEK293 cells transfected with empty vector and cell nuclei (blue) induced overnight then incubated with variable concentration of A1 Affimer. Labelled DiI-oxLDL (red) uptake is inversely proportional to the Affimer A1 concentration. Inhibitory plateau was reached at a concentration of 1 µg/ml A1 Affimer. Scale bar, 200 µm.

Chapter 4

4. Discussion

4.1 General discussion

As per the report of Public Health England, ischaemic heart disease and stroke are two of the three leading causes of death (Public Health England, 2017). Although the pathophysiology of ischaemic heart disease and stroke is multifactorial (Marzilli et al., 2012; Deb et al., 2010), but atherosclerosis is a fundamental contributor in their development (Marulanda-Londoño and Chaturvedi, 2016; Hansson, 2005). Furthermore, atherosclerosis carries significant associated morbidity, particularly in the context of its additional manifestations, such as peripheral arterial disease (Malyar et al., 2013). These clinical manifestations are major factors in the burden of health systems across the globe and constitute a large area of expenditure in direct disease management and rehabilitation as well as in the social and economic aspects of living (Herrington et al 2016).

Atherosclerosis is a complex process that is driven by a chronic inflammatory reaction that is believed to start with endothelial dysfunction resulting in influx of inflammatory cells and oxidized lipid particles in the endothelial cells, eventually leading to progressive stenosis of the arterial lumen (Hadi et al., 2005). LOX-1 receptors are members of the scavenger receptors family and their overexpression is linked to the development and progression of atherosclerosis (Akhmedov et al., 2014). The evidence from animal studies confirmed this association and also proved that the composition of the atherosclerotic plaque differs between LOX-1 knockout mice and wild-type mice (Hu et al., 2008). LOX-1 knockout mice developed collagen-enriched stable plaque while wild-type mice developed cholesterol-rich plaques in the wild-type mice which are more liable for rupture and embolization, resulting in end organ ischaemic manifestations (Hsieh et al., 2001).

Cohort studies of LOX-1 polymorphisms and its linkage to cardiovascular risk demonstrated that circulating sLOX-1 in the blood can be a biomarker for disease states (Kume et al., 2010; Kobayashi et al., 2011; Fukui et al., 2013). There is an interaction between the SR family and up regulation of one member could lead to alteration of the expression of the others. These factors pose a challenge to targeted therapy to scavenger receptors with possible interaction to wider range of targets within or outside and the scavenger receptor family (Fukui et al., 2013).

Thus, the identification of molecules that target LOX-1 function is of great interest for basic research and translation medicine. To address this question in this study, we describe the isolation and characterization of Affimers as synthetic protein-binding residues for LOX-1. Affimer-based bacteriophage library was screened using phage display and identified five independent clones that bound human LOX-1 (Tiede et al., 2014). This work describes the characterization of such agents and the future application of Affimers as diagnostic or therapeutic agents, with the aim of developing new techniques to study LOX-1. These Affimers bind directly to purified human LOX-1, but the two Affimers also demonstrated lower affinity to mouse LOX-1. Affimer-binding epitopes on LOX-1 have been mapped to the CTLD ligand-binding domain. A tetracycline-inducible human LOX-1 cell expression model was used to assess its LOX-1-specific Affimer effects on cells. Fluorophore-labelled Affimers have been shown to bind to LOX-1 proteins expressed on the cell membrane. Cell incubation with Affimers has been shown to inhibit the uptake of DiI-tagged oxLDL by LOX-1-expressing cells. Furthermore, Affimers A1 and H1 were shown to modulate oxLDL stimulation and LOX-1-dependent activation of atherogenic signalling pathways, particularly inhibition of oxLDL-stimulated LOX-1-dependent ERK1/2 activation. Affimers provide more target-specific properties, thus studying this specificity and implications may offer solutions to the challenges raised by Fukui and his group in their 2013 study.

4.2 LOX-1 therapeutic potentials and implications

The consensus is that LOX-1 is a strong candidate for therapeutic intervention. Deletion or dysfunction of the OLR1 locus in mice indicates that LOX-1 is non-essential (Mehta et al., 2007). However, caution should be taken with this view, as LOX-1 has been found to have both beneficial and detrimental functions depending on the cell or tissue type. The seminal work of Brown, Goldstein, and colleagues established the liver as a key site of lipid particle metabolism associated with vascular health and disease (Brown and Goldstein, 1986). Perturbation of lipid particle metabolism in the liver can influence atherosclerotic plaque formation and progression (Kleemann et al., 2007). Liver benefactors (Wang et al., 2022) or arterial invaders (Akinnusi et al., 2011; Miao et al., 2022; Tie et al., 2010; Yang et al., 2022) and their roles in oxLDL uptake for signal transduction and as oxLDL sensors for signal transduction, respectively. Transport, processing, and recycling of LOX-1 concurrently with signalling to different signalling pathways is further complicated by heterogeneity in the regulation of signalling pathways in different cell types and tissues. Increased LOX-1 expression in the liver appears to be beneficial. However, the opposite is true for other tissues, especially endothelium, smooth muscle, immune cells and white blood cells. Therefore, therapies targeting LOX-1 should be evaluated with caution. Systemic inhibition of LOX-1 may prove to be of little benefit or adverse side effects for patients. This is especially true when hepatic oxLDL clearance is impeded by systemic inhibition of LOX-1 function. A better approach for LOX-1-specific therapy might be based on specific targeting of fatty and lipid-rich plaques or lesions in the arterial vessel wall to preserve liver lavage function.

LOX-1 is also involved in the recognition of bacterial cells, senescent and apoptotic cells, suggesting additional roles in immunity (Murphy et al., 2006; Oka et al., 1998). This fits with its structure as a C-type lectin domain protein and its genetic localization on the short arm of human chromosome 12, a region rich in innate immunity genes. Therefore, the pathological functions of LOX-1 are specifically targeted. Interactions with oxLDL for therapeutic intervention should be carefully considered to gain beneficial

functions in immune surveillance. Currently, the exact mechanism of LOX-1 recognition by ligands is poorly defined, complicating drug or therapeutic design.

By identifying specific LOX-1 residues important for differential identification of ligands such as oxLDL and bacteria, it may be possible to target proatherogenic LOX-1 activity. Mapping different epitopes recognized by LOX-1-specific Affimers may potentially tune different antiatherogenic effects in cell and animal models. A similar strategy using antibodies has enabled better targeting of antigens for therapy (Guo et al., 2022). Negative selection can also be applied to Affimer screening by eliminating clones that bind unwanted epitopes, LOX-1 epitopes that mediate bacterial recognition or immune-related functions.

4.3 Affimer-LOX-1 applications

Affimer technology existed to overcome the pitfalls caused by using the conventional antibody-mediated targeting which was discussed in Chapter 1. However, with evolution of this technology, further uses of Affimers were noted. For instance, Affimer resin was used to isolate fibrinogen from plasma in a selective and rapid process (Pechlivani et al., 2022). The quality of this fibrinogen was better compared to the commercially available recombinant substitute (Pechlivani et al., 2022). There are pitfalls in the complex antibody-based technology with requirements of biochemical conditions resulting in increased cost of the whole procedure and more risk of technical failure given the dependency of the sequence of steps on each other (Pechlivani et al., 2022). Affimers on the other hand overcome these issues, thus can reduce the cost of the procedure and result in a more reliable result (Pechlivani et al., 2022). Similarly, this module could be applied to the use of Affimers in vascular pathology. By isolating and amplifying LOX-1-specific Affimers, they could be used as biomarkers of atherosclerosis in diagnostic and prognostic implications.

4.4 Conclusions and future work

In this work we described the process of purification and testing of five LOX-1-specific Affimers and their potential use in cellular identification of LOX-1 and blocking the pro-atherogenic pathways resulting from oxLDL interaction with LOX-1 receptors. Further work is required on the application of these interactions in animal tissue modules as well as in testing on healthy and diseased human tissues which will be a rate-limiting step in the development of diagnostic and therapeutic implications of Affimers in vascular disease. Further quantitative experimental work on the Affimers inhibition of ox-LDL uptake by LOX-1 is also required on cellular and tissue levels.

References

Abdul Zani, I., Stephen, S.L., Mughal, N.A., Russell, D., Homer-Vanniasinkam, S., Wheatcroft, S.B. and Ponnambalam, S., 2015. Scavenger receptor structure and function in health and disease. Cells, 4(2), pp.178-201.

Almeida, S.O. and Budoff, M., 2019. Effect of statins on atherosclerotic plaque. Trends in cardiovascular medicine, 29(8), pp.451-455.

Anitschkow, N. 1913. Ueber experimentelle Cholesterinsteatose und ihre Bedeutung fur die Entstehung einiger pathologischer Prozesse. Zentralbl Allg Pathol.

Antonopoulos, A.S., Margaritis, M., Lee, R., Channon, K. and Antoniades, C., 2012. Statins as anti-inflammatory agents in atherogenesis: molecular mechanisms and lessons from the recent clinical trials. Current pharmaceutical design, 18(11), p.1519.

Bertelsen, A.B., Hackney, C.M., Bayer, C.N., Kjelgaard, L.D., Rennig, M., Christensen, B., Sørensen, E.S., Safavi-Hemami, H., Wulff, T., Ellgaard, L. and Nørholm, M.H., 2021. DisCoTune: versatile auxiliary plasmids for the production of disulphide-containing proteins and peptides in the E. coli T7 system. Microbial Biotechnology, 14(6), pp.2566-2580.

Binder, C.J., Papac-Milicevic, N. and Witztum, J.L., 2016. Innate sensing of oxidation-specific epitopes in health and disease. Nature Reviews Immunology, 16(8), pp.485-497.53. Boullier, A., Gillotte, K.L., Hörkkö, S., Green, S.R., Friedman, P., Dennis, E.A., Witztum, J.L., Steinberg, D. and Quehenberger, O., 2000. The binding of oxidized low density lipoprotein to

mouse CD36 is mediated in part by oxidized phospholipids that are associated with both the lipid and protein moieties of the lipoprotein. Journal of Biological Chemistry, 275(13), pp.9163-9169.

Binz, H.K., Bakker, T.R., Phillips, D.J., Cornelius, A., Zitt, C., Göttler, T., Sigrist, G., Fiedler, U., Ekawardhani, S., Dolado, I. and Saliba, J.A., 2017, November. Design and characterization of MP0250, a tri-specific anti-HGF/anti-VEGF DARPin® drug candidate. In MAbs (Vol. 9, No. 8, pp. 1262-1269). Taylor & Francis.

Binz, H.K., Stumpp, M.T., Forrer, P., Amstutz, P. and Plückthun, A., 2003. Designing repeat proteins: well-expressed, soluble and stable proteins from combinatorial libraries of consensus ankyrin repeat proteins. Journal of molecular biology, 332(2), pp.489-503.

Biocca, S., Falconi, M., Filesi, I., Baldini, F., Vecchione, L., Mango, R., Romeo, F., Federici, G., Desideri, A. and Novelli, G., 2009. Functional analysis and molecular dynamics simulation of LOX-1 K167N polymorphism reveal alteration of receptor activity. Plos one, 4(2), p.e4648.

Blais, J.E., Wei, Y., Yap, K.K., Alwafi, H., Ma, T.T., Brauer, R., Lau, W.C., Man, K.K., Siu, C.W., Tan, K.C. and Wong, I.C., 2021. Trends in lipid-modifying agent use in 83 countries. Atherosclerosis, 328, pp.44-51.

Boisvert, W.A., Santiago, R., Curtiss, L.K. and Terkeltaub, R.A., 1998. A leukocyte homologue of the IL-8 receptor CXCR-2 mediates the accumulation of macrophages in atherosclerotic lesions of LDL receptor-deficient mice. The Journal of clinical investigation, 101(2), pp.353-363.

Bork, P., 1993. Hundreds of ankyrin-like repeats in functionally diverse proteins: mobile modules that cross phyla horizontally?. Proteins: Structure, Function, and Bioinformatics, 17(4), pp.363-374.

Bossaller, L. and Rothe, A., 2013. Monoclonal antibody treatments for rheumatoid arthritis. Expert opinion on biological therapy, 13(9), pp.1257-1272.

Bradbury, A.R. and Plückthun, A., 2015. Getting to reproducible antibodies: the rationale for sequenced recombinant characterized reagents. Protein Engineering, Design and Selection, 28(10), pp.303-305.

Buhaescu, I. and Izzedine, H., 2007. Mevalonate pathway: a review of clinical and therapeutical implications. Clinical biochemistry, 40(9-10), pp.575-584.

Cannon, C.P., Braunwald, E., McCabe, C.H., Rader, D.J., Rouleau, J.L., Belder, R., Joyal, S.V., Hill, K.A., Pfeffer, M.A. and Skene, A.M., 2004. Intensive versus moderate lipid lowering with statins after acute coronary syndromes. New England journal of medicine, 350(15), pp.1495-1504.

Canton, J., Neculai, D. and Grinstein, S., 2013. Scavenger receptors in homeostasis and immunity. Nature Reviews Immunology, 13(9), pp.621-634.

Cavieres, V., Valdes, K., Moreno, B., Moore-Carrasco, R. and Gonzalez, D.R., 2014. Vascular hypercontractility and endothelial dysfunction before development of atherosclerosis in moderate dyslipidemia: role for nitric oxide and interleukin-6. American Journal of Cardiovascular Disease, 4(3), p.114.

Chong, P.H., Seeger, J.D. and Franklin, C., 2001. Clinically relevant differences between the statins: implications for therapeutic selection. The American journal of medicine, 111(5), pp.390-400.

Conrath, K., Vincke, C., Stijlemans, B., Schymkowitz, J., Decanniere, K., Wyns, L., Muyldermans, S. and Loris, R., 2005. Antigen binding and solubility effects upon the veneering of a camel VHH in framework-2 to mimic a VH. Journal of molecular biology, 350(1), pp.112-125.

Dolk, E., van der Vaart, M., Lutje Hulsik, D., Vriend, G., de Haard, H., Spinelli, S., Cambillau, C., Frenken, L. and Verrips, T., 2005. Isolation of llama antibody fragments for prevention of dandruff by phage display in shampoo. Applied and environmental microbiology, 71(1), pp.442-450.

Ewert, S., Honegger, A. and Plückthun, A., 2004. Stability improvement of antibodies for extracellular and intracellular applications: CDR grafting to stable frameworks and structure-based framework engineering. Methods, 34(2), pp.184-199.

Fasan, R., Dias, R.L., Moehle, K., Zerbe, O., Obrecht, D., Mittl, P.R., Grütter, M.G. and Robinson, J.A., 2006. Structure–Activity Studies in a Family of β-Hairpin Protein Epitope Mimetic Inhibitors of the p53–HDM2 Protein–Protein Interaction. ChemBioChem, 7(3), pp.515-526.

Fasan, R., Dias, R.L., Moehle, K., Zerbe, O., Vrijbloed, J.W., Obrecht, D. and Robinson, J.A., 2004. Using a β-hairpin to mimic an α-helix: cyclic peptidomimetic inhibitors of the p53–HDM2 protein–protein interaction. Angewandte Chemie International Edition, 43(16), pp.2109-2112.

Firer, M.A. and Gellerman, G., 2012. Targeted drug delivery for cancer therapy: the other side of antibodies. Journal of hematology & oncology, 5(1), pp.1-16.

Fong, L.G., Parthasarathy, S., Witztum, J.L. and Steinberg, D., 1987. Nonenzymatic oxidative cleavage of peptide bonds in apoprotein B-100. Journal of lipid research, 28(12), pp.1466-1477.

Freeman, D.J., Norrie, J., Sattar, N., Neely, R.D.G., Cobbe, S.M., Ford, I., Isles, C., Lorimer, A.R., Macfarlane, P.W., McKillop, J.H. and Packard, C.J., 2001. Pravastatin and the development of diabetes mellitus: evidence for a protective treatment effect in the West of Scotland Coronary Prevention Study. Circulation, 103(3), pp.357-362.

Friedman, M. and Friedland, G.W., 1998. Medicine's 10 greatest discoveries. Yale University Press.

Gimbrone Jr, M.A. and García-Cardeña, G., 2016. Endothelial cell dysfunction and the pathobiology of atherosclerosis. Circulation research, 118(4), pp.620-636.

Gisterå, A. and Hansson, G.K., 2017. The immunology of atherosclerosis. Nature reviews nephrology, 13(6), pp.368-380.

Gitsels, L.A., Kulinskaya, E. and Steel, N., 2016. Survival benefits of statins for primary prevention: a cohort study. PloS one, 11(11), p.e0166847.

Gligorov, J., Pivot, X., Ataseven, B., De Laurentiis, M., Jung, K.H., Manikhas, A., Azim, H.A., Gupta, K., Alexandrou, A., Herraez-Baranda, L.

and Tosti, N., 2022. Safety and efficacy of adjuvant subcutaneous trastuzumab in human epidermal growth factor receptor 2-positive early breast cancer: Final results of the SafeHER study. The Breast, 64, pp.151-158.

Hafeez, U., Gan, H.K. and Scott, A.M., 2018. Monoclonal antibodies as immunomodulatory therapy against cancer and autoimmune diseases. Current opinion in pharmacology, 41, pp.114-121.

Hajar, R., 2017. Coronary heart disease: From mummies to 21st century. Heart views: the official journal of the Gulf Heart Association, 18(2), p.68.

Helma, J., Cardoso, M.C., Muyldermans, S. and Leonhardt, H., 2015. Nanobodies and recombinant binders in cell biology. Journal of Cell Biology, 209(5), pp.633-644.

Hinagata, J.I., Kakutani, M., Fujii, T., Naruko, T., Inoue, N., Fujita, Y., Mehta, J.L., Ueda, M. and Sawamura, T., 2006. Oxidized LDL receptor LOX-1 is involved in neointimal hyperplasia after balloon arterial injury in a rat model. Cardiovascular research, 69(1), pp.263-271.

Holt, L.J., Herring, C., Jespers, L.S., Woolven, B.P. and Tomlinson, I.M., 2003. Domain antibodies: proteins for therapy. TRENDS in Biotechnology, 21(11), pp.484-490.

Ignatowski, A., 1909. Über die Wirkung des tierischen Eiweisses auf die Aorta und die parenchymatösen Organe der Kaninchen. Virchows Archiv für pathologische Anatomie und Physiologie und für klinische Medizin, 198(2), pp.248-270.

Jenkins, T.P., Fryer, T., Dehli, R.I., Jürgensen, J.A., Fuglsang-Madsen, A., Føns, S. and Laustsen, A.H., 2019. Toxin neutralization using alternative binding proteins. Toxins, 11(1), p.53.

Jim, M.H., Ho, H.H., Siu, C.W., Miu, R., Chan, C.W.S., Lee, S.W.L. and Lau, C.P., 2007. Value of ST-segment depression in lead V4R in predicting proximal against distal left circumflex artery occlusion in acute inferoposterior myocardial infarction. Clinical Cardiology: An International Indexed and Peer-Reviewed Journal for Advances in the Treatment of Cardiovascular Disease, 30(1), pp.36-41.

Kaboord, B. and Perr, M., 2008. Isolation of proteins and protein complexes by immunoprecipitation. 2D PAGE: sample preparation and fractionation, pp.349-364.

Kataoka, H., Kume, N., Miyamoto, S., Minami, M., Morimoto, M., Hayashida, K., Hashimoto, N. and Kita, T., 2001. Oxidized LDL modulates Bax/Bcl-2 through the lectinlike Ox-LDL receptor-1 in vascular smooth muscle cells. Arteriosclerosis, thrombosis, and vascular biology, 21(6), pp.955-960.

Kattoor, A.J., Kanuri, S.H. and Mehta, J.L., 2019. Role of Ox-LDL and LOX-1 in Atherogenesis. Current medicinal chemistry, 26(9), pp.1693-1700.

Kim, Y.R., Park, J.H., Lee, H.J., Pyun, W.B. and Park, S.H., 2012. The effect of doubling the statin dose on pro-inflammatory cytokine in patients with triple-vessel coronary artery disease. Korean Circulation Journal, 42(9), pp.595-599.

Kobayashi, N., Hata, N., Kume, N., Seino, Y., Inami, T., Yokoyama, S., Shinada, T., Tomita, K., Kaneshige, T. and Mizuno, K., 2011. Soluble Lectin-Like Oxidized Low-Density Lipoprotein Receptor-1 as an Early Biomarker for ST Elevation Myocardial Infarction–Time-Dependent Comparison With Other Biomarkers–. Circulation Journal, 75(6), pp.1433-1439.

Kodama, T., Freeman, M., Rohrer, L., Zabrecky, J., Matsudaira, P. and Krieger, M., 1990. Type I macrophage scavenger receptor contains α-helical and collagen-like coiled coils. Nature, 343(6258), pp.531-535.

Köhler, G. and Milstein, C., 1975. Continuous cultures of fused cells secreting antibody of predefined specificity. nature, 256(5517), pp.495-497.

Konstantinov, I.E., Mejevoi, N. and Anichkov, N.M., 2006. Nikolai N. Anichkov and his theory of atherosclerosis. Texas Heart Institute Journal, 33(4), p.417.

Kore, R.A., Bagchi, A.K., Varughese, K.I. and Mehta, J.L., 2022. The structural basis of effective LOX-1 inhibition. Future Medicinal Chemistry, 14(10), pp.731-743.

Koutsoumpeli, E., Tiede, C., Murray, J., Tang, A., Bon, R.S., Tomlinson, D.C. and Johnson, S., 2017. Antibody mimetics for the detection of small organic compounds using a quartz crystal microbalance. Analytical chemistry, 89(5), pp.3051-3058.

Krittayaphong, R., Phrommintikul, A., Boonyaratvej, S., Ayudhya, R.K.N., Tatsanavivat, P., Komoltri, C., Sritara, P. and CORE Investigators, 2019. The rate of patients at high risk for cardiovascular disease with an optimal

low-density cholesterol level: a multicenter study from Thailand. Journal of Geriatric Cardiology: JGC, 16(4), p.344.

Kronzon, I. and Saric, M., 2010. Cholesterol embolization syndrome. Circulation, 122(6), pp.631-641.

Kuller, L., Borthani, N., Furberg, C., Gardin, J., Manolio, T., O'Leary, D., Psaty, B. and Robbins, J., 1994. Prevalence of subclinical atherosclerosis and cardiovascular disease and association with risk factors in the Cardiovascular Health Study. American journal of epidemiology, 139(12), pp.1164-1179.

Kume, N., Mitsuoka, H., Hayashida, K., Tanaka, M., Kominami, G. and Kita, T., 2010. Soluble lectin-like oxidized LDL receptor-1 (sLOX-1) as a sensitive and specific biomarker for acute coronary syndrome—comparison with other biomarkers. Journal of cardiology, 56(2), pp.159-165.

Kwak, B.R., Mulhaupt, F. and Mach, F., 2003. Atherosclerosis: anti-inflammatory and immunomodulatory activities of statins. Autoimmunity reviews, 2(6), pp.332-338.

LaRosa, J.C., Grundy, S.M., Waters, D.D., Shear, C., Barter, P., Fruchart, J.C., Gotto, A.M., Greten, H., Kastelein, J.J., Shepherd, J. and Wenger, N.K., 2005. Intensive lipid lowering with atorvastatin in patients with stable coronary disease. New England Journal of Medicine, 352(14), pp.1425-1435.

Lequin, R.M., 2005. Enzyme immunoassay (EIA)/enzyme-linked immunosorbent assay (ELISA). Clinical chemistry, 51(12), pp.2415-2418.

Levitan, I., Volkov, S. and Subbaiah, P.V., 2010. Oxidized LDL: diversity, patterns of recognition, and pathophysiology. Antioxidants & redox signaling, 13(1), pp.39-75.

Liao, J.K., 2002. Isoprenoids as mediators of the biological effects of statins. The Journal of clinical investigation, 110(3), pp.285-288.

Lipovšek, D.J.P.E., 2011. Adnectins: engineered target-binding protein therapeutics. Protein Engineering, Design & Selection, 24(1-2), pp.3-9.

Lu, R.M., Hwang, Y.C., Liu, I.J., Lee, C.C., Tsai, H.Z., Li, H.J. and Wu, H.C., 2020. Development of therapeutic antibodies for the treatment of diseases. Journal of biomedical science, 27(1), pp.1-30.

Lu, Z.F., Doulabi, B.Z., Wuisman, P.I., Bank, R.A. and Helder, M.N., 2007. Differentiation of adipose stem cells by nucleus pulposus cells: configuration effect. Biochemical and Biophysical Research Communications, 359(4), pp.991-996.

Luppa, P.B., Sokoll, L.J. and Chan, D.W. 2001. Immunosensors—principles and applications to clinical chemistry. Clinica Chimica Acta. 314(1–2), pp.1-26.

Magi, B. and Liberatori, S., 2005. Immunoblotting techniques. Immunochemical Protocols, pp.227-253.

Malekmohammad, K., Sewell, R.D. and Rafieian-Kopaei, M., 2019. Antioxidants and atherosclerosis: mechanistic aspects. Biomolecules, 9(8), p.301.

Manglik, A., Kobilka, B.K. and Steyaert, J., 2017. Nanobodies to study G protein–coupled receptor structure and function. Annual review of pharmacology and toxicology, 57, pp.19-37.

Mannarino, E. and Pirro, M., 2008. Endothelial injury and repair: a novel theory for atherosclerosis. Angiology, 59(2_suppl), pp.69S-72S.

Marques, L.R., Diniz, T.A., Antunes, B.M., Rossi, F.E., Caperuto, E.C., Lira, F.S. and Gonçalves, D.C., 2018. Reverse cholesterol transport: molecular mechanisms and the non-medical approach to enhance HDL cholesterol. Frontiers in Physiology, 9, p.526.

McClure, R.S., Brogly, S.B., Lajkosz, K., McClintock, C., Payne, D., Smith, H.N. and Johnson, A.P., 2020. Economic burden and healthcare resource use for thoracic aortic dissections and thoracic aortic aneurysms—A population-based cost-of-illness analysis. Journal of the American Heart Association, 9(11), p.e014981.

Mehta, J.L. and Li, D., 2002. Identification, regulation and function of a novel lectin-like oxidized low-density lipoprotein receptor. Journal of the American College of Cardiology, 39(9), pp.1429-1435.

Mehta, N.J. and Khan, I.A., 2002. Cardiology's 10 greatest discoveries of the 20th century. Texas Heart Institute Journal, 29(3), p.164.

Milutinović, A., Šuput, D. and Zorc-Pleskovič, R., 2020. Pathogenesis of atherosclerosis in the tunica intima, media, and adventitia of coronary arteries: An updated review. Bosnian journal of basic medical sciences, 20(1), p.21.

Mitchell, T., Chao, G., Sitkoff, D., Lo, F., Monshizadegan, H., Meyers, D., Low, S., Russo, K., DiBella, R., Denhez, F. and Gao, M., 2014. Pharmacologic profile of the Adnectin BMS-962476, a small protein biologic alternative to PCSK9 antibodies for low-density lipoprotein lowering. Journal of Pharmacology and Experimental Therapeutics, 350(2), pp.412-424.

Moore, K.J. and Freeman, M.W., 2006. Scavenger receptors in atherosclerosis: beyond lipid uptake. Arteriosclerosis, thrombosis, and vascular biology, 26(8), pp.1702-1711.

Morbiducci, U., Kok, A.M., Kwak, B.R., Stone, P.H., Steinman, D.A. and Wentzel, J.J., 2016. Atherosclerosis at arterial bifurcations: evidence for the role of haemodynamics and geometry. Thrombosis and haemostasis, 115(03), pp.484-492.

Münch, R.C., Janicki, H., Völker, I., Rasbach, A., Hallek, M., Büning, H. and Buchholz, C.J., 2013. Displaying high-affinity ligands on adeno-associated viral vectors enables tumor cell-specific and safe gene transfer. Molecular therapy, 21(1), pp.109-118.

Ogura, S., Kakino, A., Sato, Y., Fujita, Y., Iwamoto, S., Otsui, K., Yoshimoto, R. and Sawamura, T., 2009. LOX-1 the multifunctional receptor underlying cardiovascular dysfunction. Circulation Journal, 73(11), pp.1993-1999.

Ouriel, K., 2001. Peripheral arterial disease. The lancet, 358(9289), pp.1257-1264.6

Plaxco, K.W., Spitzfaden, C., Campbell, I.D. and Dobson, C.M., 1997. A comparison of the folding kinetics and thermodynamics of two homologous fibronectin type III modules. Journal of molecular biology, 270(5), pp.763-770.

Plückthun, A., 2015. Designed ankyrin repeat proteins (DARPins): binding proteins for research, diagnostics, and therapy. Annual review of pharmacology and toxicology, 55, pp.489-511.

Popovic, B., Millin, A., Bakthavatsalam, D., Velayutham, M., Post, S. and Nagarajan, S., 2017. LOX-1 Primarily Contributes to M1 Macrophage Induced Foam Cell Formation. Arteriosclerosis, Thrombosis, and Vascular Biology, 37(suppl_1), pp.A217-A217.

Pothineni, N.V.K., Karathanasis, S.K., Ding, Z., Arulandu, A., Varughese, K.I. and Mehta, J.L., 2017. LOX-1 in atherosclerosis and myocardial ischemia: biology, genetics, and modulation. Journal of the American College of Cardiology, 69(22), pp.2759-2768.

Ramamurthy, V., Krystek Jr, S.R., Bush, A., Wei, A., Emanuel, S.L., Gupta, R.D., Janjua, A., Cheng, L., Murdock, M., Abramczyk, B. and Cohen, D., 2012. Structures of adnectin/protein complexes reveal an expanded binding footprint. Structure, 20(2), pp.259-269.

Raniolo, S., Vindigni, G. and Biocca, S., 2016. Cholesterol level regulates lectin-like oxidized low-density lipoprotein receptor-1 function. Biomedical Spectroscopy and Imaging, 5(s1), pp.S87-S99.

Ridker, P.M. and Cook, N.R., 2013. Statins: new American guidelines for prevention of cardiovascular disease. The Lancet, 382(9907), pp.1762-1765.

Ritman, E.L. and Lerman, A., 2007. The dynamic vasa vasorum. Cardiovascular research, 75(4), pp.649-658.

Rodon, J., Omlin, A., Herbschleb, K.H., Garcia-Corbacho, J., Steiner, J., Dolado, I., Zitt, C., Feurstein, D., Turner, D., Dawson, K.M. and Stumpp, M.T., 2015. Abstract B25: First-in-human Phase I study to evaluate MP0250, a DARPin blocking HGF and VEGF, in patients with advanced solid tumors. Molecular Cancer Therapeutics, 14(12_Supplement_2), pp.B25-B25.

Ross, R., 1999. Atherosclerosis—an inflammatory disease. New England journal of medicine, 340(2), pp.115-126.

Rossouw, J.E., Lewis, B. and Rifkind, B.M., 1990. The value of lowering cholesterol after myocardial infarction. New England Journal of Medicine, 323(16), pp.1112-1119.

Roth, G.A., Mensah, G.A., Johnson, C.O., Addolorato, G., Ammirati, E., Baddour, L.M., Barengo, N.C., Beaton, A.Z., Benjamin, E.J., Benziger, C.P. and Bonny, A., 2020. Global burden of cardiovascular diseases and risk factors, 1990–2019: update from the GBD 2019 study. Journal of the American College of Cardiology, 76(25), pp.2982-3021.

Sabatine, M.S., Giugliano, R.P., Keech, A.C., Honarpour, N., Wiviott, S.D., Murphy, S.A., Kuder, J.F., Wang, H., Liu, T., Wasserman, S.M. and Sever, P.S., 2017. Evolocumab and clinical outcomes in patients with

cardiovascular disease. New England journal of medicine, 376(18), pp.1713-1722.

Scandinavian Simvastatin Survival Study Group, 1994. Randomised trial of cholesterol lowering in 4444 patients with coronary heart disease: the Scandinavian Simvastatin Survival Study (4S). The Lancet, 344(8934), pp.1383-1389.

Schiffrin, E.L., 2002. Beyond blood pressure: the endothelium and atherosclerosis progression. American journal of hypertension, 15(S5), pp.115S-122S.

Scott, A.M., Allison, J.P. and Wolchok, J.D., 2012. Monoclonal antibodies in cancer therapy. Cancer immunity, 12(1).

Sentinelli, F., Filippi, E., Fallarino, M., Romeo, S., Fanelli, M., Buzzetti, R., Berni, A. and Baroni, M.G., 2006. The 3′-UTR C> T polymorphism of the oxidized LDL-receptor 1 (OLR1) gene does not associate with coronary artery disease in Italian CAD patients or with the severity of coronary disease. Nutrition, metabolism and cardiovascular diseases, 16(5), pp.345-352.51. Mango, R., Predazzi, I.M., Romeo, F. and Novelli, G. 2011. LOX-1/LOXIN: the yin/yang of atheroscleorosis. Cardiovasc Drugs Ther. 25(5), pp.489-494.

Shah, B. and Mayer, L., 2010. Current status of monoclonal antibody therapy for the treatment of inflammatory bowel disease. Expert review of clinical immunology, 6(4), pp.607-620.

Sharma, M., Ansari, M.T., Abou-Setta, A.M., Soares-Weiser, K., Ooi, T.C., Sears, M., Yazdi, F., Tsertsvadze, A. and Moher, D., 2009. Systematic

review: comparative effectiveness and harms of combination therapy and monotherapy for dyslipidemia. Annals of internal medicine, 151(9), pp.622-630.

Shi, Y., Cosentino, F., Camici, G.G., Akhmedov, A., Vanhoutte, P.M., Tanner, F.C. and Lüscher, T.F., 2011. Oxidized low-density lipoprotein activates p66Shc via lectin-like oxidized low-density lipoprotein receptor-1, protein kinase C-β, and c-Jun N-terminal kinase kinase in human endothelial cells. Arteriosclerosis, thrombosis, and vascular biology, 31(9), pp.2090-2097.

Stack, E.C., Wang, C., Roman, K.A. and Hoyt, C.C., 2014. Multiplexed immunohistochemistry, imaging, and quantitation: a review, with an assessment of Tyramide signal amplification, multispectral imaging and multiplex analysis. Methods, 70(1), pp.46-58.

Stary, H.C., Chandler, A.B., Dinsmore, R.E., Fuster, V., Glagov, S., Insull Jr, W., Rosenfeld, M.E., Schwartz, C.J., Wagner, W.D. and Wissler, R.W., 1995. A definition of advanced types of atherosclerotic lesions and a histological classification of atherosclerosis: a report from the Committee on Vascular Lesions of the Council on Arteriosclerosis, American Heart Association. Circulation, 92(5), pp.1355-1374.

Sternke, M., Tripp, K.W. and Barrick, D., 2019. Consensus sequence design as a general strategy to create hyperstable, biologically active proteins. Proceedings of the National Academy of Sciences, 116(23), pp.11275-11284.

Stumpp, M.T., Binz, H.K. and Amstutz, P., 2008. DARPins: a new generation of protein therapeutics. Drug discovery today, 13(15-16), pp.695-701.

Sun, Y. and Chen, X., 2011. Ox-LDL-induced LOX-1 expression in vascular smooth muscle cells: role of reactive oxygen species. Fundamental & clinical pharmacology, 25(5), pp.572-579.

Swirski, F.K., Libby, P., Aikawa, E., Alcaide, P., Luscinskas, F.W., Weissleder, R. and Pittet, M.J., 2007. Ly-6C hi monocytes dominate hypercholesterolemia-associated monocytosis and give rise to macrophages in atheromata. The Journal of clinical investigation, 117(1), pp.195-205.

Thompson, R.C., Allam, A.H., Lombardi, G.P., Wann, L.S., Sutherland, M.L., Sutherland, J.D., Soliman, M.A.T., Frohlich, B., Mininberg, D.T., Monge, J.M. and Vallodolid, C.M., 2013. Atherosclerosis across 4000 years of human history: the Horus study of four ancient populations. The lancet, 381(9873), pp.1211-1222.

Tiede, C., Bedford, R., Heseltine, S.J., Smith, G., Wijetunga, I., Ross, R., AlQallaf, D., Roberts, A.P., Balls, A., Curd, A. and Hughes, R.E., 2017. Affimer proteins are versatile and renewable affinity reagents. Elife, 6, p.e24903.

Tiede, C., Tang, A.A., Deacon, S.E., Mandal, U., Nettleship, J.E., Owen, R.L., George, S.E., Harrison, D.J., Owens, R.J., Tomlinson, D.C. and McPherson, M.J., 2014. Adhiron: a stable and versatile peptide display scaffold for molecular recognition applications. Protein Engineering, Design and Selection, 27(5), pp.145-155.

Toth, P.P., 2008. Subclinical atherosclerosis: what it is, what it means and what we can do about it. International journal of clinical practice, 62(8), pp.1246-1254.

Vazquez-Lombardi, R., Phan, T.G., Zimmermann, C., Lowe, D., Jermutus, L. and Christ, D., 2015. Challenges and opportunities for non-antibody scaffold drugs. Drug discovery today, 20(10), pp.1271-1283.

Wang, Y., Dubland, J.A., Allahverdian, S., Asonye, E., Sahin, B., Jaw, J.E., Sin, D.D., Seidman, M.A., Leeper, N.J. and Francis, G.A., 2019. Smooth muscle cells contribute the majority of foam cells in ApoE (Apolipoprotein E)-deficient mouse atherosclerosis. Arteriosclerosis, thrombosis, and vascular biology, 39(5), pp.876-887.

Waters, D.D., Ho, J.E., DeMicco, D.A., Breazna, A., Arsenault, B.J., Wun, C.C., Kastelein, J.J., Colhoun, H. and Barter, P., 2011. Predictors of new-onset diabetes in patients treated with atorvastatin: results from 3 large randomized clinical trials. Journal of the American College of Cardiology, 57(14), pp.1535-1545.

Wei, C., Wan, L., Yan, Q., Wang, X., Zhang, J., Yang, X., Zhang, Y., Fan, C., Li, D., Deng, Y. and Sun, J., 2020. HDL-scavenger receptor B type 1 facilitates SARS-CoV-2 entry. Nature metabolism, 2(12), pp.1391-1400.

White, S.J., Sala-Newby, G.B. and Newby, A.C., 2011. Overexpression of scavenger receptor LOX-1 in endothelial cells promotes atherogenesis in the ApoE−/− mouse model. Cardiovascular Pathology, 20(6), pp.369-373.

Xu, S., Ogura, S., Chen, J., Little, P.J., Moss, J. and Liu, P., 2013. LOX-1 in atherosclerosis: biological functions and pharmacological modifiers. Cellular and Molecular Life Sciences, 70, pp.2859-2872.